Analysis of risks related to maritime hydrogen-based propulsion solutions

Master thesis

MSc Marine Technology

Guan-Wei Chen (Wayne)

Analysis of risks related to maritime hydrogen-based propulsion solutions

Master thesis

by

Guan-Wei Chen (Wayne)

to obtain the degree of Master of Science in Marine Technology
with the specialization in Marine Engineering & Ship Design
at the Delft University of Technology,
to be defended publicly on Tuesday, May 16, 2023 at 10:00 a.m. (CEST).

Student number:	5446902	
Project duration:	August, 2022 – May, 2023	
Report number:	MT.22/23.030.M.	
Thesis committee:	Dr. ir. L. van Biert,	TU Delft, chair, supervisor
	Dr. ir. M. Godjevac,	Future Proof Shipping, supervisor
	Dr. ir. A.A. Kana	TU Delft, committee member
	Dr. ir. M. Yang	TU Delft, committee member

TU Delft

Preface

Completing this thesis marks the end of my academic journey as a master's student in marine technology at TU Delft. The road has been long and challenging, but the knowledge and experience gained throughout the process have been invaluable. This research is the result of countless hours of hard work, dedication, and collaboration with my thesis supervisors.

First and foremost, I would like to express my deep gratitude to my daily supervisor, Dr. Milinko Godjevac, for his unwavering guidance and support throughout the entire process. Our insightful discussions and weekly office day with friendly future-proof shipping colleagues will always be memorable. I would also like to extend my thanks to my university supervisor, Dr. Lindert van Biert, for his valuable feedback and encouragement during the proposal stage of this project, which was critical in motivating me to pursue this research.

Next, I am deeply grateful to all my friends in the Netherlands and Taiwan for their support, encouragement, and positive feedback, which provided me with invaluable companionship and a sense of community during my studies.

Lastly, I would like to acknowledge my family, who have always unconditionally supported and encouraged me since the day I decided to study abroad. I cannot express enough gratitude for their unwavering support and belief in my abilities.

Completing this thesis would not have been possible without the support and encouragement of these individuals and communities, and I am forever grateful for their contributions.

Guan-Wei Chen (Wayne)
Delft, May 2023

Summary

The maritime sector is actively investigating new solutions for zero emissions in response to climate change. One of the promising options is hydrogen-based propulsion, but there are currently no prescriptive rules or legislation to approve the design of such innovative, unproven technology. The International Maritime Organization (IMO) requires a quantitative risk assessment to demonstrate that the safety level of hydrogen-fueled vessels is equivalent to that of conventional-fueled vessels. To address this challenge, a risk-based design approach is needed, and the quantitative risk assessment process plays a crucial role in the early design stage.

This research contributes to the technical understanding and potential of zero-emission maritime hydrogen propulsion solutions, by designing a quantitative risk assessment system for analyzing and evaluating risks associated with this innovative technology. The developed risk-analysis system could be a useful tool for future development. While compressed hydrogen design has matured and undergone relevant risk studies, its low volumetric energy density limits its sailing distance. Liquid hydrogen provides a more energy-dense solution, enabling longer-distance sea-going missions, but its application in the maritime industry lacks related risk studies. Therefore, this study aims to design a quantitative risk assessment system for maritime liquid hydrogen propulsion that can analyze and evaluate risks adequately.

The methodology of this study includes a conceptual design of a liquid hydrogen-fueled vessel, followed by hazard identification and scenario selection. The Bayesian theory was used to assess the leak frequencies of components operating with liquid and gaseous hydrogen from published literature, with adjustments made for the harsh maritime environment and mechanical systems. Ignition probability models were proposed, and validated consequence models were used to simulate hazards. Risks are presented as individual and societal risks and compared to acceptance criteria to determine the acceptability of the design. Mitigation measures were proposed and examined. The study also compared the risks associated with liquid and compressed hydrogen configurations.

The conclusion of this study shows that the risks associated with maritime liquid hydrogen-based propulsion solutions can be acceptably managed with appropriate mitigation measures. Specifically, the results indicate that for the FPS Rijn vessel, the risks are acceptable for up to 20% of operational time without any mitigation measures, as long as the liquid hydrogen system is located at least 45 meters away from crew rooms. However, with the implementation of mitigation measures, such as those proposed in this study, it is possible to operate the vessel 100% of the time with acceptable risks. Additionally, a comparison of liquid and compressed hydrogen designs demonstrate that liquid hydrogen designs have a similar risk level as compressed hydrogen designs but offer advantages in terms of space-saving and longer-distance characteristics, making them a promising candidate for maritime zero-emission propulsion solutions in the future.

Nonetheless, it is essential to validate the consequences and liquid hydrogen leak frequencies more rigorously, as limited information is currently available for this innovative technology. Overall, this research explores the risks of maritime hydrogen-fueled applications and challenges the perception of hydrogen as an impossible and dangerous substance.

Contents

List of Figures

List of Tables

Nomenclature

In this nomenclature, one can find all of the variables used in the report, including a definition and the unit of the variable.

α_1	Intercept of the leak frequency relation to leak area	$-$
α_2	Slope of the leak frequency relation to leak area	$-$
$\bar{R}$	Combustion energy-scaled distance	$-$
ΔH	Heat of combustion	kJ/g
ΔP	Pressure difference	Pa
$\Delta \bar{P_s}$	Dimensionless maximum static overpressure	-
$\dot{m}$	Release mass flow rate	kg/s
η	Efficiency	$-$
$_{H_2}$	Mass of hydrogen	kg
μ	Mean	$-$
ρ_0	Release density	kg/m^3
ρ_a	Atmosphere density	kg/m^3
ρ	Storing density	kg/m^3
σ	Standard deviation	$-$
τ_a	Atmospheric transmissivity	$-$
τ_G	Global flame residence time	$-$
τ_j	Precision	$-$
A	Leakage area	m^2
a_p	Planck-mean absorption coefficient for an optically thin flame	$-$
$A_{fireball}$	Surface area of the fireball	m^2
C	Discharge coefficient	$-$
D	Fireball sphere diameter	m
d, d_j	Leakage diameter	m
E	Combustion energy of the fuel-air mixture in stoichiometric quantity	J/kg
f	frequency	$-$
F_s	Fraction of heat radiated	$-$
F_{view}	View factor	$-$
G_{eva}	Evaporation rate	$kg/m2/s$
g_{rms0}	Reference root mean square vibration amplitude	$g(m/s^2)$

g_{rms}	Root mean square vibration amplitude	$g(m/s^2)$
h	Distance of a flat target located outside the fireball	m
h_c	Heat of combustion	J/Kg
k	Ratio of specific heat capacity at constant pressure to constant volume	–
k_t	Temperature dactor	–
L	Fatal distance of the flash fire	m
L, L_f	Flame length of the jet fire	m
LHV	Lower heating value	kJ/kg
m_f	Mass of fuel involved	kg
N	Number of components	–
P	Generated power	kW
P	Positive overpressure	Pa
$p()$	Probability	–
P, P_{01}, P_0	Storing pressure	Pa
P_a	Atmospheric pressure	Pa
$P_{ignition}$	Ignition probability	–
q	Heat radiation	W/cm^2
$q(r)$	Heat flux density at r	W/cm^2
q_s	Burning rate	kg/s
R	Distance from the explosion center	m
R	Pool fire radius	m
r	Distance from the flame center	m
Re	Reynold number	–
t	Sailing time	hr
t_d	Duration of the fireball	s
T_f	Adiabatic flame temperature	K
T_{01}	Storing temperature	K
T_{atm}	Atmosphere temperature	K
u	Wind speed	m/s
VF	Vibration factor	–
W_f	Flame width of the jet fire	m
x	Radiation fraction	–
X_{IG}	Ignition distance	m
γ	Safety coefficient	–

Acronyms

Acronym	Definition
GHG	Greenhouse Gas
IMO	International Maritime Organization
ICS	International Chamber of Shipping
QRA	Quantitative Risk Assessment
SOTA	State Of The Art
ICE	Internal Combustion Engine
CH2	Compressed Hydrogen
LH2	Liquid Hydrogen
CCH2	Compressed- Cryogenic Hydrogen
CO2	Carbon Dioxide
N2	Nitrogen
LNG	Liquid Natural Gas
LFL	Lower Flammable Limit
SNL	Sandia National Laboratories
NASA	National Aeronautics and Space Administration
DNV	Det Norske Veritas
IGF Code	International Code of Safety for Ships using Gases or other Low-flashpoint Fuels
RBD	Risk-Based Design
HAZID	Hazard Identification
PEM	Proton Exchange Membrane
FRR	Fire Resistance Rating
CFD	Computational Fluid Dynamic
IR	Individual Risk
SR	Societal Risk
MIE	Minimum Ignition Energy
DDT	Deflagration to Detonation Transition
IDEALHY	Integrated Design for Efficient Advanced Liquefaction of Hydrogen
BLEVE	Boiling Liquid Expanding Vapour Explosion
FTA	Fault Tree Analysis
ETA	Event Tree Analysis
BT	Bow Tie Analysis
OREDA	Offshore Reliability Data Handbook
HSE	Health and Safety Executive
TCS	Tank Connection Space
FFI	Norwegian Defence Research Establishment
BAM	Federal Institute for Materials Research and Testing
TNO	Nederlandse Organisatie voor Toegepast Natuurwetenschappelijk Onderzoek
OGP	International Association Oil & Gas Producers
FN	Frequency-Number
ALARP	As Low As Reasonable Practical
FPS	Future Proof Shipping B.V.
FC	Fuel Cell
ESD	Emergency Shut-Down
PBU	Pressure Build-Up Unit
ACH	Air Changes Per Hour
VF	Vibration Factor
PSD	Power Density Function
FFT	Fast Fourier Transform
CH4	Methane
RIVM	National Institute of Public Health and the Environment, the Netherlands
BST	Baker-Strehlow-Tang
QRM	Quantitative Risk Matrix
HPPS	High-Pressure Piping Subsystem
LPPS	Low-Pressure Piping Subsystem

1
Introduction

1.1. Background

Global warming caused by greenhouse gas (GHG) emissions has had a detrimental impact on the environment, with the shipping industry being responsible for approximately 2.5-3% of such emissions worldwide [84]. To address this issue, the International Maritime Organization (IMO) set a target in April 2018 to reduce greenhouse gas emissions from shipping by 50% by 2050, compared to 2008 levels [85]. However, the International Chamber of Shipping (ICS) has called for an increase in this target to achieve net-zero emissions by 2050.

To meet the objective of decreasing GHG emissions, implementing several technologies, including alternative fuels, is imperative. One such promising solution is the hydrogen-based propulsion system, which generates only water and heat as byproducts. However, the extreme characteristics of hydrogen, such as its broad flammability range, low density, and low ignition energy, can result in unfavorable consequences. These traits make hydrogen a highly combustible and prone-to-leak fuel, leading to fires and explosions. On ships, hydrogen is usually stored either as a highly pressurized gas (250-700 bar) or as a cryogenic liquid (20K) with a slight over-pressure (1-10 bar) to increase energy density, leading to higher risk due to increased potential for hydrogen leakage. Currently, the majority of maritime hydrogen-based propulsion systems utilize compressed hydrogen storage because of their better understanding and maturity. However, these gaseous applications limit the sailing distance capability, making them suitable only for inland, short-distance missions. Liquid hydrogen storage, on the other hand, surpasses gaseous storage in terms of energy density by 2-4 times. Therefore, liquid hydrogen systems are more appropriate for zero-emission, long-distance maritime missions.

Since regulations and standards for maritime hydrogen-based propulsion systems are incomplete, establishing a knowledge base for their future development is necessary. As an innovative and untested design, a safety level equivalent to that of conventional-fuelled vessels is required, and it is the only regulation that governs alternative designs [51]. Furthermore, as a novel and unproven technology, risk should be quantified instead of ranked qualitatively [50]. Thus, a risk-based design should be comprehensively researched before implementing the technology on ships to avoid safety and economic consequences from potential accidents.

In conclusion, achieving the target of lowering GHG emissions while enabling long-distance missions requires a liquid hydrogen-based propulsion system. However, without preliminary regulations or standard design procedures, applying a risk-based design concept is crucial to ensure adequate safety levels for real-life applications. Therefore, a quantified risk assessment tool for maritime liquid hydrogen-based solutions must be developed, where risk can be assessed within the acceptable criteria during the preliminary design phase.

1.2. Aim of the research

The research presented in this thesis aims at developing a quantitative risk assessment tool for maritime liquid hydrogen-based propulsion solutions, which can be applied in the early preliminary design stage. As a crucial part of the risk-based design framework, this tool should be able to analyze the risks thoroughly and rationally. This leads to the following research objective:

To develop a quantitative risk assessment system that can effectively analyze and evaluate the risks associated with liquid hydrogen-based propulsion solutions in the maritime industry.

The objective can be pursued by answering the following research sub-questions:

1. What is the system configuration of the maritime liquid hydrogen propulsion system, and how can potential hazards and scenarios be identified and assessed to evaluate the risks?

2. What are the most suitable methods for quantitatively and accurately assessing the risks (likelihoods and consequences) of maritime liquid hydrogen propulsion systems?

3. What is the comparative feasibility, in terms of risks and capabilities, of maritime liquid hydrogen propulsion systems and existing compressed hydrogen propulsion systems?

4. What are the quantified risks of maritime liquid hydrogen propulsion systems, and what mitigation measures can be implemented to reduce these risks to acceptable levels?

5. To what extent can this quantified risk assessment system be applied? What are the limitations of this tool, and can this design framework also be applied to different alternative fuels?

1.3. Thesis structure

The thesis presents the work in the following sequence:

Chapter 2 gives the overview of the literature review. The state-of-the-art hydrogen technology in the shipping industry and literature regarding hydrogen quantitative risk assessment studies were reviewed, whereas the research gaps were found, and the main research objective was concluded in this chapter.

Chapter 3 summarises the research objective and research questions of this thesis, where the conclusion from the literature review phase was summarised here and formed the basic motivation of this research.

Chapter 4 presents the methodology behind this research, where each process of quantitative risk assessment was investigated and discussed. Start with designing the whole logical map of the system, then implementing relative theories or advancing old information to design an innovative quantitative risk assessment system.

Chapter 5 shows the compiled result of the quantitative risk assessment system. Risks in terms of individual risk and societal risk were calculated, while these quantified risk values were compared to the risk criteria to determine the safety of the system. The individual risks from the different scenarios were also presented in this chapter, where the most severe scenario was assessed, and the solutions to mitigate it was proposed.

Chapter 6 addresses the critical discussion regarding the methodologies and results of this research. The system's uncertainties were discussed, and a few possible solutions and developments for future research have been suggested. Additionally, risks in respect of individual and societal risks were also assessed, and the analytical comparison with the existing published hydrogen quantitative risk assessment tool was carried out.

Chapter 7 concludes the findings and highlights of this research. And the answers to research questions are presented.

Chapter 8 summarises the previous discussions, providing possible solutions and recommendations for future research.

This page intentionally left blank

2

Literature study

The aim of this chapter is to investigate the state-of-the-art (SOTA) hydrogen risk assessment and identify research gaps in the application of hydrogen-based solutions in the maritime industry, based on reviewed knowledge and information. The chapter will begin by focusing on hydrogen technologies and properties, followed by an examination of risk assessment studies, including quantitative risk analysis (QRA) procedures and SOTA studies on maritime hydrogen applications. Both CH2 and LH2 systems using the QRA procedure will be reviewed. Finally, in chapter 3, the research objective and research questions regarding the analysis of the risk associated with hydrogen-based propulsion systems will be concluded.

2.1. Hydrogen as a marine fuel

Several studies have been conducted on hydrogen-fueled vehicles [45, 111, 104]. These articles suggested that fuel cells are one of the most promising zero-emission power sources, as hydrogen combustion engines have lower efficiency, as indicated by Seyed et al. [45]. By using hydrogen as a fuel and air as an oxidant, the electrochemical reactions inside the fuel cell produce electricity for propulsion. However, fuel cells have different types based on their operating temperature, materials, and efficiency, despite having similar working principles. In the shipping industry, fuel cells outperform conventional internal combustion engines (ICEs) in terms of efficiency and low emissions. Nonetheless, diesel is still more economical and has a significantly higher energy density than any of the hydrogen storage methods, as demonstrated in Figure 2.1, when it comes to fuel storage.

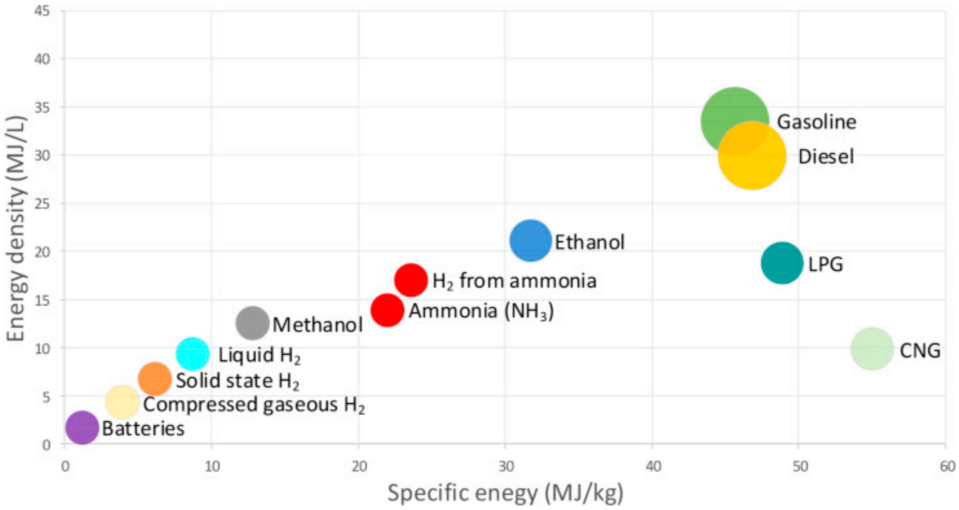

Figure 2.1: Comparison of volumetric energy density for different fuels [120].

Upgrading the volumetric energy density of hydrogen storage is essential for its widespread adoption as a fuel. The primary solutions for achieving this are through compression or liquefaction, such as compressed hydrogen (CH2), liquid hydrogen (LH2), and compressed-cryogenic hydrogen (CCH2). However, other methods like hydrogen carriers have also been experimented with and researched by van Hoecke et al. [42].

A comparison of different energy systems in terms of weight and volume is presented in Figure 2.2. It is evident that an ICE system remains the lightest solution, but the weight of LH2 storage is comparable to that of the conventional ICE solution. Figure 2.3 shows the energy demand for producing 1 kg of hydrogen for different hydrogen storage methods. CH2 has the lowest energy demand, while hydrogen carriers such as CO2-based and N2-based storage require higher energy. This economic advantage due to the low energy demand has resulted in the commercialization and wide application of CH2.

Various CH2 vessels have been produced with different structures, as shown in Figure 2.4. Type I cylinders can only store hydrogen up to 300 bar, while the other three can increase to 700 bar due to their structural strength. Despite having the lowest energy density and the highest weight, type I has the most considerable market share of 93% for its low price. In contrast, type IV cylinders have the overall highest energy density due to the utilization of composite materials. However, the low volumetric energy density of CH2 storage limits its sailing durability. Therefore, at present, inland vessels or short-mission shipping are the only viable applications.

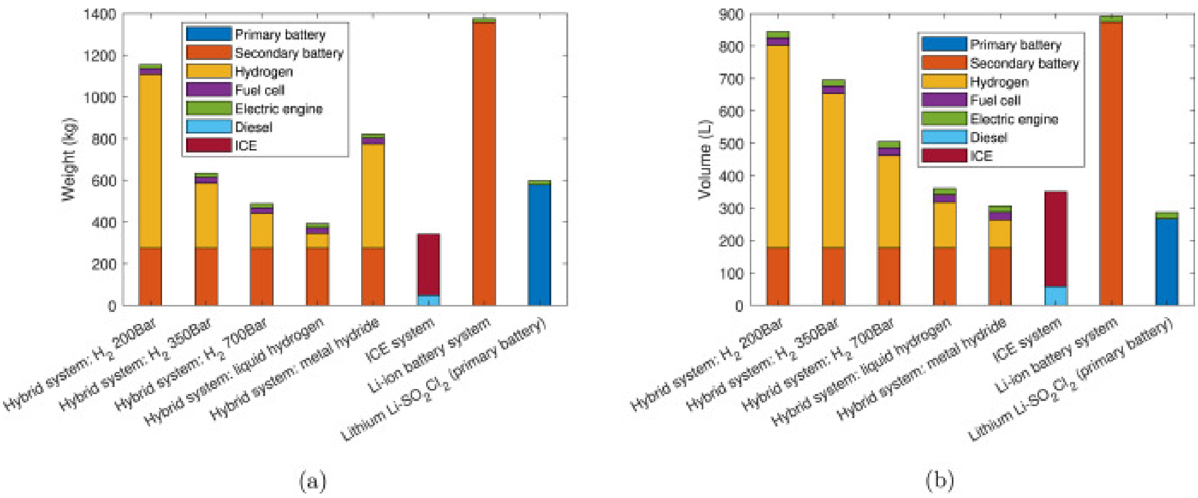

Figure 2.2: Estimated weight and volume of 75kW hydrogen fuel cell solutions- comparison with the battery and the diesel ICE systems [16].

LH2 has a higher volumetric energy density compared to CH2. Additionally, its cost of production is lower than most other hydrogen storage methods, as shown in Figure 2.3. Figure 2.4 presents a comparison of the volumetric and gravimetric energy density of CH2 in different configurations with liquid hydrogen, revealing that LH2 has a significantly higher energy density than all types of CH2 storage. According to Tashie-Lewis and Nnabuife [9], LH2 is still the more attractive option for extended-duration operations and missions because of its high energy density. Moreover, LH2 storage can operate under atmospheric pressure, providing an additional advantage over CH2 storage. However, the energy required to liquefy the hydrogen and the boil-off behavior of LH2 increase its cost and decrease its applicability [9].

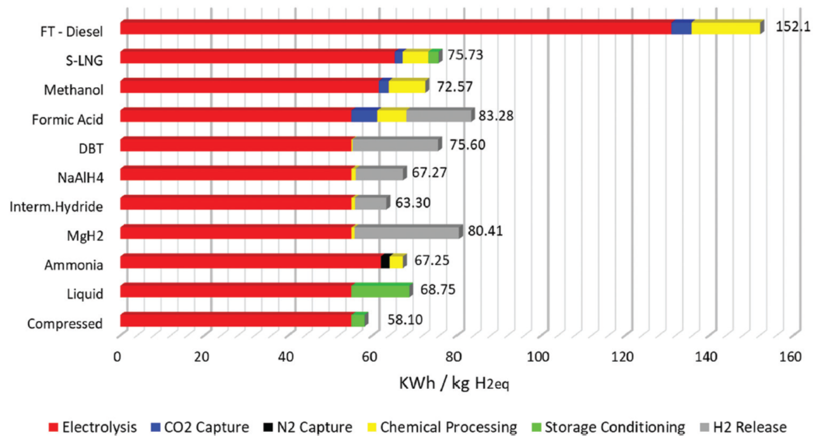

Figure 2.3: Energy comparison for the storage requirements for the selected hydrogen storage carriers [42].

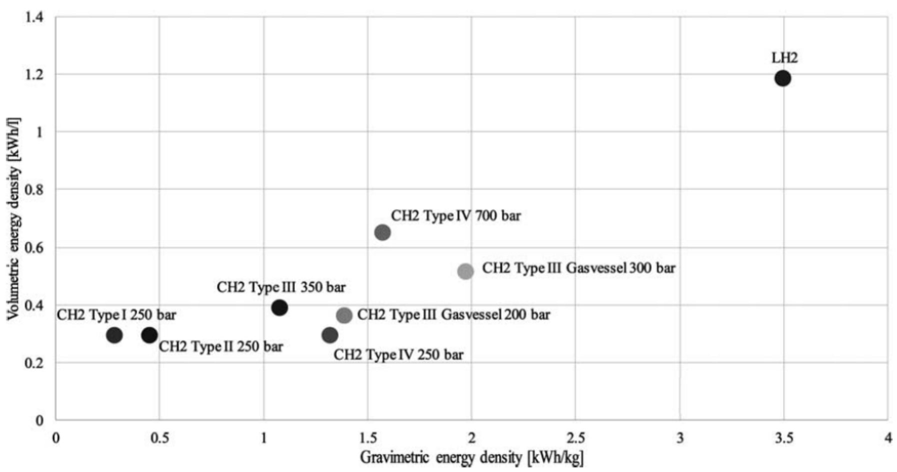

Figure 2.4: Volumetric and gravimetric energy density of different hydrogen storage technologies [97].

2.1.1. Hydrogen properties

The development of hydrogen technology for maritime applications is majorly limited by its life-cycle cost and safety [9], which are highly related to its extreme physical properties. Hydrogen, being the first element in the periodic table of elements and the most abundant chemical substance in the universe, has been measured and documented for its extreme properties. It is a colorless and odorless gas at room temperature and pressure, making it difficult to detect by humans. Additionally, its low viscosity and high diffusivity can cause hydrogen to leak out of components and diffuse quickly, necessitating unique sealing designs for hydrogen storage. Hydrogen is known for its high combustibility, with a minimum ignition energy (MIE) of only $0.017mJ$, which is ten times less than that of liquid natural gas (LNG) [93]. Its extremely low ignition energy and the wide flammability range from 4% to 75% of hydrogen in the air are also disadvantages. Table 2.1 compares the physical properties of hydrogen and methane.

Table 2.1: Physical properties of hydrogen and other fuels, data collected from [64, 45, 42, 93].

Property	Hydrogen	Methane
Density (STP, g/L)	0.083	0.659
Minimum Ignition energy (in air, mJ)	0.017	0.27
Flammable limits (in air, %)	4-75	5-17
Boiling point (Degree)	-253	-161
Viscosity ($Pa * s * 10^{-5}$)	0.0083	0.0651
Diffusion coefficient in air (cm^2/s)	0.61	0.16
Auto ignition temperature (Degree)	585	540
Amount of energy, heat of combustion (kJ/g)	120	50
Adiabatic flame temperature (Degree)	2045	1875

Hydrogen must be manipulated safely during transportation, storage, and production with these extreme physical properties to avoid leakage, ignition, and even explosion. According to Yang et al. [119], who analyzed 120 existing hydrogen incident data from 1999 to 2019, resulting in that equipment failure-induced hydrogen leakage is the main cause of the accidents, leading to a 10.27% of injury rate and 5.32% of facility rate, where the latter is twice the LNG accidents. Accordingly, it is necessary to evaluate the risk of hydrogen systems before their real application.

2.1.2. Challenges of moving from land-base to maritime

Hydrogen has been used in industry for decades, and land-based experiences are proven to be safe enough to operate and transport. For instance, NASA is the first institute that uses hydrogen as a fuel in the space industry. It also conducted a series of large-scale LH2 release experiments to investigate the safety-related issues of hydrogen [116]. Furthermore, extensive research on risk assessment of land-based hydrogen fueling stations improved its maturity in terms of safety. However, due to the severe conditions such as ship motions, humidity, and limited space, further measures to increase the safety requirements should be established for maritime applications. According to DNV [64], the following factors are the primary challenges that influence the safety requirement and measures of maritime hydrogen applications:

- Unlike land-based applications, ships operate in the open seas environment, which is self-reliant and cannot be supported by the outside immediately.
- The limited space of ships constrains the safety distances, and the isolated environment restricts the possible way for crew or passengers to escape.
- The power demand for shipping is much greater than for land-based transportation such as cars and buses. Therefore, the larger scale of hydrogen storage would have a higher impact on safety issues.
- The offshore environmental conditions are humid and salty. Moreover, the vibrations from machines or acceleration and inclination due to ship motions are also challenges.

2.1.3. Maritime hydrogen-based design framework

As noted earlier, hydrogen fuel cell shipping appears to be a promising solution for a zero-emission future. However, there are currently no specific prescriptive rules and regulations in place for using hydrogen as a marine fuel. The IMO International Code of Safety for Ships using Gases or other Low-flashpoint Fuels (IGF code) [51] provides regulatory frameworks for low flash-point marine fuels, including hydrogen. However, while the IGF code contains detailed prescriptive descriptions for LNG fuel, other fuels are referred to as an alternative design. Currently, the alternative design only needs to provide the same risk level as the conventional fuel design.

Due to the absence of prescriptive regulations, the approval process for the alternative design will be based on a risk-based approval process. Risk-based design (RBD) is a design process that provides a concrete, comprehensive, and flexible design framework developed for new technologies and novel solutions not covered by prescriptive rules. The generic process was illustrated in Figure 2.5 using Lloyd's Register Risk Based Designs [94]. In addition, a more specific RBD process was proposed by DNV, as can be seen in Figure 2.6, which shows the 'Approval of preliminary design' for hydrogen-fuelled ships. This procedure is based on the IMO document 'Guidelines for approving alternatives and equivalents as provided in various IMO instruments' (MSC.1/Circ 1455, 2013) [50]. In addition, this design approach can be divided into two stages: preliminary design space and final design development. In the first stage, the project owner should develop general information about the ship system in the preliminary design phase, such as general arrangement, components, and boundary conditions. Then, an iterative process of executing risk, including concept quantitative risk assessment and explosion analysis, is required. Finally, preliminary approval will be granted after all design-related hazards and failure modes are identified and the parties agree upon analytical results. Otherwise, an iterative procedure would be recirculated until a feasible design solution was found. The second stage, the final approval phase, can be assessed after the preliminary has been approved. The analyses from the former phase will be updated to fit the final design, whereas the approval of the final design is required to gain approval from the administration, such as the flag state.

Notably, within this RBD framework, a risk assessment is required before the design is approved. Particularly in hydrogen as a fuel concept, as an unproven and novel technology, hydrogen is categorized as technology status four by IMO, which is the highest value for this new technology. Therefore, a quantified risk assessment will be required as the basic HAZID may not be applicable to rank the risk due to the limited understanding of such a new technology.

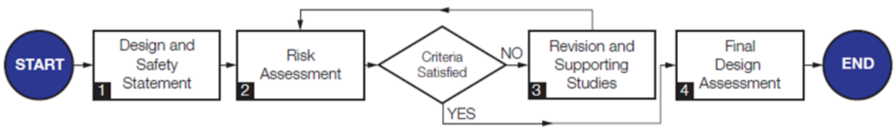

Figure 2.5: Generic Process for Risk Based Designs (RBD) [94].

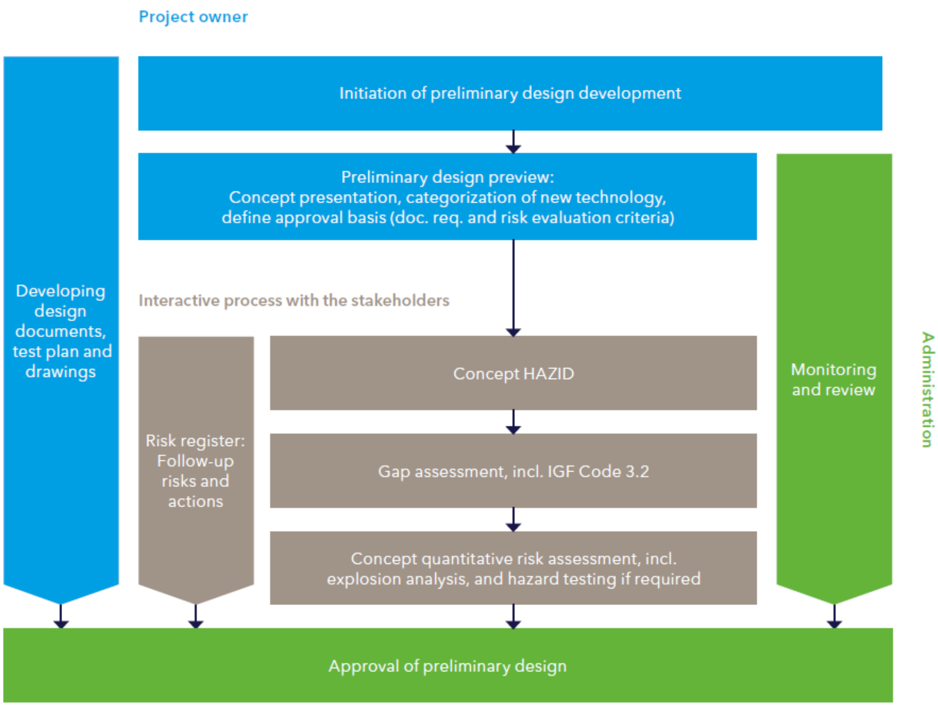

Figure 2.6: Proposed steps in the process towards 'Approval of preliminary design' for hydrogen-fuelled ships [64].

2.1.4. Maritime hydrogen-based propulsion solution

Several hydrogen-powered vessels have been sailing at rivers or lakes for a decade, with hydrogen stored in the compressed gas form [17, 16]. Within these applications, hydrogen fuels the proton exchange membrane (PEM) fuel cells to constitute a zero-emission solution. PEM fuel cell is widely applied in the maritime industry due to their lightweight and low-temperature characteristics. The system layout of CH2 was also conceptually proposed by Aarskog et al. [3], and DNV [64], as can be seen in figure 2.7. On the other hand, recent experience with LH2 is limited in the marine industry. The proposed design of the maritime LH2 propulsion system was only found in DNV [64] and Mylonopoulos et al. [77], or other company's manuals such as MAN Energy Solutions [101], where the design is derived from the maturer LNG-fuelled system and inland LH2 vehicles.

Figure 2.7 and 2.8 shows the proposed system layout of CH2 and LH2 propulsion system from DNV [64] and MAN [101]. Safety-related components such as a venting system, hydrogen leakage detection system, and fire extinguishing system are implemented in both systems. Apart from the differences in vessel type and system pressure, handling the cryogenic hydrogen required additional components to ensure safety. To feed the fuel cells, the liquefied hydrogen should be evaporated to the gaseous form. Hence, an evaporator and gaseous buffer tank are required for producing gaseous hydrogen and storing hydrogen as a buffer. The latter can also mitigate the issue of insufficient driving force due to sloshing. Moreover, the pressure build-up devices and pressure-relief valves mounted on the tank can ensure that the pressure inside the tank is sufficiently safe to transport hydrogen.

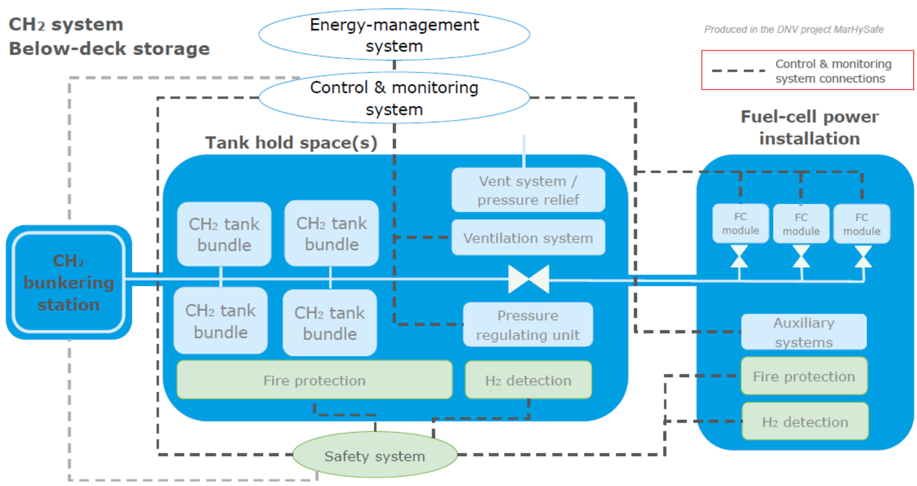

Figure 2.7: System layout for compressed gas hydrogen storage [64].

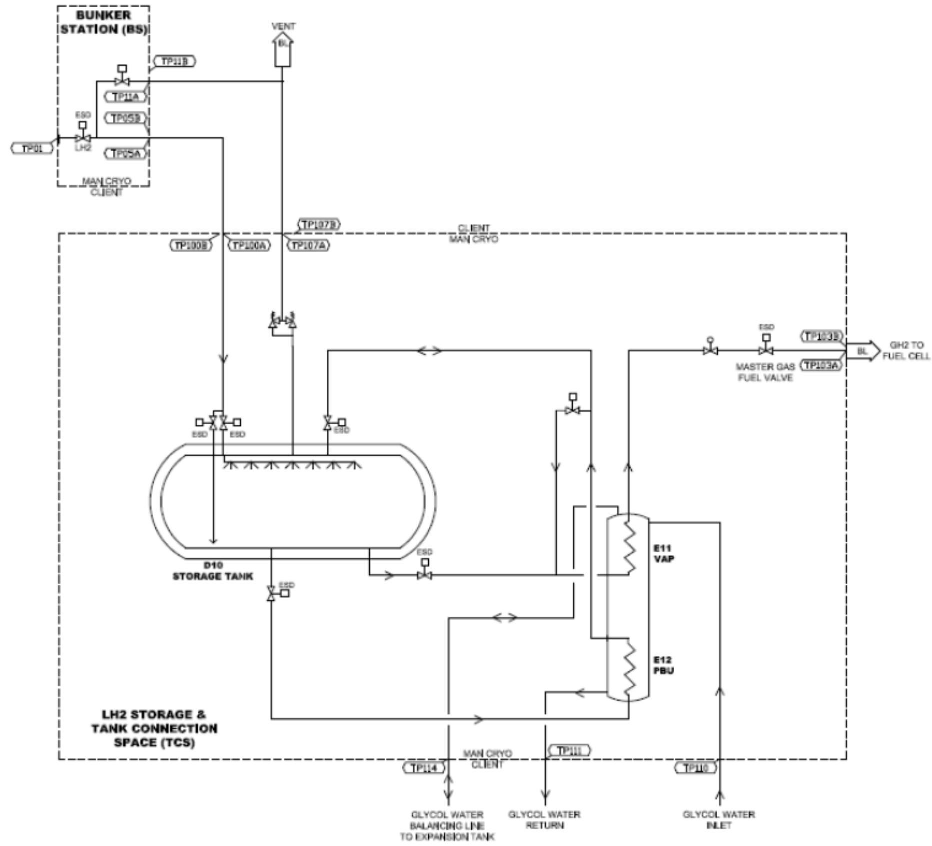

Figure 2.8: System layout for liquefied hydrogen storage [101].

2.1.5. Risk assessment on maritime hydrogen-fulled applications

Aiming at implementing maritime hydrogen-based solutions to lower global GHG emissions, the safety of this alternative design should be proven at the same level as the conventional fuel design. Risk assessment is a standardized procedure that will be elaborated on in the next chapter. Moreover, due to the novelty of hydrogen-fuelled in the maritime industry, there was little literature investigating the risks of the maritime hydrogen-fuelled solution. Therefore, more common studies, such as hydrogen fuelling stations and hydrogen-fuelled inland vehicles, are also reviewed to gain insight into the risk assessment field.

Risk concepts on compressed hydrogen

A number of studies provide the QRA on compressed hydrogen systems, [59, 3, 35, 25, 21, 123]. HyRAM is a software carried out by Sandia National Laboratories (SNL) [25]. It widely covers QRA on CH2 for different system configurations, where the users can define the system parameters and scenarios by themselves. However, Dadashzadeh et al. [21] pointed out that the consequence model in HyRAM does not consider all hazards thoroughly. In the research of Kikukawa et al. [59], the $70Mpa$ hydrogen fueling station's risk assessment was conducted, and the consequences were modeled by interpolating the experiments and under assumptions due to lack of data. As a result, it showed that the $70Mpa$ hydrogen fuelling station is in the same risk range as the $35Mpa$ station. Using the same assessment procedure, Dadashzadeh et al. [21] performed the QRA on onboard hydrogen storage. In this study, the risk was defined in the form of fatality rate and fatality cost per vehicle per year, while the fire resistance of the tank was evaluated as a possible function of the fire resistance rating (FRR). Using different risk evaluation methods, Li et al. [123] evaluated risks in the form of societal risk for a refueling station in Shanghai. Same as presenting society risk as a result, a study for the CH2 reforming process was investigated by Mohammadfam and Zarei [75].

Aside from the land applications, O. Hansen [35] and Aarskog et al. [3] conducted QRAs in maritime applications, while Aarskog et al. [3] established the first conceptual QRA on CH2 propulsion systems for maritime vehicles. The resulting risks were compared with defined thresholds based on different system scenarios. O. Hansen [35] also evaluated the acceptability of CH2 in other applications such as trains and buildings. Dense gas behavior and expected extensive hazard distance make LH2 handling more severe than CH2. Due to the lack of experimental hydrogen data and the complicated consequential physics, both studies employed computational fluid dynamic (CFD) technology to validate the correctness and adapt to different geometries appropriately. In contrast, Huang and Ma [48] reduced uncertainties caused by a shortage of data by implementing a Bayesian network modeling and predicted risks using the grid-based risk mapping method.

Unfortunately, the lack of experimental data and fewer hydrogen facilities are common problems among all these studies. Consequently, the risks are commonly performed as the worst-case scenario in order to solve the high uncertainties issues conservatively.

Risk concepts on liquefied hydrogen

As an important way of increasing the operating durability of the vehicles, LH2 risks have only been carried out in a limited number of studies, [35, 60, 121, 19, 77]. In the research of Klebanoff et al. [60], the potential risks caused by the LH2 system for a high-speed fuel cell ferry were carried out and compared to the liquid natural gas system. The historical experiments and hypothetical mechanisms were reviewed due to the similar combustion energy of both fuels. On the other hand, the first QRA on liquid hydrogen was conducted by Yoo et al. [121] for the refueling station. In this literature, the comparison of the liquid and compressed hydrogen refueling stations were conducted.

The estimated result for LH2 differs from the qualitative evaluation conducted by O. Hansen [35], which indicated that the CH2 fuelling station has a higher individual risk (IR). However, the overpressure model used in the study was only applied to the compartment and may not be applicable to the hydrogen refueling station. Correa-Jullian and Groth [19] proposed an innovative event sequence diagram and event tree scenario for the LH2 fueling system, emphasizing the need to collect data to obtain a confident QRA result. Meanwhile, Caliendo and Genovese [12] examined the risk analysis of transporting dangerous goods like LH2. In a separate study, Mylonopoulos et al. [77] conducted the first safety assessment for a high-speed LH2 ferry and analyzed the qualitative HAZID for the proposed design, as well as the semi-quantified CFD result of the hydrogen leak. However, the semi-quantified result only provided molecular hydrogen concentration in the given scenarios, without quantified information such as overpressure and heat radiation caused by explosions and fires.

Overall, research on LH2 risk assessment is lacking compared to CH2. Recent studies, such as [121] and [35], have yielded conflicting results regarding the risks associated with LH2, highlighting the need for systematic risk assessments to gain a better understanding of the hazards and associated risks.

2.2. Risk study on hydrogen systems

In this chapter, the risk assessment methods for hydrogen are reviewed in detail, both for CH2 and LH2 systems. Prescriptive regulations for the maritime hydrogen-based propulsion solution still need to be developed. Currently, only the IMO IGF code [51] has mentioned that an alternative design should provide an equivalent level of safety as the relevant low-flash point fuel. Moreover, it also required that ”A risk assessment must be performed to assess risks arising from the alternative design.” Therefore, hydrogen-fueled propulsion systems, which considered an alternative design, should perform a risk assessment before the real-life application. In this chapter, the definition and the standardized procedure are introduced, followed by reviewing the state-of-the-art literature on hydrogen applications that are not only focusing on specific maritime applications but also on other industries. Moreover, a QRA approach is discussed and investigated step-by-step, including hazard identification, scenario, frequency assessment, consequence assessment, and risk evaluation.

2.2.1. Risk assessment

Risk assessment has been an effective tool for characterizing risk acceptability, which applies in different fields such as nuclear, and environmental problems, and the topic of this research: hydrogen. By definition, risk can be presented as:

$$Risk = \Sigma Frequencies * consequences \tag{2.1}$$

ISO/IEC guidelines [52] provide the terminology, definitions, and recommendations for risk assessment procedures. Risk assessment can be divided into two categories: qualitative and quantitative risk assessment [27]. The primary difference between the two methods lies in the risk evaluation. Qualitative risk assessment evaluates the frequency and consequence of an event qualitatively [117], [62]. For example, the likelihood and severity of an event are classified into different categories, and risk is evaluated using a risk matrix, as shown in Figure 2.9 [62]. On the other hand, quantitative risk assessment presents the risk in numerical values, such as potential loss of lives per year or frequency of damage per year. To assess the risk more precisely, this research will focus on the quantitative risk assessment approach.

		Likelihood			
		A	B	C	D
Consequence		Improbable	Remote	Occasional	Probable
1	Extremely Severe Damage	H	H	H	H
2	Severe Damage	M	H	H	H
3	Damage	M	M	H	H
4	Small Damage	L	L	M	H
5	Minor Damage	L	L	L	M

Figure 2.9: Risk matrix [62].

Several empirical studies were conducted through a QRA procedure across different fields. Figure 2.10 shows a frequent structure of QRA. Based on this procedure, QRA has often been separated into a few steps: 1)Hazard identification, 2)accident scenario selection, 3)frequency assessment, 4)consequence assessment, 5)risk compilation, and 6) risk assessment. These steps in the field of hydrogen technologies will be reviewed individually in the following subsections.

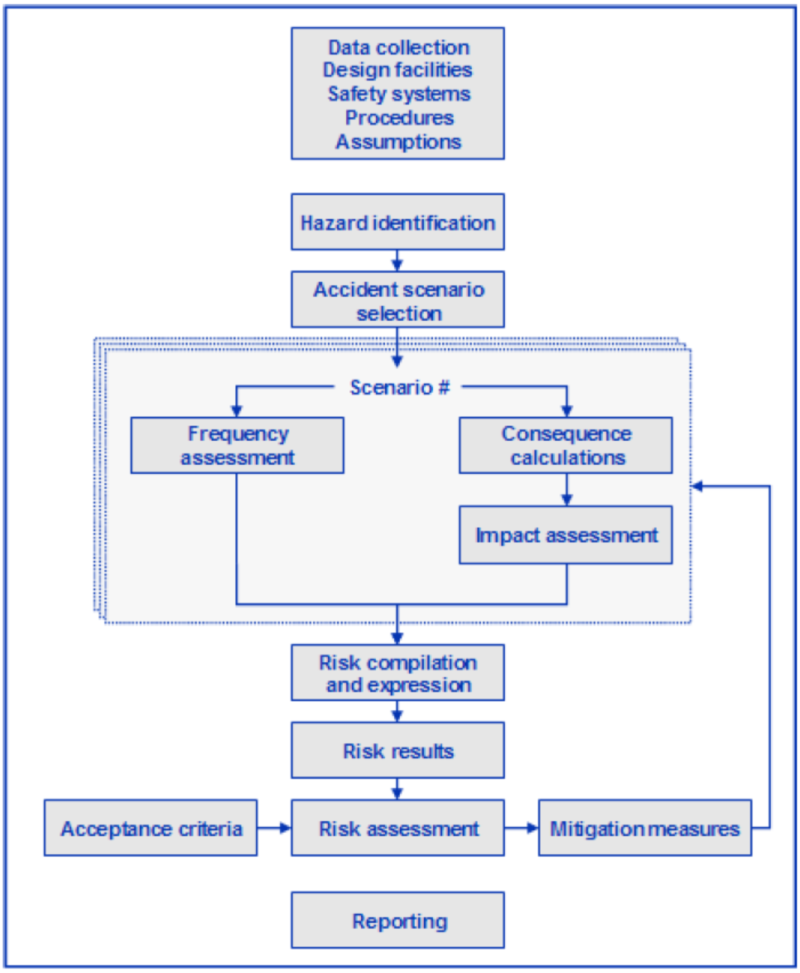

Figure 2.10: Generic quantitative risk assessment procedure [27].

2.2.2. Hazard identification

The hazards associated with different hydrogen storage systems vary, and hydrogen leakage is the primary cause of these, as mentioned in Section 2.1.1. Numerous studies have identified hazards associated with hydrogen. Blast pressure, jet fire, and explosion (deflagration and detonation) are potential hazards associated with compressed hydrogen, as identified by HyRAM [25], Kikukawa et al. [59], and Aarskog et al. [3]. However, since the LH2 system operates at cryogenic temperatures of 20K, it presents different hazards, including cryogenic spills, cold plume frostbite, and combustive phenomena, as identified in the literature by O. Hansen [35], Klebanoff et al. [60], and Yoo et al. [121].

As the first step in QRA, the mechanisms of hydrogen hazards have garnered significant interest among researchers. Hydrogen is characterized as a highly reactive and combustible substance, with a wide flammability range of 4-75%V/V and a low minimum ignition energy (MIE) of 0.017mJ. Ono et al. [83] obtained the MIE of a hydrogen-dry air mixture using previous studies that conducted an MIE at approximately 25% concentration, as shown in Figure 2.11. Despite this, the mechanisms and physics of ignition behavior were not well understood. In early research by Gummer and Hawksworth [53], mechanisms were postulated by investigating incidents of hydrogen releases. The authors concluded that a single mechanism is unlikely to ignite the hydrogen-air mixture, but a combination of postulated mechanisms may lead to ignition. With more data and experiments, Yang et al. [119] and S. Tretsiakova-McNally [108] reviewed existing research and identified the reasons that induce spontaneous ignition:

- Reverse Joule-Thomson Effect

The Joule-Thompson effect occurs when a gas undergoes expansion through a throttling valve or other similar devices. During this process, the gas experiences a decrease in temperature if it is below the Joule-Thompson inversion temperature. In the case of hydrogen, the inversion temperature is at 193K [29], which is lower than that of CH2 stored in the vessel, resulting in a reverse Joule-Thomson effect and an increase in temperature. While the literature suggests that the resulting temperature increase would not reach the self-ignition temperature of hydrogen [125], this effect still raises the possibility of ignition.

- Electrostatic Ignition
  Electrostatic discharges are classified into three types: spark discharge, brush discharge, and corona discharge. Spark discharge occurs when the electric field strength between two electrodes surpasses a certain threshold in volts per centimeter. Studies by Gummer et al. [53] and Tretsiakova-McNally et al. [108] suggest that the required voltage to ignite a hydrogen-air mixture is below 2kV, which can be easily generated on people and individuals standing on an isolated surface. Brush and corona discharge only require a single electrode to undergo an electrical breakdown. The difference between these two phenomena lies in the conductor geometry and discharge behavior, both being induced by high voltage or electrical field. A brush discharge usually happens at a curved electrode, while a corona discharge may occur at the needlepoint. When the electric field strength exceeds the dielectric strength of the surrounding substance, the former induces a larger scale of energy, and multiple brush-like plasma channels can be seen near the electrode. Meanwhile, the latter concentrates the field strength on a needlepoint, leading to a current that passes to the atmosphere as the form of corona [57]. The equivalent energies of the brush discharge were estimated to be about 4mJ for flat polyethylene sheets, according to Ackroyd and Newton [4]. Although corona discharge is generally considered a weak ignition source, it has been observed to ignite the hydrogen-air mixture during weather conditions corresponding to a high electric field, such as thunderstorms [53].

- Diffusion Ignition
  The formation of shock waves can have a significant impact on the behavior of the hydrogen and air mixture. To investigate this effect, high-pressure release experiments have been conducted. Wolanski and Wojcicki showed that ignition could occur at pressures below the self-ignition threshold. In contrast, several studies have suggested that diffusion ignition is more likely to occur at higher initial pressures and longer tube lengths [118, 74].

- Mechanical friction and impact ignition
  The heat generated by mechanical friction is another potential ignition source for hydrogen. When the energy generated by the mechanical friction is higher than the MIE of hydrogen, ignition can occur. In fact, a hydrogen ignition event has been reported to occur when mechanical friction was used as the heat source [119].

- Hot Surface Ignition
  When a hot surface is in contact with a hydrogen-air mixture, it can partially heat the mixture and lead to ignition. However, the temperature of the hot surface must be higher than the ignition temperature of the mixture for ignition to occur. The specific temperature required will depend on factors such as the shape and area of the hot surface. For example, research conducted by HyFact found that the ignition temperature of hydrogen was lower when it was in contact with a hot wire compared to a hot plate of the same temperature and area. This suggests that the shape and area of the hot surface can have a significant impact on ignition behavior [89].

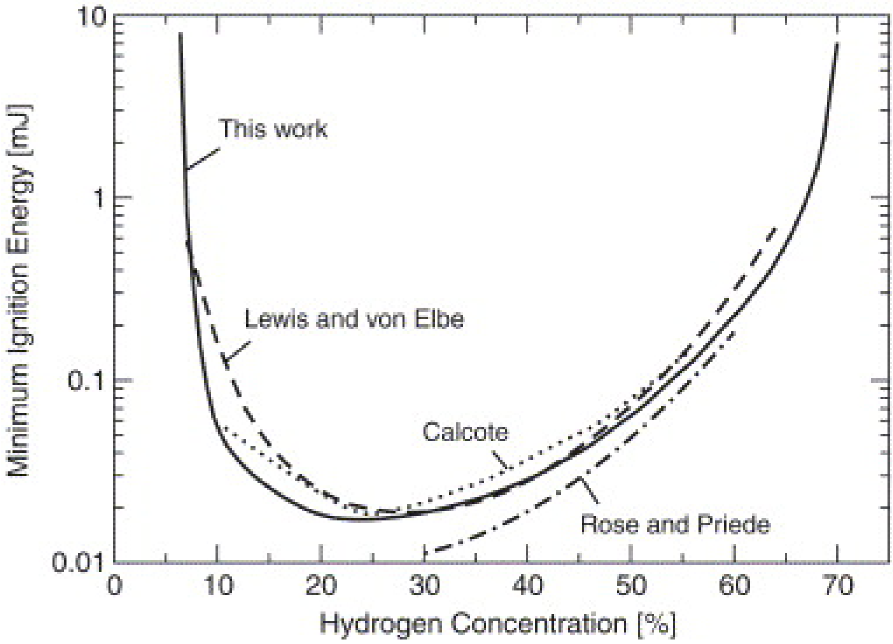

Figure 2.11: Minimum ignition energy of the hydrogen-dry air mixture [83].

The behavior of hydrogen jet leaks from compressed vessels has been studied by Yang et al. [119] before identifying the hazards of ignition. The hydrogen jet can be classified into three types based on the pressure ratio: subsonic, critical-state, and under-expanded jet. In CH2 fuel cell vehicles, an under-expanded jet is expected to disperse and mix with air. After ignition, the hazards can be divided into four categories: jet fire, flash fire, deflagration, and detonation. Flame area, heat radiation, and over-pressure are commonly used criteria to characterize these hazards, as shown in Table 2.2 in most literature studies. However, due to the complexity of the phenomenon and the lack of probability data, no single study covers all of the consequences. Therefore, for simplicity, immediate and delayed ignition are often considered separately, with jet fire being the primary consequence of the former and flash fire and explosion being the primary consequences of the latter.

Similarly, several studies have investigated the mechanisms behind the transfer of fire to deflagration and detonation. Klebanoff et al. [60] emphasized the importance of the ignition source, which can be classified as weak (<50mJ) or strong (>4MJ) depending on the ignition energy. Explosion limits, confined spaces, and detonation cell size were identified as other contributing factors by R. Knystautas [92] and Ng and Lee [81]. For detonation to occur, the hydrogen-air fraction must lie between 18.3-59% (Lower Explosion Limit-Upper Explosion Limit), and the combustion volume should be larger than the detonation cell size. Matsui and Lee [71] quantitatively determined the MIE required for direct detonation, which was found to be 4.16 MJ. However, a detonation can also occur below the explosion limits, known as Deflagration to Detonation Transition (DDT). Sherman et al. [100] found that DDT can occur for as little as 12% hydrogen-air fractions in the FLAME tunnel. The presence of confinement, increasing hydrogen concentration, and run-up distance contribute to the flame acceleration and DDT. The presence of obstacles also increases turbulent formation, leading to feedback that accelerates the flame speed. Figure 2.12 demonstrates that DDT can occur even outside the range of explosion limits with obstacles.

Table 2.2: Hazards of hydrogen, with information collected from [13, 60, 54, 36, 69].

Hazards	Description	Criteria
Fire	Fire is an ordinary combustion with a low propagation speed, and it happens when the ignition energy exceeds the MIE in the flammability range. The sound and overpressure are negligibly harmful to the surrounding. Fires can be classified into jet, flash, and pool fires. • A jet fire occurs at the instant ignition, commonly used in pressurized, high-speed releases with a high radiation fraction. • A flash fire is a release of flammable vapor that mixes with air and expands, finally igniting. • A pool fire happens when the flammable liquid mixture is being ignited.	Temperature, Ignition distance, Heat radiation
Deflagration	Fast combustion, where the flame propagates at subsonic speeds, the induced over-pressures and sound can cause injury to humans and rupture buildings. Deflagrations are initiated by a weak ignition source.	Overpressure, Heat radiation
Detonation	Extremely fast combustion propagates at supersonic speeds, which can produce loud bangs and damaging over-pressures. Detonations are initiated by strong ignition sources or weak ignition sources with fully-developed space.	Overpressure, Heat radiation
Cold plume	The leakage of cryogenic hydrogen mixed with the surrounding air, the low-temperature area near the leakage source, can cause frostbite on humans and the material embrittlement to components.	Temperature

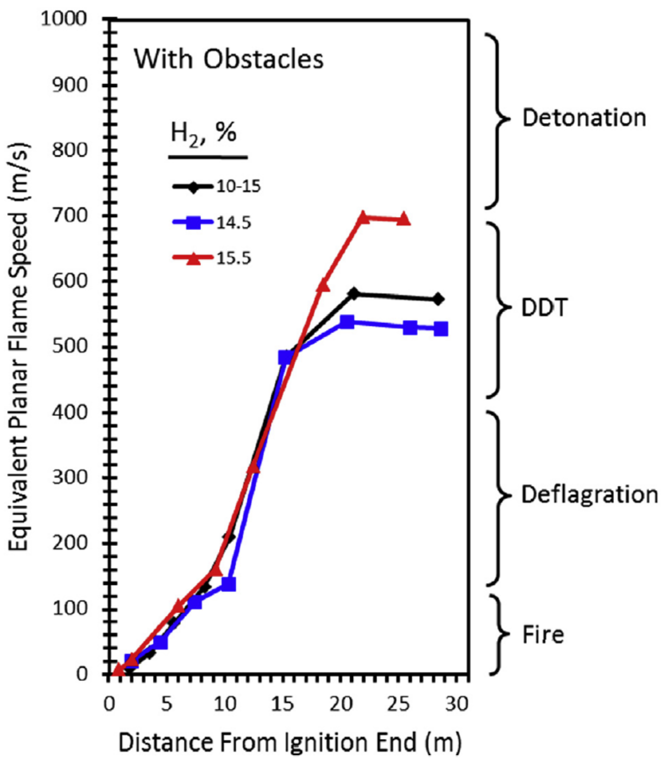

Figure 2.12: Detonation happens below the explosion limits(<18.3%) with obstacles, figure cited from [60] and data reported in [100].

Of equal importance, LH2 poses a significant risk of jet fire and explosion, especially due to its cryogenic temperature. The IDEALHY project [68, 32] conducted an analysis of hazardous incidents caused by LH2 leakage, as depicted in Figure 2.13. The project also included a qualitative analysis of LH2 transportation and supply through high-pressure pipelines [32]. O. Hansen [36] highlighted that the low temperature of LH2 could solidify oxygen and nitrogen in the air, with boiling and freezing temperatures of 90K and 54K for oxygen, 77K and 63K for nitrogen, respectively, leading to the formation of a condensed air phase with liquefied or solidified oxygen and nitrogen in the near-field area. Incident data and experiments reviewed by Jallais et al. [54] and Lyons et al. [69] confirm the hydrogen pool phenomenon, particularly in the case of significant, sudden LH2 releases. These hydrogen-oxygen enriched properties are known for their highly combustible nature. Kumamoto et al. [63] reported an MIE of only 0.0057mJ for 35% oxygen-enriched air with hydrogen.

On the other hand, the cryogenic nature of LH2 may cause hydrogen embrittlement in certain materials, such as ferritic steels, which can become brittle at low temperatures. However, austenitic steels and aluminum are not affected [60, 23]. In addition, studies have shown that the cryogenic jet flame may have a longer ignition distance, and a decrease in temperature can increase heat radiation and radiation fraction [87, 122]. A boiling liquid expanding vapor explosion (BLEVE) is defined as ”a physical explosion of a vessel containing a liquid at a temperature significantly higher than its boiling point at atmospheric pressure.”, which can result in a sudden depressurization and super-heated state of the liquid, causing an overpressure and fireball. Although BLEVEs are rare compared to other ignited events [110], LH2 also presents additional hazards such as cold plumes, pool fires, and a higher level of hazardous ignited behavior.

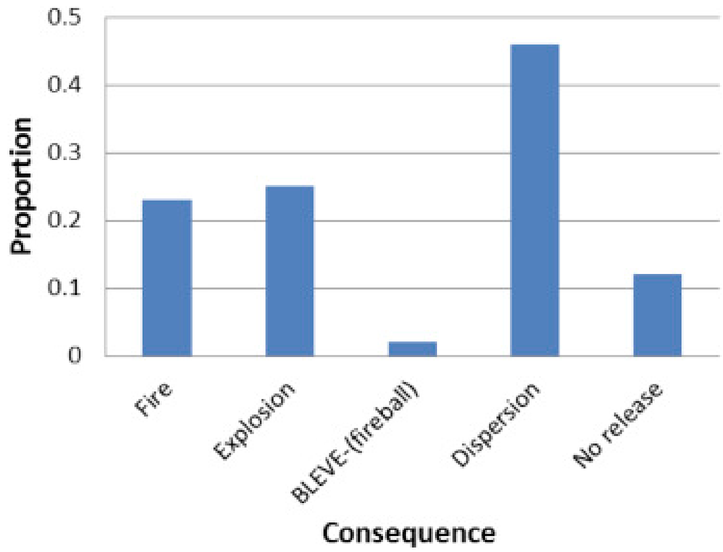

Figure 2.13: Proportion of each LH2 hazards from incidents [68].

2.2.3. Scenario selection

After identifying the hazards associated with hydrogen fueling stations, it is necessary to define and select accident scenarios. The selected scenarios and their corresponding consequences vary depending on the system configuration. For example, fueling stations for compressed hydrogen (CH2) and liquid hydrogen (LH2) have different system configurations, as shown in Figure 2.14, which leads to different considered components and scenarios [121]. Hydrogen leakage is reported as the main concern for accidents [119], and scenarios for causing hydrogen leakage should be defined. These scenarios are commonly divided into components of random leakage, and accidental ruptures [25, 35, 121, 3]. Components can become aged and fatigued after a long-term operation, leading to leakage when they reach their material limits. Conversely, large-scale ruptures due to accidents can result in an instant and significant leakage. The HyRAM model [25] provides an overview of accident scenarios, where random leakages can lead to hole sizes ranging from 0.01% to 10%, and catastrophic ruptures can result in 100% leakage. Aarskog et al. [3] also used this concept, but it was applied to a CH2 ferry. However, O. Hansen [35] suggests that catastrophic rupture is not a credible scenario in maritime operations due to its low frequency of occurrence, which is roughly 10^{-7} to 10^{-6} per year. Therefore, low-frequency high-consequence scenarios were not assessed. Instead, Yoo et al. [121] defined scenarios involving catastrophic rupture of main equipment and small or medium-scale random leaks from the dispenser. Additionally, a fault tree analysis (FTA) is an accepted method for identifying accident scenarios. Ehrhart et al. [25] also performed an FTA for random components and catastrophic rupture leakage.

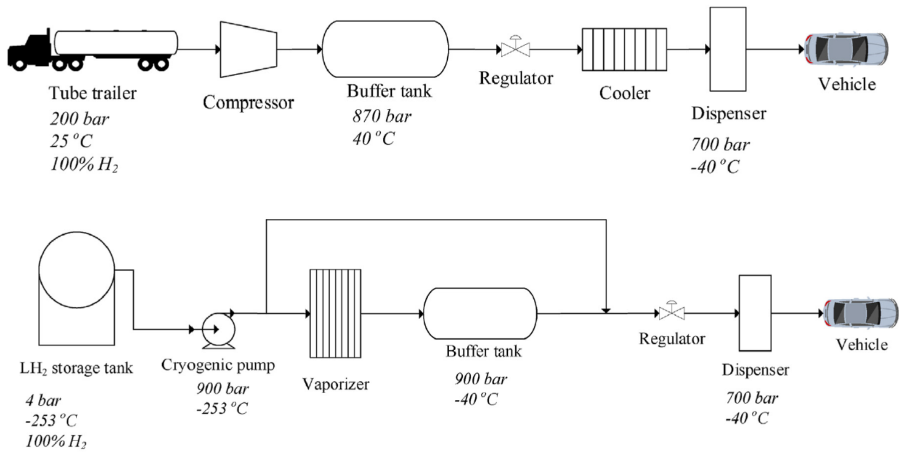

Figure 2.14: Examples of system configuration of CH2 and LH2 fueling stations [121], the component differences contribute to different scenarios.

Once the scenarios have been selected in the FTA diagram, they can be transcribed to an event tree analysis (ETA) that maps the corresponding consequences based on hazard identification. In the case of the CH2 system, HyRAM proposed an ETA that only considered jet fire and explosion consequences, as shown in Figure 2.15. To conduct a comprehensive risk assessment, the combination of FTA and ETA is commonly used in the form of a bow tie analysis (BT), which visualizes the causes and consequences of the scenarios. For instance, Figure 2.16 depicts the BT for the hydrogen generation unit. Bow tie analysis is a useful analytical tool for risk assessment that helps identify and manage potential hazards.

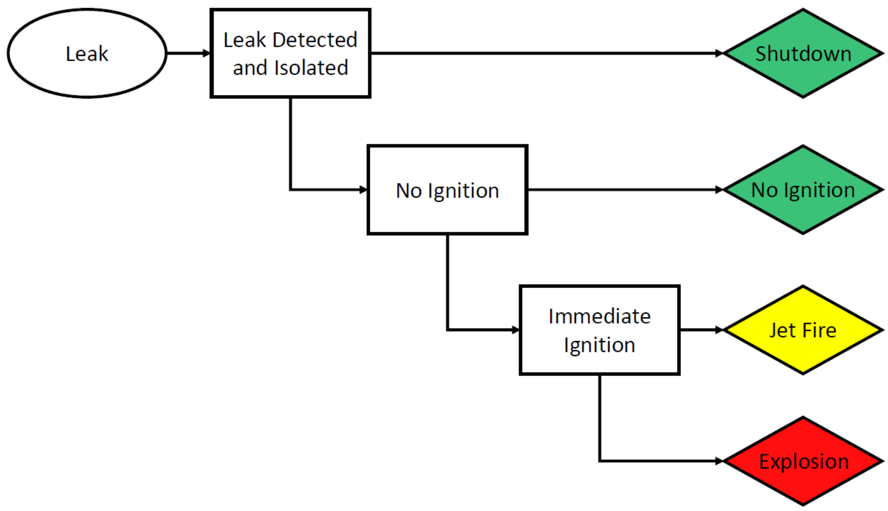

Figure 2.15: Event tree analysis of compressed hydrogen systems [25].

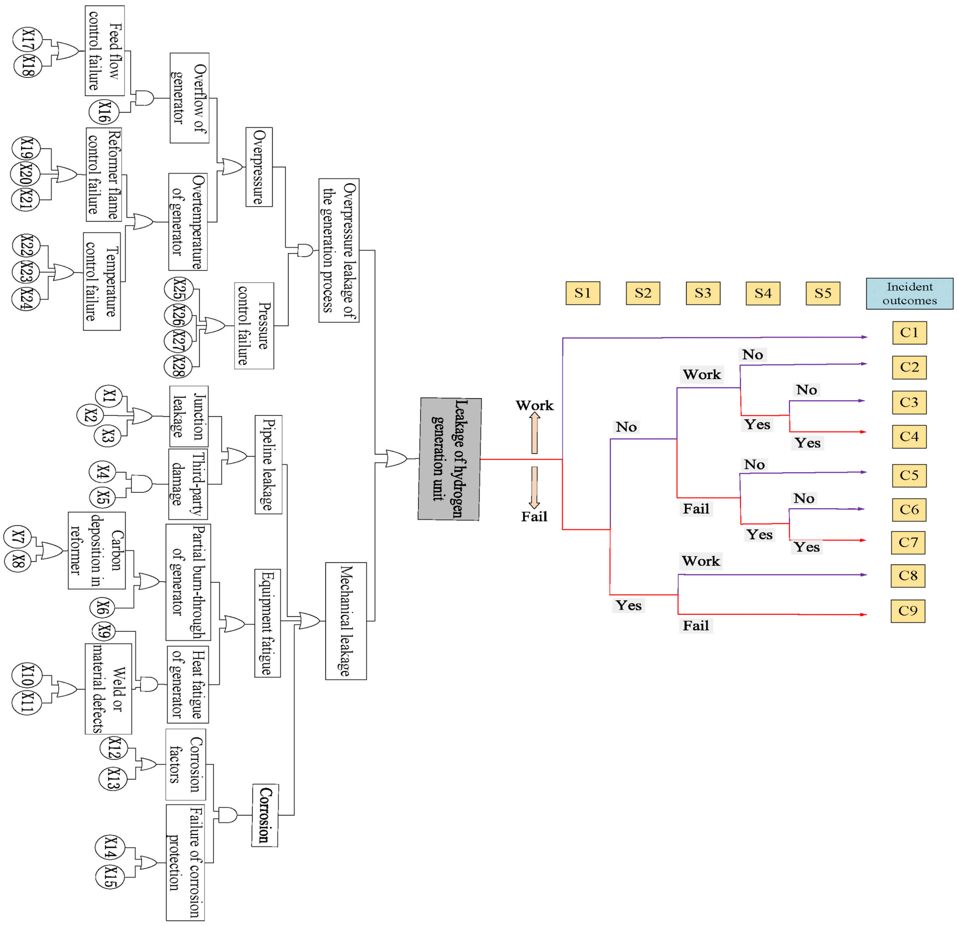

Figure 2.16: Bow tie diagram of the hydrogen generation process [14].

2.2.4. Frequency assessment

To perform a quantitative result in the QRA process, each leakage scenario corresponds to a specific frequency, such as leakage frequency per year, failure rate, and accidental rupture frequency. The most common CH2 random leakage frequencies were derived by Lachance et al. [55]. The author implemented the Bayesian method for updating the leakage of the component's frequency data from chemical processing, compressed gas, nuclear power plant, and offshore petroleum industries. The given frequencies assumed that the mean leak frequency of any component is linearly related to the logarithm of the fractional area of the leak. These data were applied in the risk study in [25, 35, 121, 3]. Figure 2.17 shows the distribution of leak frequency for each component in HyRAM [25], where the geometric mean value was used for frequency assessment. Additionally, data investigated by HSE [38, 102], Uijt de Haag and Ale [86], and DNV offshore reliability data handbook (OREDA) [88] show failure rate or frequency for different failure modes and components but are not specific to hydrogen nor covering wide-range of leakage holes.

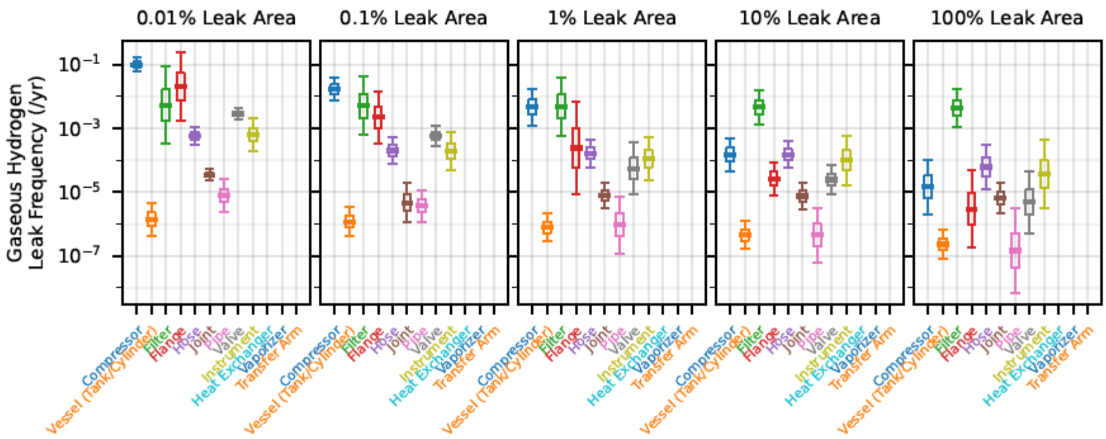

Figure 2.17: Compressed hydrogen leak frequency listed in HyRAM [25].

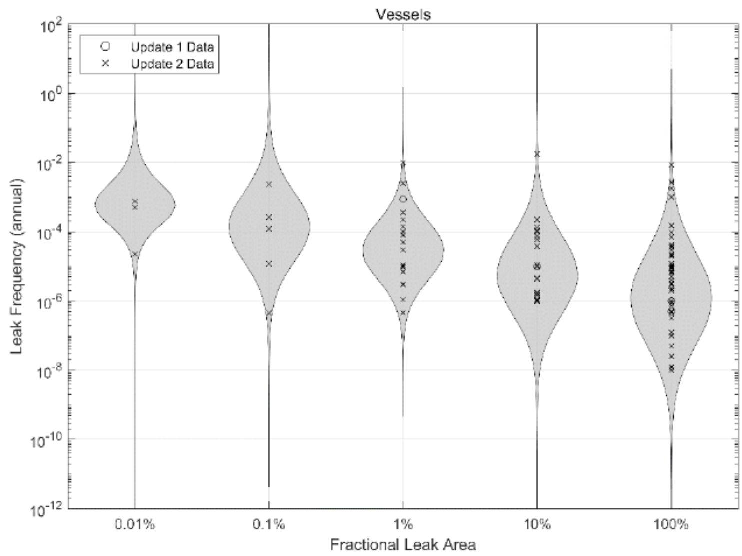

Figure 2.18: Liquid hydrogen leak frequency of the vessel [20].

In addition to CH2, the unique cryogenic and permeating characteristics of LH2 can cause its leakage frequencies to differ from the proposed frequencies. Brooks et al. [20] collected data from both CH2 and LNG systems and used Bayesian analysis to propose leakage frequencies for LH2 components. Due to the characteristics of LH2 falling between CH2 and LNG, Bayes' theory can update existing data to obtain expected values for the LH2 system. Figure 2.18 illustrates the LH2 leak frequencies under the assumption of a normal distribution of the log-leak frequency for each fractional leak area. This estimation shows a similar trend of decreasing frequency with increasing leak size.

Catastrophic rupture is another factor causing hydrogen leakage, and it is commonly assumed that the event would lead to large-scale leakage [25, 121, 3]. Based on Uijt de Haag and Ale [86] and HSE [38] guidelines, the recommended rupture frequencies for different components were advised, in the scale of 10^{-7} to 10^{-6} per year. Collecting from the incident data, these values were applied in the risk studies mentioned above.

2.2.5. Probability assessment

A few ignition probability models have been suggested to assess the hydrogen risk quantitatively. Tchouvelev et al. [107] proposed the ignition probability for hydrogen based on the ignition probability data of methane. The author compared the flammable cloud volume, MIE, and the flammable limits of the two substances, resulting in a higher ignition probability of hydrogen. In addition, the probability of immediate and delayed ignition is set to be 2:1 as reported in DNV historical ignition probability data [107]. Figure 2.19 provides the ignition probability of hydrogen investigated by Tchouvelev et al. [107], which is widely used in most hydrogen risk studies such as HyRAM [25]. However, in 2021, Aarskog et al. [3] pointed out that the given step function did not consider gas accumulation by confinement or congestion. An updated model is shown in fig 2.19. It was also compared with the ignition probability of methane from OGP [82], which assumed the ignition probability would increase with hydrogen accumulation. The immediate and delayed ignition ”remained unchanged at a ratio of 2:1.

Other probability studies have been found from The Guidelines for Quantitative Risk Assessment, also known as the ”Purple book” [86], and the IDEALHY project [32] are among the sources that provided ignition probabilities for different types of sources and substances. The Purple book proposed a direct ignition probability of 0.2 for stationary installations with a leakage rate lower than $10kg/s$ for highly reactive gases, with a subsequent 40% and 60% probability for explosion and flash fire, respectively. These probabilities were employed in studies by Li et al. [123, 124]. However, the definitions of ”large-scale release” and ”high reactive gas” were not clearly defined in this model.

The IDEALHY project proposed ignition probabilities based on a review of LH2 incidents from road transportation and storage/liquefaction activities. The model suggests a 100% ignition probability for large and confined releases and a 50% probability for releases to the atmosphere. However, the definitions of ”large-scale release” and ”confined release” were also unclear in this model. Moreover, both models do not consider the probability of delayed ignition or the consequences of immediate ignition, such as flash fires.

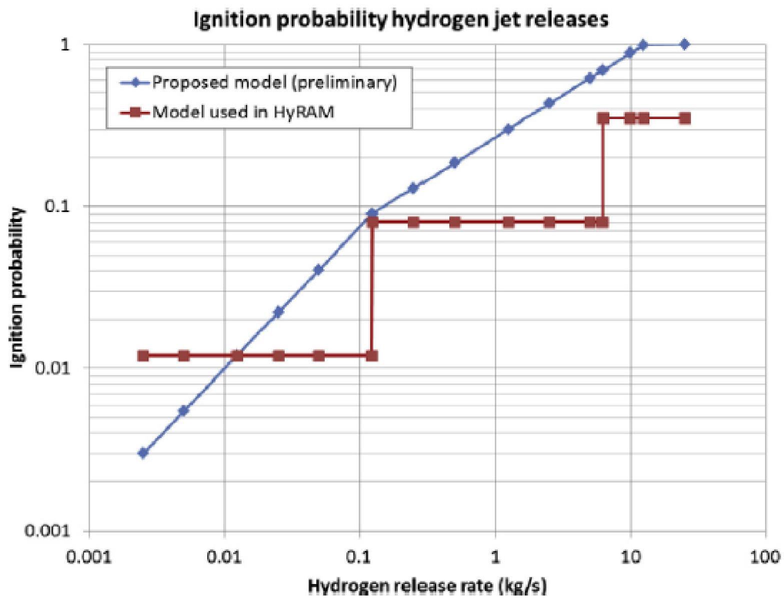

Figure 2.19: Proposed ignition probability from Aarskog et al. [3] and HyRAM [35].

2.2.6. Consequence modelling

In this subsection, the experimental and numerical methods that have been used in the existing literature to predict the consequences of hydrogen leakage scenarios will be presented. While there has been extensive research on CH2 consequences, there is a lack of literature that precisely simulates the consequences of LH2. Therefore, we will also review some experimental reports and relevant numerical studies of LH2 to understand the progress and research gaps in this field. Specifically, we will review both experimental and CFD consequence models of fires and explosions for CH2 and discuss the limitations of existing models.

Compressed Hydrogen

In the early stage of CH2 consequence modeling, mathematical models were interpolated from the existing experimental data. For instance, Kikukawa et al. [59] estimated the blast pressure and jet flame length employing extrapolating from the experimental data of Okabayashi et al. [105], and Takeno et al. [106]. The blast pressure was then presented as a function of leak size and propagated distance. At the same time, the flame length was derived proportional to the initial pressure and leak size. On the other hand, distinguished from jet fires, the fireball consequence under the scenario of storage tank failure in a fire was presented by Dadashzadeh et al. [21]. This consequence was predicted using the validated mathematical model from Hord J. [44] and scaled from the experiment data from Weyandt NC. [79]. The blast wave from the explosion was also modeled in this study by Molkov et al. [76, 99], where the over-pressure and distance were derived as functions of tank pressure and volume.

The literature has progressed from experimental data interpolation to the consolidation and validation of mathematical models for hydrogen fires and dispersion behaviors. NFPA-2 [80] incorporated data from previous hydrogen experiments and studies [47, 46] to propose mathematical models for unignited and ignited events, presenting results for different leak sizes, initial pressure, concentration, and heat radiation, as can be seen in Figure 2.20. These models were implemented in Lloyd's Register screening tool, which was used by O. Hansen [35] and Aarskog et al. [3] for consequence modeling. While Yoo et al. [121] modeled the heat radiation and overpressure from explosions for both CH2 and LH2 refueling stations, the theory applied was for the flash fire [26] and confined explosion [91], which may not apply to all scenarios. Moreover, the consequences of LH2 were not thoroughly considered, and factors such as different leakage frequencies and additional consequences, including cold plumes and pool fires, should be updated in the model.

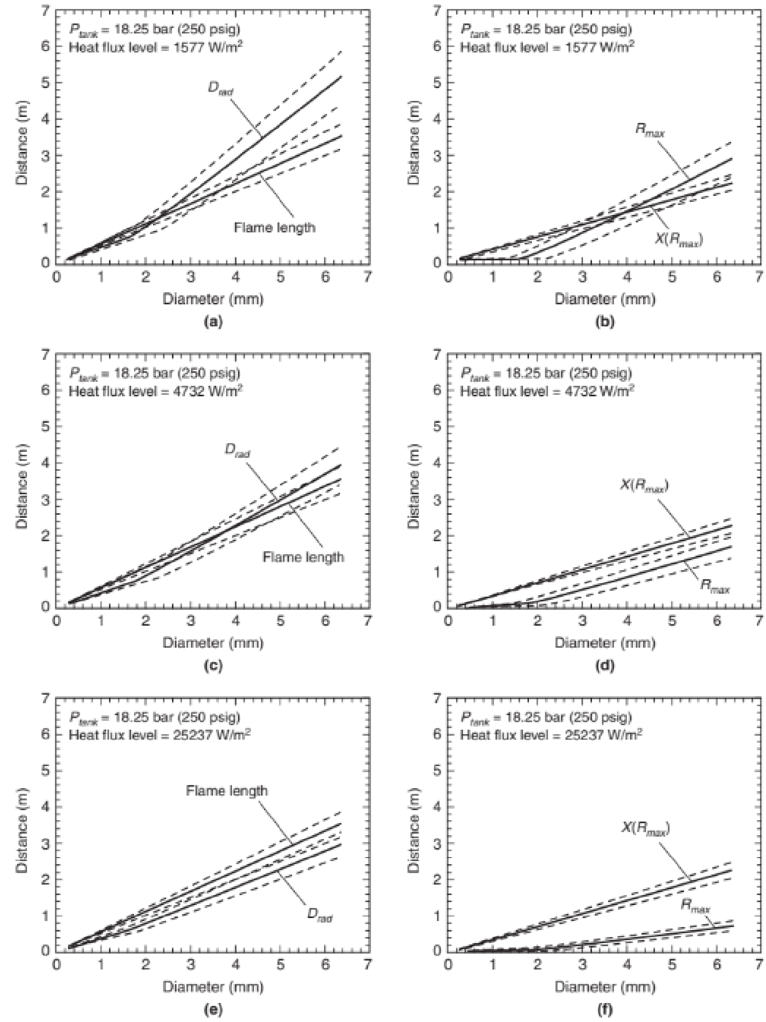

Figure 2.20: Simulation of heat radiation distance for ignited hydrogen [80].

Explosions are considered the most severe hazard among all hydrogen consequences. Therefore, several explosion behavior models have been suggested in the literature. One of the widely used methods is the TNO-Multienergy method [112], which investigated a series of blast pressure load models for different substances with combustion strengths ranging from 1-10. Hydrogen has extremely high combustion energy and was assigned a strength of ten in the literature [3]. Another method for estimating the blast pressure is the Baker-Strehlow-Tang (BST) method proposed by Baker et al. [8], which presents the blast pressure as a function of the Mach number. A suggested matrix for determining the blast pressure by the Mach number was also provided. To evaluate the accuracy of blast pressure estimation, Mélani et al. [72] reviewed the TNO-Multienergy and BST methods with a few experimental results of a hydrogen explosion. The review showed that the TNO-Multienergy method has a better prediction performance than the BST method. However, the accuracy of the TNO-Multienergy method is highly dependent on the strength number, and the literature proposed a guideline for determining the hydrogen strength number.

Alternatively, some CFD calculations are applied to predict hydrogen dispersion and overpressure from the explosion. In light of the simplicity of the TNO-Multienergy model, O. Hansen [34] conducted a series of FLACS CFD calculations to predict the blast wave over-pressure. Furthermore, the simulated results were compared with the TNO-Multienergy method and experimental data for validation, as shown in Figure 2.21. The results are reasonably similar to the experimental data but under-predicted the far-field pressure in test 4 of the HSE experiment. Aiming to solve the under-prediction issue, a significant improvement in predicting the far-field blast has been derived by implementing the DDT phenomenon in the model [33].

In contrast, HyRAM [25] does not directly consider the hazards of heat radiation or overpressure. Instead, it translates these consequences into fatality models for jet fires and blast waves. The fatality probability can then be calculated by substituting the results into a Gaussian distribution. This approach simplifies the consequence analysis process and efficiently computes the risk of hydrogen accidents. However, it should be noted that this method may only capture some aspects of the consequences of hydrogen accidents and may underestimate the risks in some scenarios. Further research and validation are needed to ensure the accuracy and reliability of this approach.

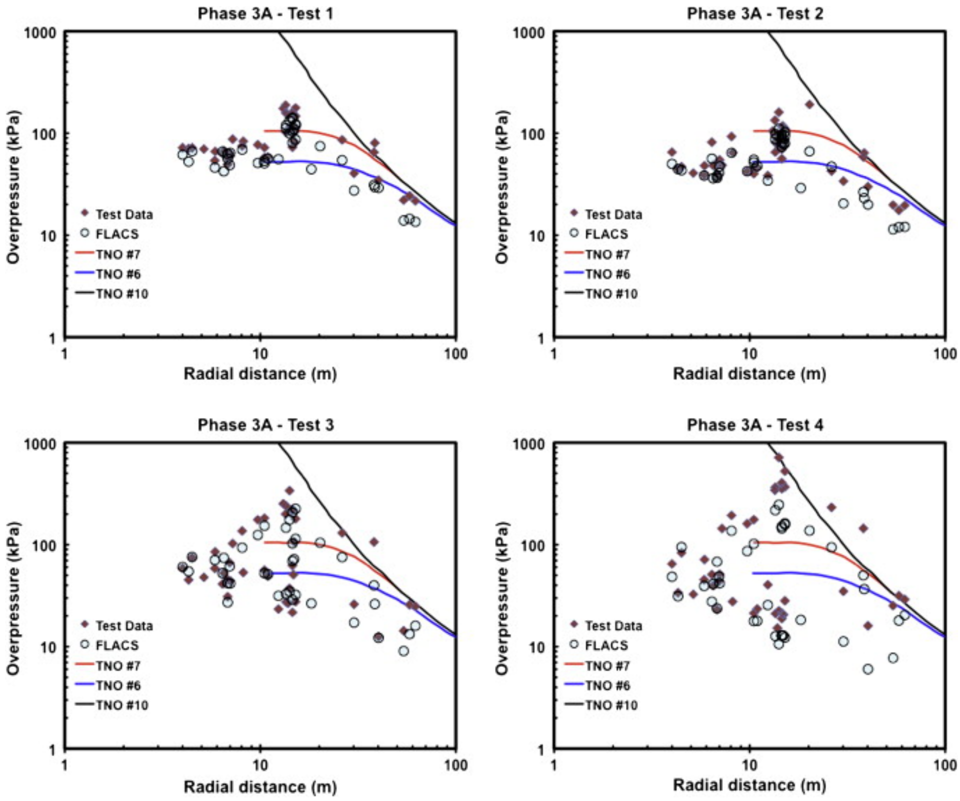

Figure 2.21: FLACS simulation against experiment data and TNO-Multienergy method [34].

Liquid Hydrogen

There is a limited body of literature regarding the risk assessment of LH2. Only a few studies have investigated the risk associated with LH2, including those conducted by Kikukawa et al. [58] and Yoo et al. [121] in the early stages, and Klebanoff et al. [60], who provided a qualitative comparison with the LNG system. However, KIKUKAWA et al.'s [58] modeling approach lacked validation, and Yoo et al. [121] used the same methods for modeling both LH2 and CH2 consequences. Therefore, further experimental studies on LH2 and related literature, such as CFD and mathematical assessment, are also reviewed to fill the knowledge gaps.

- **Large scale experiment**

  Most of the literature on LH2 risk assessment is based on laboratory-scale spilling tests, with only a few large-scale experiments performed. The first unignited LH2 tests with a 1500-gallon (5678L) spill were conducted by NASA [116], with an average spill time of 30 seconds. The flammable cloud was found to travel beyond 50 meters, with a cloud rise rate of 0.5-1.0 m/s in test 6. HSE also conducted experiments for both unignited [98] and ignited scenarios [31], with a flow rate of 60 liters per minute. The unignited behavior was consistent with the NASA experiment, where the dispersion phenomenon was significantly influenced by wind speed. The ignited experiments used a 1kJ source to ignite the hydrogen-air mixture. The ignition failed in test 7, where the wind speed was too low to disperse the hydrogen cloud. The results showed that the buoyancy effect dominated the cloud dispersion effect. In test 6, a second explosion was observed when the flame was overpressured to the release point, possibly due to the oxygen-enriched air from the solid or the immediate mixture of LH2 and solidified air. The experiment also included ignition in the pool. Still, only a small visible flame was observed due to the weak igniting source of 1J. Therefore, experimental studies on LH2, CFD, and mathematical assessments are essential to accurately assess the risk of LH2 spilling.

To perform more precise scenarios in terms of outdoor bunkering leakage and indoor tank connection space (TCS) release, the Norwegian Defence Research Establishment (FFI) [56] conducted a series of release experiments for different flow rates, unignited or ignited consequences, and outdoor or confined space releases. The outdoor leakage experiment with a release rate of 9.7 to 49.9 kg/min showed that horizontal releases dispersed the hydrogen to a farther distance, whereas downward releases resulted in pool generation and higher heat radiation when ignited. In the closed room release with a ventilation mast at a release rate from 11 to 40.1 kg/min, the hydrogen concentration near 100% was built up in 30 seconds, and the hydrogen did not disperse horizontally outside the ventilation mast. Figure 2.22 shows the result of outdoor release test 4, indicating that even at a leakage rate of $0.828kg/s$ horizontally, no LH2 pool was formed. The temperature of LH2 pool presence is also shown here for comparison.

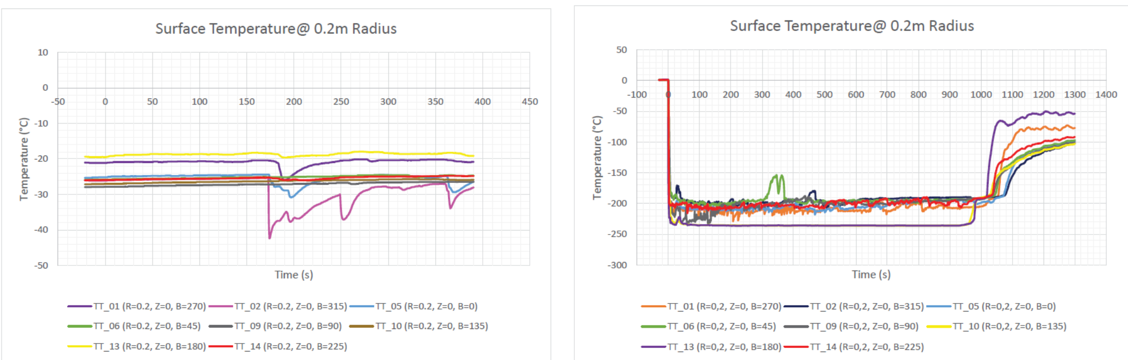

Figure 2.22: Measured temperature of test 4 on the ground showed no LH2 pool presence (left), while the temperature of test 3 with LH2 pool (right) [56].

- **Physical approach**

Numerous researchers have investigated circular nozzle experiments to model flame characteristics, including heat radiation and flame length, as a function of various parameters. Figure 2.23 and 2.23 show the investigation from Friedrich et al. [1] by conducting LH2 leakage from the round orifice at temperatures of 35-65K and pressures of 0.7-3.5MPA, the scaling function for hydrogen concentration, thermal radiation, and flame length have been established. In Hecht and Panda [41] study, the unignited LH2 dispersion behavior was observed via Raman scattering images. The proposed model of the decay behaviors showed similarities with the experimental data. The empirical formulation of 1% hydrogen concentration distance was derived and validated by Kobayashi et al. [61]. It was also confirmed that the hydrogen leakage rate increases as the temperature decreases, and an investigation of flow coefficients for different tank configurations were also reported. Other experimental studies for flame characteristics such as Panda and Hecht [87] carried out that the jet flame length is linearly dependent on the square root of the jet Reynold number, and the cryogenic would increase the radiative heat flux compared to the room temperature jet. Panda and Hecht [87] also observed that the average ignition mole fraction is 0.14 (hydrogen-air).

Furthermore, Yu et al. found that flame size is not only dependent on flow rate but also on stagnation pressure and temperature. Therefore, they formulated a correlation between flame length and width, given by Equations 2.2 and 2.3, respectively. Moreover, in light of the radiation fraction, Yu et al. established a correlation model to predict heat radiation as a function of parameters such as stagnation pressure and temperature. This model advances previous models by Molina et al. and Panda and Hecht, which were not applicable under certain conditions.

$$\frac{L_f}{d_j} = 530 * {P_0}^{0.43} * (\frac{T_{atm}}{T_0})^{0.35} \tag{2.2}$$

$$\frac{W_f}{d_j} = 95 * {P_0}^{0.43} * (\frac{T_{atm}}{T_0})^{0.35} \tag{2.3}$$

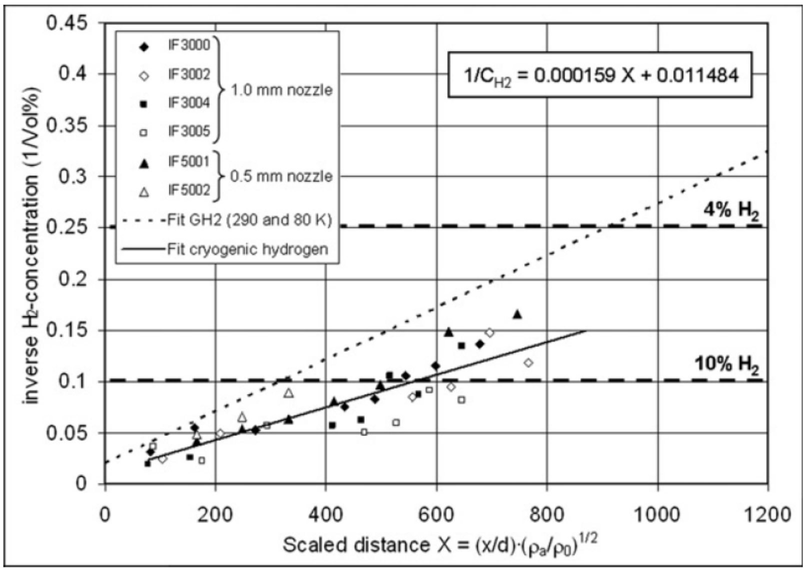

Figure 2.23: Concentration against scaled distance from the experiment [1].

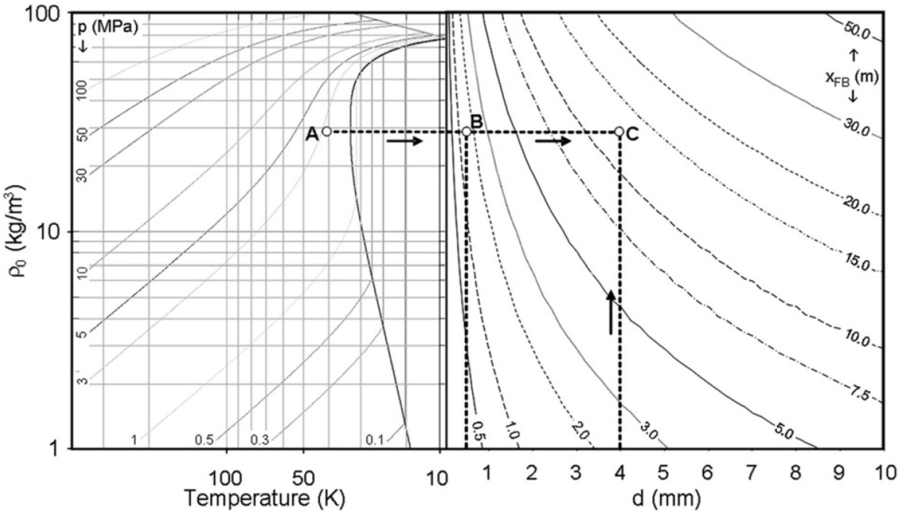

Figure 2.24: Maximum ignition distances prediction against diameter and initial conditions [1].

In addition to circular nozzles, some researchers have also investigated the flame characteristics of high-aspect-ratio-shaped releases, which are more representative of real-life situations. Chowdhury and Hecht [18] and Hecht et al. [40] conducted experiments on ignited LH2 releases with aspect ratios ranging from 2 to 64. Surprisingly, the results showed that aspect ratio did not significantly influence flame length or heat radiation. Chowdhury and Hecht also suggested that using a round tube would accurately represent different release geometries, indicating that further investigation into the effect of aspect ratio on flame behavior may not be necessary.

The occurrence of hydrogen pool and pool fire is typically associated with large-scale leakage, which is often the result of continuous high-flow rate leakage or catastrophic instant rupture. D. Little Inc. [66] developed hydrogen pool fire models for rapid and continuous release based on aircraft accident data, with the pool diameter being a function of the leakage rate. Figure 2.25 shows the fitting curve for these models. Additionally, a CFD calculation code LAuV was investigated and found to be in good agreement with an LH2 spill experiment conducted by the Federal Institute for Materials Research and Testing (BAM), predicting a pool diameter and duration of 20m and 13s for a $40m^3$ instant release [113]. Holborn et al. [43] also performed a FLACS CFD simulation. Although the dispersion results showed a significant difference from experimental data, the predicted pool size estimates were consistent with the observed data, with a steady-state evaporation rate of $0.22kg/m^2/s$ for pooling on a concrete surface. Figure 2.26 shows the predicted pool diameter. Following the accumulation of the LH2 pool, M. Afzali [5] compared existing evaporation models and found that the GASP model had the best agreement with the experimental data.

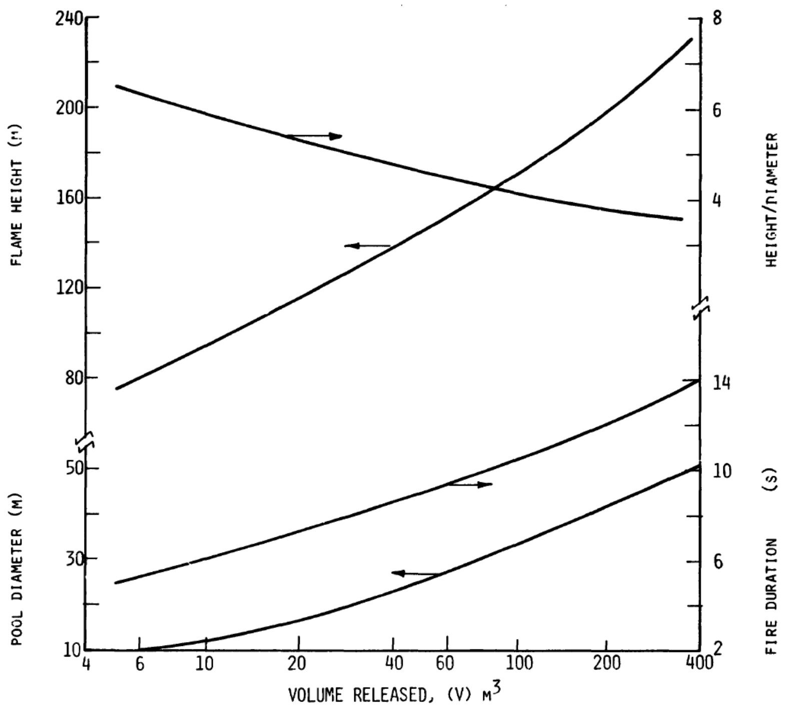

Figure 2.25: Predicted pool diameter and pool flame height for an instantaneous LH2 release [66].

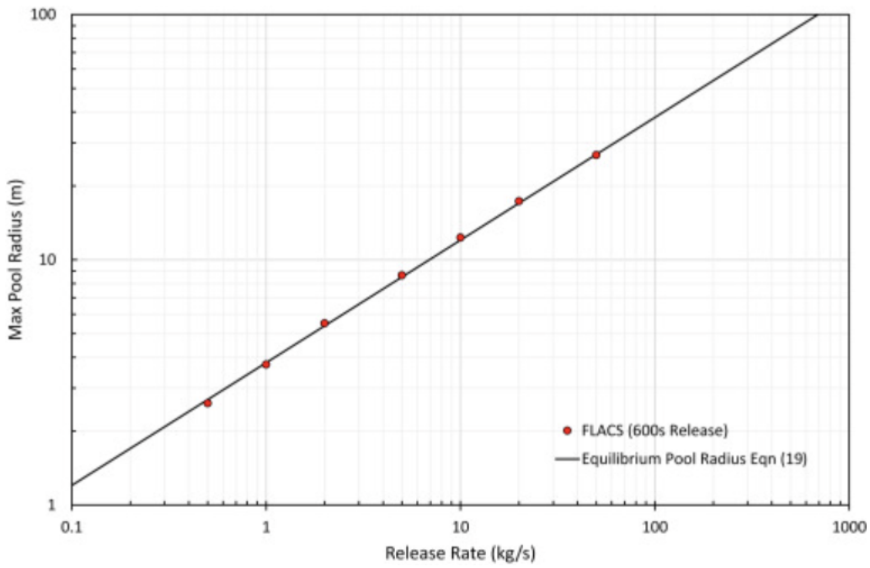

Figure 2.26: Predicted pool diameter against spill rate[43].

Cold plumes and BLEVE are additional consequences of LH2 leakage. However, the majority of hydrogen risk literature neglects these behaviors due to their lower harmful effects and low likelihood, respectively. The cold plume is an unignited release of LH2, where the cryogenic hydrogen rapidly decreases the ambient temperature. Although only one published study has simulated the cold plume behavior, Li et al. [65] have modeled the safe distance of the LH2 cryogenic cloud. The results show that the harmful distance of the cold cloud extends farther than that of the fireball in catastrophic releases, with a threshold of -313K. Although the study does not describe the modeling approach, the result provides insight into the potential harm of the cold cloud, as shown in Figure 2.27.

BLEVE, as mentioned in Section 2.2.2, is considered a consequence of tank failure, which only occurs when external fire increases the pressure inside the tank. Ustolin et al. [110, 109] reviewed empirical models of BLEVE behavior, comparing them with experimental data obtained from the BMW test. The authors also proposed the most probable model to assess BLEVE behavior. Although existing models do not accurately predict the consequence, they do agree with the experimental data's overall trend. However, more experimental data is needed to reduce the uncertainties in consequence prediction.

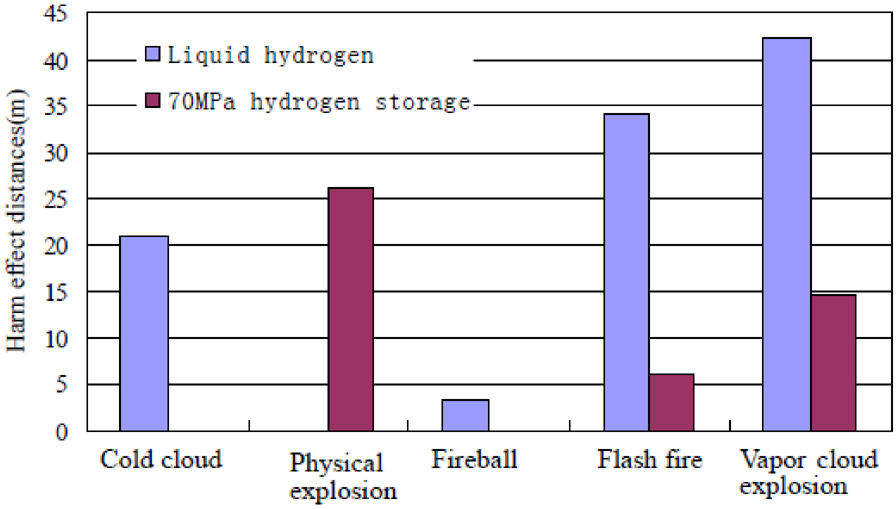

Figure 2.27: Prediction of LH2 catastrophic rupture consequences [65].

- **Numerical approach**

Regarding numerical approaches, only a few CFD studies have been conducted to compare with the aforementioned experimental results. One study focused on predicting the LFL distance of dense LH2 gas dispersion, which was found to be significantly larger than that of LNG [36]. Holborn et al. [43] and Statharas et al. [103] also conducted numerical simulations to predict LH2 dispersion behavior and compared their results with NASA and BAM experiments. While their numerical results showed general agreement with the experimental data, some differences were still apparent. Both spill rate and wind speed are critical factors that influence LH2 dispersion behavior. Liu et al. [67] developed a numerical and mathematical model to predict the safety distance. They formulated a correlation between spill rate, wind speed, and safety distance, as shown in equation 2.4 and figure 2.28.

$$L = \dot{m}^a (b{U_0}^2 + c\dot{m}^d U_0 + e) \;\; ; \;\; \dot{m} = spill \;\; rate \;\; ; \;\; U_0 = wind \;\; speed \tag{2.4}$$

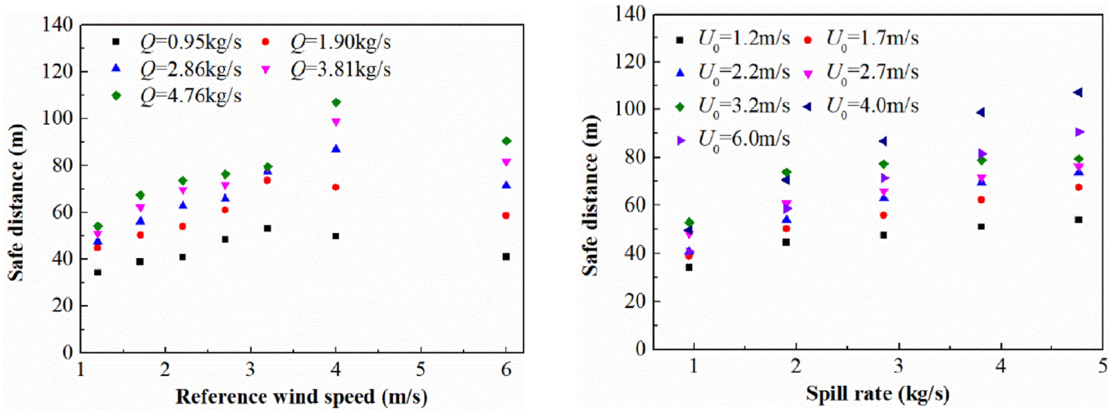

Figure 2.28: Safe distance against wind speed (left) and spill rate (right) [67].

2.2.7. Risk evaluation& assessment

Risk evaluation is an important step in the risk assessment process, which involves multiplying the probabilities of an event occurring with the consequences that would result. However, to determine whether a particular risk is acceptable or not, it is essential to compare the resulting risk value with established standards or thresholds. In section 2.2.6, the consequences of potential hazards such as fires and explosions are estimated by evaluating heat radiation, flame length, and overpressure. The release of LH2 also presents an additional hazard of cryogenic temperature. In some studies, risk has been presented in terms of safety distance, which is the maximum distance at which harm can occur [49]. In hydrogen risk studies, thresholds for safety have been established and applied.

In the case of a jet fire, the most common threshold for causing 100% lethality is a heat radiation level of $37.5kW/m^2$ within a minute, as per the guidelines provided by International Association Oil & Gas Producers (OGP) [82], EUROPEAN INDUSTRIAL GASES ASSOCIATION AISBL [49], and DMI [24]. Some lethality models based on thermal dose, which consider exposure time and heat radiation, have also been formulated. For example, TNO Purple book [86] and other researchers [25] have provided formulas in the form of $P_r = a + 2.56 * ln(Q^(4/3) * t)$, where the parameter 'a' can be adjusted based on the indoor or outdoor conditions.

As a result, A fatality threshold of $37.5kW/m^2$ has been widely used in studies such as [3, 121, 75], while a value of $12.5kW/m^2$ has been associated with a 1% lethality rate. For pool and flash fires, which involve radiation fractions that cause less harm [66], the fatality criteria is often based on flame envelope or the lower flammability limit (LFL) distance (4% concentration) [75, 124]. However, the literature suggests different threshold values for the LFL zone: Mohammadfam and Zarei [75] reported that the 1/2 LFL zone causes inhalation effects, while O. Hansen [35] found that a 4% concentration only results in upward flame propagation until it reaches 8%, when the flame can burn sideways and downwards. A summary of fire-related criteria is presented in Tables 2.3 and 2.4. Meanwhile, the safety distance for fire events is suggested to be $9.5kW/m^2$ and the LFL zone [65].

Table 2.3: Thresholds for jet fire, data collected from [3, 75, 82, 24].

Heat radiation, kW/m^2	Damage	Fatality
4	First-degree burns after 20 s	0%
12.5	Sufficient energy to induce ignition on wood and plastic	1%
37.5	Equipment and equipment damage	100%

Table 2.4: Thresholds for flash fire and pool fire, data collected from [75, 82, 24, 124].

Criteria	Damage	Fatality
1/2LFL	Inhalation effects	0%[75]
LFL	Imminent death, only burn upwards	100% [124][75]
2 LFL	Imminent death, be able to burn sideways and downwards	100%[35]

Several studies have proposed criteria for explosion-induced overpressure. For instance, the Oil and Gas Producers (OGP) carried out the lethality probability for explosive overpressure for onshore and offshore applications [82]. For personnel in the offshore module, a 100% lethality would be induced by only 0.2-0.3 bar over-pressures, which is much lower than the onshore outdoor application. According to Glasstone and Dolan [28], a 0.2 bar of over-pressure would cause serious injuries, and Aarskog et al. [3] proposed a 10% fatality rate. In contrast, Mohammadfam and Zarei [75] proposed a 5% fatality rate for 0.17 over-pressure. Moreover, most people will be killed when exposed to a 10 psi (0.69 bar) over-pressure [28]. Therefore, Mohammadfam and Zarei [75] proposed 100% lethality for 0.83 bar over-pressure, while Yoo et al. [121] proposed 1.38 bar over-pressure to cause 100% death. However, except for OGP, none of these studies considered the problem of open or confined spaces. For instance, Li et al. [124] assumed that 0.3 bar over-pressure would result in 100% lethality, which is probably under the assumption of an indoor explosion. Regarding the cold cloud event for LH2, its lethality is omitted from the guidelines and relevant studies due to a lack of data on how the human body reacts to extremely low temperatures. Only a safe distance of $-40°C$ has been mentioned for cold cloud events by Li et al. [65].

Table 2.5: Thresholds for over-pressure, data collected from [28].

Over-pressure (bar)	Description
0.07	Light injuries from fragments occur
0.14	People injured by flying glass and debris
0.21	Serious injuries are common, fatalities may occur
0.34	Injuries are universal, fatalities are widespread
0.69	Most people are killed
1.38	Fatalities approach 100%

Once the vulnerability thresholds have been determined, the risks can be quantified in terms of fatality rate, which is calculated as the frequency of an incident occurring multiplied by the probability of the fatality rate, and then multiplied by the number of fatalities that occurred within a specified boundary. The fatality rate can be classified into individual risk (IR) and societal risk (SR). IR is defined as the risk to a person in the proximity of a hazard [15], and is calculated as follows: $IR_{x,y} = \Sigma IR_{x,y,i}$, where $IR_{x,y,i}$ is the outcome from incident case i, f_i is the frequency of incident outcome i, and $p_{f,i}$ represents the probability that incident outcome case i will result in a fatality at location x,y.

On the other hand, society risk (SR), by definition, is the risk to a group of people [15]. A frequent measure of SR is the Frequency-Number (FN) curve, which can be presented as equation (2.5). Where F_N stands for the frequency of all incident outcome cases affecting N or more people per year, while F_i is the frequency of incident outcome case i per year, and N_i represents the number of fatalities from incident outcome case i.

$$F_N = \Sigma F_i \;\; for \;\; all \;\; outcome \;\; cases \;\; i \;\; for \;\; which \;\; N_i >= N \tag{2.5}$$

Various criteria based on individual or societal risks have been proposed to determine the acceptability of risk. The Risk Acceptance Criteria for Hydrogen Refueling Stations, as outlined in Norsk Hydro [6] and Haugom [37], states that the Individual Risk (IR) should not exceed 10^{-4} per year for both first-party and second-party risks. For third-party Societal Risk (SR), the Dutch VROM criteria suggest that the risk should be lower than the acceptable F-N curve, which is expressed as $F = 10^{-3}N^{-2}$ per year, where F represents the fatality rate and N is the number of fatalities. Figure 2.29 depicts the ALARP area (As Low As Reasonably Practicable) as the area between the risk acceptance curve and the lower line. The HSE R2P2 [39] proposes that the tolerable limits for workers and the public should be 10^{-3} per annum and 10^{-4} per annum, respectively. Additionally, Aarskog et al. [3] suggest that vessels utilizing new technologies should have a safety level of no more than 1.0 fatality per 10^{9} passenger km.

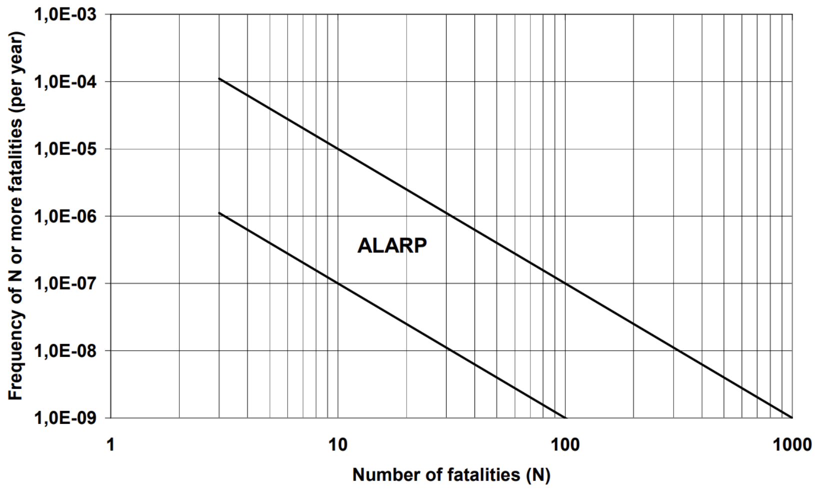

Figure 2.29: Society risk criteria [37].

Table 2.6 summarizes the safety criteria suggested by various studies, including the Risk Acceptance Criteria for Hydrogen Refueling Stations [6, 37] that has been widely implemented [121, 75, 124]. Individual risk (IR) is commonly presented as a contour map, as shown in Figure 2.30 adopted by Li et al. [124]. On the other hand, societal risk (SR) is generally compared to the ALARP area, as shown in Figure 2.31 [75]. In maritime applications, Aarskog [3] converted the safety level of 1.0 fatality per 10^{9} passenger km into an IR of 7×10^{-5} per year for people working 30 hours per week based on the ferry's operation profile. This safety level is 1.4 times stricter than that proposed by [6] and [37].

Table 2.6: Risk criteria.

Criteria	Reference	Fatality Rate(Probability/year)
IR	[6][37]	10^{-4}
	[39]	$10^{-3}$for workers, 10^{-4} for the public
	[3]	1.0 fatality per 10^{9} passenger km
Criteria	**Reference**	**Fatality Rate(numbers/year)**
SR	[6][37]	Lower than $F = 10^{-3}N^{-2}$

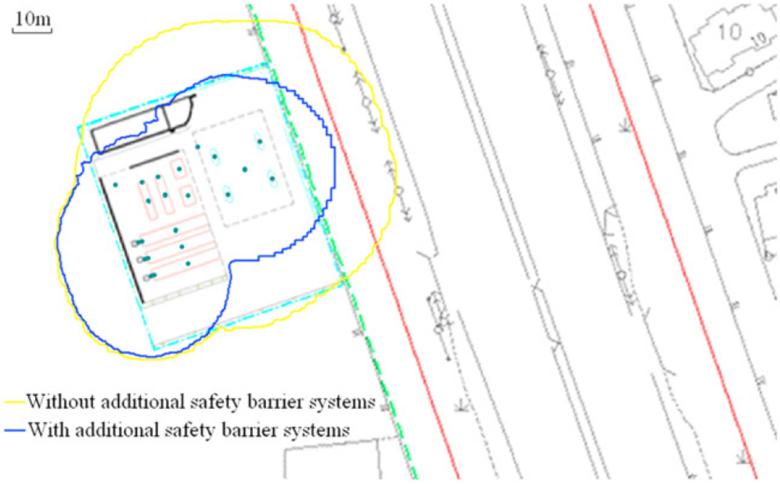

Figure 2.30: Individual risk contours of 10^{-6} per year [124].

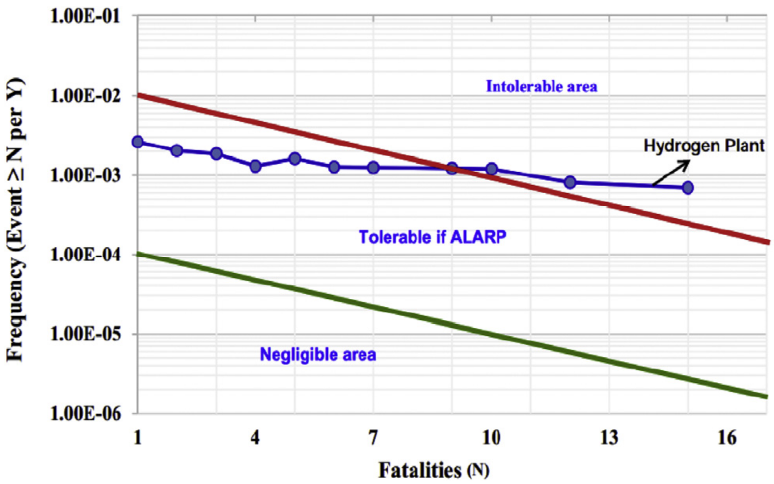

Figure 2.31: Society risk in comparison with ALARP area [75].

2.3. Conclusion of the literature review

The majority of research on quantitative risk analysis (QRA) for hydrogen has focused on onshore applications, such as refueling stations. Only a limited number of studies have addressed the risks associated with maritime propulsion systems, as summarized in Table 2.7. A comprehensive QRA is necessary at the design stage of any innovative hydrogen system to ensure that it meets the same safety standards as existing designs. While [3, 35, 77] have quantitatively assessed the risks of hydrogen-based propulsion in maritime applications, there remains a critical need for the development of a QRA tool specifically designed for such systems.

To enable longer distance missions, compressed hydrogen-based propulsion systems are no longer a viable option due to their low volumetric power density. Instead, liquid hydrogen-based propulsion systems are being considered as a more future-proof solution. However, the related risk of LH2 propulsion systems has not been robustly assessed, nor has its feasibility been evaluated for maritime applications. Qualitative risk assessments of LH2-based solutions have been conducted by [60] and [77], but their results do not meet the proposed regulations of the International Maritime Organization (IMO) [50].

The QRA process for hydrogen systems has been reviewed, and the lack of information and historical data on hydrogen has raised concerns about the correctness and accuracy of the analysis, as noted by [3] and [123]. The major uncertainties in the assessment are likely to lie in the frequency and consequence assessments. In consequence assessment, for instance, ignition probability models for CH2 were derived from the physical differences with methane by [3] and [107]. However, there is no existing ignition model for LH2, which is known to result in a higher combustible mixture due to the dense gas behavior. Additionally, the extra hazards of LH2 and how to model their consequences have not been covered by any of the risk studies listed in Table 2.7. Hence, a more detailed and accurate approach to assess the risk of LH2 propulsion systems is necessary.

Table 2.7: Risk studies related to hydrogen

Title	Author	Type
Survey of Hydrogen Risk Assessment Methods rev 2	DNV, 2005	CH2, review
Risk assessment of Hydrogen fueling stations for 70MPa	KIKUKAWA et al. 2008	CH2, qualitative
Risk assessment for liquid hydrogen fueling stations	KIKUKAWA et al. 2008	LH2, qualitative
Quantitative risk assessment on 2010 Expo hydrogen station	Li et al. 2011	CH2, QRA
Safety risk modeling and major accidents analysis of hydrogen and natural gas releases	Iraj Mohammadfam and Esmaeil Zarei, 2015	CH2, QRA
Comparison of the safety-related physical and combustion properties of liquid hydrogen and liquid natural gas in the context of the high-speed fuel-cell ferry	Klebanoff et al. 2017	LH2, comparison
Risk assessment methodology for onboard hydrogen storage	Dadashzadeh et al. 2018	CH2, QRA
A grid-based risk screening method for fire and explosion events of hydrogen refuelling stations	Huang and Ma, 2018	CH2, BN
Hydrogen infrastructure: Efficient risk assessment and design optimization approach to ensure safe and practical solution	O. Hanson, 2020	CH2, QRA
Concept risk assessment of a hydrogen driven high speed passenger ferry	Aarskog et al. 2020	CH2, QRA
Quantitative Risk Assessment on the Transport of Dangerous Goods Vehicles Through Unidirectional Road Tunnels: An Evaluation of the Risk of Transporting Hydrogen	Caliendo and Genovese, 2020	LH2, QRA
Comparative risk assessment of liquefied and gaseous hydrogen refueling stations	Yoo et al. 2021	CH2&LH2, QRA
Hydrogen Plus and Other Alternative and Fuels Risk and Assessment Models and (HyRAM+) Version and 4.1 and Technical Reference and Manual	Sandia National Laboratories, 2022	CH2&LH2, QRA
Hydrogen vs. Batteries: Comparative Safety Assessments for a High-Speed Passenger Ferry	Mylonopoulos et al. 2022	LH2, semi-QRA

This page intentionally left blank

3 Research methodology

This chapter provides insight into this thesis. First, the research gap from the literature review is summarised in detail. Next, a recap of the research objective and the extended research questions corresponding to the research gas is formulated. Lastly, the research methodology is discussed to provide a better understanding of the whole design framework and logic.

3.1. Research gap

- **Quantitative risk assessment for hydrogen-fuelled marine vehicle**

  In compliance with the IGF code, alternative designs for ships must demonstrate an equivalent level of safety to conventional designs. As a new and innovative fuel, hydrogen must undergo a rigorous quantitative risk analysis to ensure its safety. However, there have been only a handful of studies conducted on the risk analysis of hydrogen-based solutions in the maritime industry, with inconsistent results and methods. Thus, there is a need to address the gaps in the quantitative risk assessment methodology for maritime hydrogen-fuelled vehicles to better govern and improve their safety.

- **Maritime liquid hydrogen-based propulsion solution**

  At present, the limitations of compressed hydrogen storage volumes restrict the sailing range of hydrogen-fuelled ships to short-distance missions. LH2, with its higher energy density, presents a potential solution for extending the range of such vessels to sea-going missions. However, research on LH2 risk analysis in the maritime industry is scarce, and studies on its application are even fewer. As a result, there are significant gaps in understanding the risks associated with LH2 systems. Additionally, the IMO requires QRA at the preliminary design phase for innovative designs to ensure they meet the same safety standards as conventional designs. [50].

- **Increasing the accuracy of the risk assessment process**

  In the field of QRA for hydrogen applications, a common challenge is the high level of uncertainty associated with each step of the process, which can significantly impact the final results. Thus, carefully selecting appropriate methods to mitigate this challenge is crucial. Therefore, one of the primary objectives of this research is to identify the most suitable QRA methods for maritime hydrogen-fuelled systems and update outdated information accordingly.

3.2. Research objective

Based on the conclusion of the literature review and gap analysis, the primary research objective is:

To develop a quantitative risk assessment system that can effectively analyze and evaluate the risks associated with liquid hydrogen-based propulsion solutions in the maritime industry.

The objective can be pursued by answering the following research sub-questions:

1. What is the system configuration of the maritime liquid hydrogen propulsion system and how can potential hazards and scenarios be identified and assessed to evaluate the risks?

   In the process of conducting QRA, it is crucial to define system scenarios after identifying potential hazards associated with the system. As such, a conceptual design for a liquid hydrogen-based propulsion system needs to be developed, including all relevant components and geometries. However, since this system has not been extensively utilized in the maritime industry, information can only be obtained from companies' inland vehicle designs and product manuals. Therefore, proposing a conceptual design for a liquid hydrogen propulsion system and investigating and selecting relevant LH2-related hazards and scenarios is necessary.

2. What are the most suitable methods for quantitatively and accurately assessing the risks (likelihoods and consequences) of maritime liquid hydrogen propulsion systems?

   Hydrogen risk studies often oversimplify consequences due to the complexity of the system, and outdated or unvalidated modeling approaches contribute to high uncertainty. For example, existing ignition probability models for compressed hydrogen by Aarskog et al. [3], and Tchouvelev et al. [107] cannot be applied to liquid hydrogen, highlighting the need for a new probability model. Addressing the shared problem of high uncertainty requires an approach that improves QRA fidelity through suitable consequence modeling, updated probability models, and comprehensive consequence analysis.

3. What is the comparative feasibility, in terms of risks and capabilities, of maritime liquid hydrogen propulsion systems and existing compressed hydrogen propulsion systems?

   Several researchers have conducted QRAs on compressed hydrogen, and some have discussed the feasibility of compressed hydrogen-based propulsion systems for maritime applications. For example, Dadashzadeh et al. [21], Aarskog et al. [3], and O. Hansen [35] have all explored these topics. However, since compressed hydrogen is limited in terms of sailing distance, it is essential to examine the applicability of the LH2 system as a long-distance shipping solution. Additionally, comparing the capability and risks of the two systems can provide valuable insights for future development and decision-making in the maritime industry.

4. What are the quantified risks of maritime liquid hydrogen propulsion systems, and what mitigation measures can be implemented to reduce these risks to acceptable levels?

   This research question is linked to the previous ones. After designing the system, selecting the scenarios, and modeling the consequences, the risk model for maritime LH2-based propulsion solutions can be executed. Then, the evaluated risks can be compared with the criteria from the published guidelines, such as HSE R2P2 [39] and DNV [37, 6]. Eventually, the acceptability of the risk can be answered, and an early QRA system for maritime Liquid hydrogen-based solutions can be applied widely in the industry. And this QRA tool for maritime LH2-based solutions could be helpful at the preliminary design stage.

5. To what extent can this quantified risk assessment system be applied? What are the limitations of this tool, and can this design framework also be applied to different alternative fuels?

   The ”model extension” block at the bottom of the flowchart aims to enhance the risk-based design process by providing a tool that can analyze the quantified risks of not only the given conceptual design but also a wide range of future LH2 designs. This tool is crucial for improving the development of future technologies.

3.3. Methodology

To help answer the research objective and questions, the design flow chart of the research methodology is presented, as shown in Figure 3.1. Blocks with different colors represent the stage of the process, which in order are system definition, analysis of the event, model implementation, and result. Additionally, the gray iteration loops between the blocks ensure the adaptability of each method to accomplish the rigorous result.

After getting insight into the risks and maritime hydrogen-based solutions through the literature study. The first step is to define the system's parameters based on the operation profile of the ship, where the components required, and educational assumptions will be

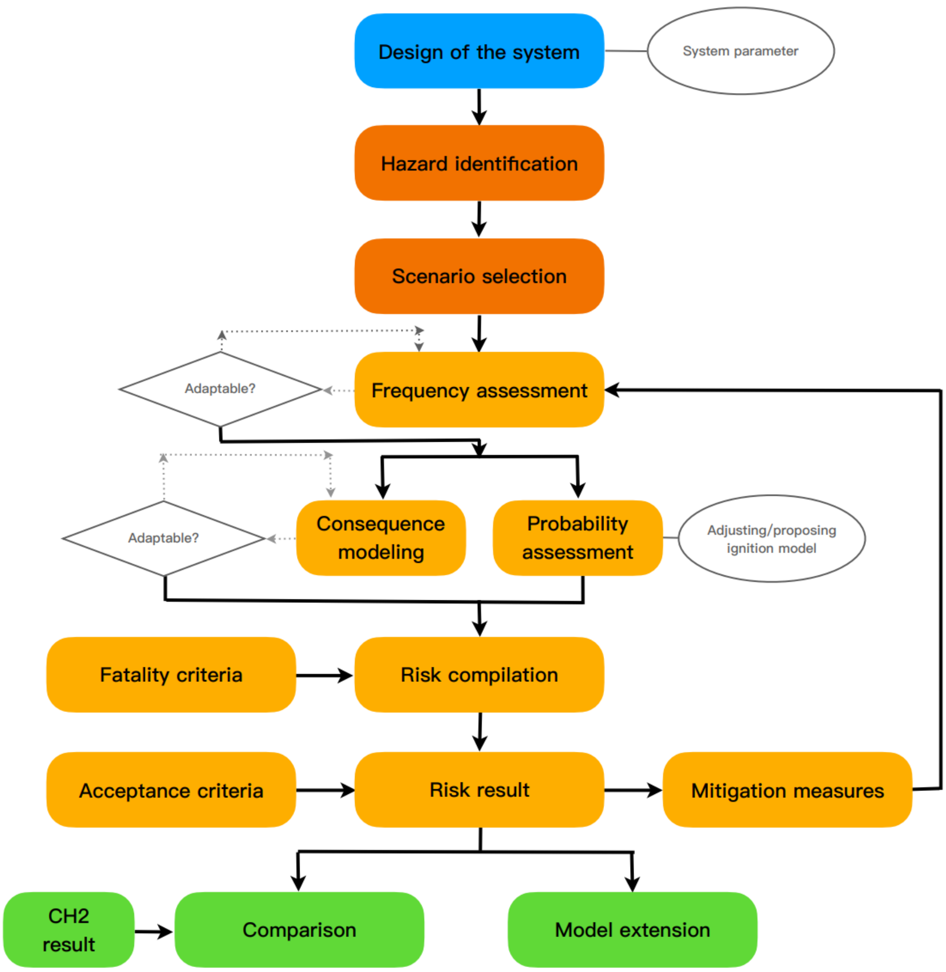

Figure 3.1: Flow chart of the research methodology, it covers the system logic (orange blocks), quantified process (light orange blocks), and the final comparison study with the CH2 design (green blocks).

This page intentionally left blank

4
System development

In this chapter, the overall principles and theories that have been implemented into the quantitative risk assessment tool for maritime liquid hydrogen propulsion systems are presented. The structure of this chapter follows the generic QRA process outlined in Section 2.2.1. The chapter begins with a proposal of the conceptual design of a maritime LH2-based propulsion solution based on the upcoming FPS vessel Rijn. Following this, potential hazards and corresponding scenarios are formulated using FTA and ETA techniques. The frequency assessment section analyzes the leakage frequency of each component while adapting to liquid hydrogen and maritime environment. The probability of combustive events is investigated based on the ETA hierarchy, and the final consequences are modeled using validated physical models from the literature.

4.1. Conceptual design of the LH2-based solution

When designing the propulsion system of a vessel, an essential aspect to consider is its operational profile, including missions and demands, especially for alternative fuels, due to the limited energy density and safety concerns. The proposed system is for an LH2-fueled inland vessel, FPS Rijn, that transports cargo from Rotterdam to Duisburg, taking approximately 16 hours downstream and 22 hours upstream. The electric power of FPS Rijn is generated by proton-exchange membrane fuel cells (PEMFC), with an estimated installed power of $1MW$. The system configuration of this conceptual design is shown in Figure 4.1, consisting of the following subsystems with initial parameters estimated based on information from the literature through scaling and assumptions:

- LH2 storage tank
- LH2 piping system
- Pressure build-up system and vaporiser system
- Venting system
- GH2 buffer tank
- GH2 piping system
- PEMFC system

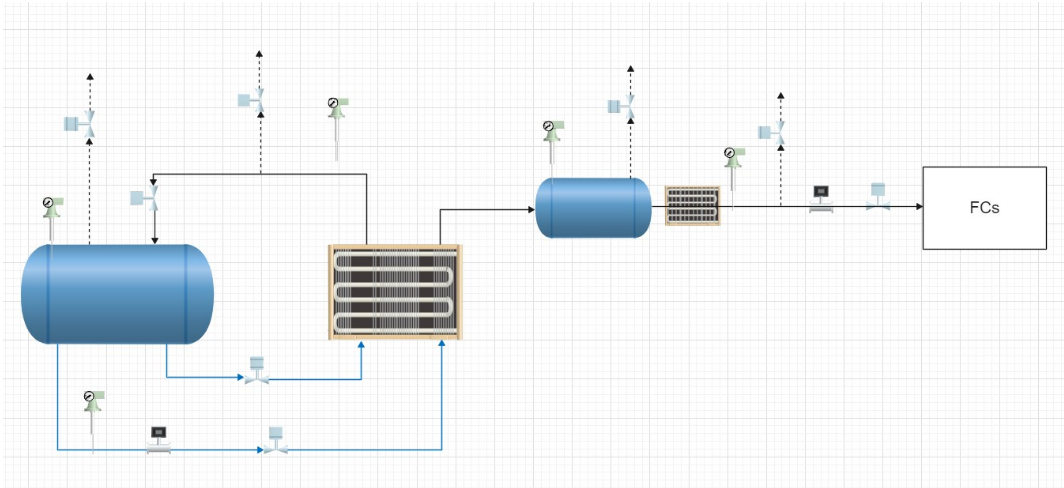

Figure 4.1: Proposed system layout for the maritime LH2-based propulsion system, it comprises LH2 part (blue line), GH2 part (black line), and venting line (black dotted line).

4.1.1. LH2 storage tank

Due to the cryogenic properties of LH2, it is necessary to insulate the tank from the atmosphere. A vacuum-insulated design is proposed, wherein the annular space is evacuated and filled with superinsulation foil. In terms of material selection, HE-resisted materials, such as austenitic steels and aluminum, will be used to prevent hydrogen embrittlement, which can cause ductile to brittle behavior. To determine the appropriate tank size, the required amount of hydrogen can be calculated based on the operational profile of FPS Rijn using Equation 4.1.

$$m_{H_2} = \frac{P(kW) * t(h) * 3600}{\eta(\%) * LHV(kg/kg)} \tag{4.1}$$

In the above equation, P represents the power generated by the fuel cells, t is the sailing time, η denotes the product of efficiencies, and LHV is the lower heating value of hydrogen, which is approximately $120,000kJ/kg$. By substituting the operation profile of the ship, the total hydrogen consumption for a round trip is approximately $2800kg$. Therefore, a Linde $3000kg$ hydrogen container HYLICS with 5% ullage and designed to withstand $12barg$ pressure is selected [22].

Table 4.1: LH2 tank characteristics [22].

Parameter	Value	Unit
Pressure	12	bar
Frame size	40ft container	-
Hydrogen capacity	3000	kg
Temperature	20	K
Ullage	5	%

4.1.2. LH2 piping system

The LH2 piping system includes the components upstream of the vaporizer and relies on the pressure difference between the tank and pipes to drive the flow of LH2. Operating pressure is estimated to be within the range of $10 - 11; barg$, and the inner diameter of the pipes is assumed to be 12 mm. Valves are employed in the piping system to regulate the flow rate and act as emergency shut down devices (ESD) if necessary.

Table 4.2: LH2 piping characteristics.

Parameter	Value	Unit
Pressure	10-11	bar
Inner diameter	12	mm
Temperature	20	K

4.1.3. Pressure build-up unit and vaporiser

To ensure sufficient driving force, the pressure level inside the tank must be controlled by a pressure build-up unit (PBU), which includes a pressure sensor, valves, and pipes for regulating flow rate and transport. When the pressure drops below a critical value, the LH2 is evaporated to gaseous hydrogen by the vaporiser. The gaseous hydrogen is then circulated back to the LH2 tank to build up pressure. Additionally, another vaporiser is used to evaporate the LH2 to a gaseous state for use in the fuel cells, as the hydrogen supplied to the fuel cells must be in a gaseous state.

4.1.4. GH2 buffer tank

The GH2 buffer tank provides hydrogen supplements under unfavorable conditions. For instance, the sloshing of the LH2 tank due to motions may cause hydrogen transport capacity. The nominal consumption of hydrogen for a fuel cell unit is $59kg/MWh$. Therefore, it was assumed that the buffer tank should be able to supply one hour of sailing capability. Therefore, a $60kg$ buffer tank was selected in a 20ft container to store the GH2. Due to the required mass of $60kg$ and the limited volume of $33m^3$, the required density should be at least $1.82kg/m^3$. Therefore, operating conditions of $9bar$ and $123K$ meet the design requirements.

4.1.5. GH2 piping system

The GH2 piping system is divided into two parts: the first part starts from the vaporizer to the buffer tank, with the same dimensions and operating pressure as the previous LH2 piping system. An orifice is implemented before the buffer tank to decrease the system pressure to achieve the required storing capacity at $123K$ and $10bar$. The second part supplies the 1MW fuel cell stacks with a total hydrogen mass flow rate of $16.39g/s$, estimated based on FC manuals. To meet this demand, a $3.28g/s$ mass flow rate with an inner diameter of 12mm is proposed, with an operation temperature and pressure of 300K and $6bar$. A small heat exchanger is implemented in this second part of the GH2 piping.

Table 4.3: GH2 piping characteristics.

Parameter	Value (1st;2nd)	Unit
Pressure	10; 6	bar
Inner diameter	12; 12	mm
Temperature	123; 300	K

4.1.6. PEMFC system

As the final component of the proposed system, the PEMFCs are responsible for generating power for the entire ship. Based on the 1MW power demand, a PEMFC system comprising five Bollard FC wave units, each with a rated power of $200kW$, has been selected [2]. The operating pressure of the system is in the range of $3.5 - 6bar$, and the dimensions of each unit are $1.209m$×$0.741m$×$2.195m$. The mini GH2 pipes transport $3.28g/s$ of hydrogen to each FC module.

Table 4.4: PEMFC characteristics [2].

Parameter	Value	Unit
Rated Power	200	kW
Minimum Power	55	kW
Weight	1000	kg
Built Level	1.97	m^3
Pressure	3.5-6.5	bar
Temperature	0- 45	$°C$

4.1.7. Venting system

The venting system plays a critical role in ensuring the safety of the LH2 propulsion system. It is responsible for controlling the release of hydrogen during emergency or error situations, where it is necessary to empty the hydrogen from the system. One of the key challenges in operating and handling LH2 propulsion systems is their complexity, which arises due to the presence of both LH2 and GH2 subsystems. Unlike GH2, which can be vented outside automatically due to its lower density than air, liquefied hydrogen requires a separate venting system. Since most of the hydrogen is stored in the LH2 tank, which contains both LH2 and GH2, two venting pipes, one from the top and the other from the bottom of the tank, must be implemented. The top venting system releases cryogenic gaseous hydrogen to the air, whereas the bottom venting line requires an additional step of evaporating through the vaporizer, given the higher density of LH2. The venting outlet is located 10 meters above the main deck to ensure safe dispersion of hydrogen.

The Venting capability is required to have at least a 30 air changes per hour (ACH) ventilation rate in a tank connection space (TCS). An inner diameter of the vent mast was assumed to be 150-200 mm to limit the release velocity. Since the design of the venting system was assumed to be a safe operating system, the hazards for this were not considered in the scope of this thesis.

4.1.8. Other units

In order to safely manage both liquid and gaseous hydrogen phases, various units that connect the subsystems are utilized. Gaskets or flanges are employed to connect components, while different valves are implemented to control flow and pressure. Flow control valves are used to regulate flow rate, and pressure-reducing valves are designed to decrease pressure levels through orifices to the required conditions. Additionally, pressure-relief valves are installed in every subsystem. These valves open to release hydrogen to the venting system when the pressure exceeds critical values. The frequency assessment of these units will be presented in Section 4.5 based on estimation from literature data and company manuals.

4.2. Hazard identification

The hazards of liquid hydrogen have been introduced in section 2.2.2. For most of the literature, LH2 was simulated and assumed to have the same hazardous consequences as GH2. However, the physical differences between these two storage types vary in the corresponding hazards. Essentially, hazards of hydrogen can be divided into two categories: fires and explosions. But for the cryogenic LH2, an additional cold effect should also be considered.

Figure 4.2 presents a simplified ETA of a maritime LH2-based propulsion system. The diagram depicts the system's complex ETA in several stages, each characterized by different states. The condition of each state determines the subsequent states, ultimately leading to hazardous consequences. The states and final events are summarized in Tables 4.5 and 4.6. The final consequences primarily depend on the hydrogen phase, LH2 or GH2, within the system. The differences in properties of hydrogen phases dominate the hazards of release events. Release types are classified as continuous, small-scale, and large-scale. Small-scale releases refer to random small-scale component leakages.

In contrast, large-scale releases result in hydrogen pool formation (LH2) or the emptying of hydrogen mass within a minute (GH2).

In addition, the behavior of hydrogen also depends on the release rate. For instance, when the LH2 release rate is around $1kg/s$, liquid hydrogen may accumulate on the ground due to a lack of large-scale experiments. Moreover, the ignition state is crucial for determining the final hazards, with direct and delayed ignition being the two possibilities. In small-scale releases, a direct ignition results in a jet fire. In contrast, delayed ignition causes a flash fire due to the accumulation of hydrogen fluid over time. The final state determines whether an explosion will occur and its type. Deflagration is the only type of explosion considered in this study, as the conditions required for detonation are unlikely to happen in a hydrogen-fueled vessel. The intensity of the ignition source and the geometry of the environment determines the type of explosion. Appendix B contains the full-detailed ETA diagram, shown in Figure B.1.

To summarize the hazards identified in the five-stage event tree, there are six potential outcomes, which can be classified into two categories: ignited events and non-ignited events, and further differentiated by GH2 and LH2 hazards. These hazards are outlined in Table 4.6. Ignited events include a jet fire, which is an immediate ignition of high-speed release that poses risks to human safety due to high flame temperatures and heat radiation. A flash fire, on the other hand, is a more widespread fire that poses risks primarily within the 4% hydrogen-air concentration area. A fireball occurs when a significant amount of ignitable gas is released and ignited instantly, causing heat flux and overpressure in the surrounding environment. A pool fire can only occur following a large-scale LH2 release, where an oxygen-rich pool of hydrogen accumulates on the ground and ignites. The main risk associated with a pool fire is the flame area, as the radiation fraction is insufficient to cause fatality. Explosions, as noted in Section 2.2.2, can occur only under specific conditions, including a strong ignition source, confinement, and an explosive atmosphere. Therefore, explosions are assumed to be the outcome of delayed ignition in a confined space.

Moreover, for the type of explosions, only deflagrations are considered in this research since detonations are not likely to happen. Detonation is an extremely fast combustion with much higher speed and overpressure than deflagration. But it requires an extremely strong ignition source of up to $4MJ$ and enough confined space to propagate, which is not likely to happen in a hydrogen-fuelled vessel.

On the other hand, cold plume and hydrogen pool are two types of unignited events that can occur in the maritime LH2-based propulsion system. They are triggered by continuous and instantaneous release, respectively. The density of liquid hydrogen is higher than air until it is mixed with ambient air with a concentration lower than approx. 40% [36]. Therefore, LH2 spray vapor would show a dense gas behavior in the near-field high hydrogen concentration area. This physical phenomenon is called a ”cold plume” due to its cryogenic property. For an instantaneous large-scale release condition, since the evaporation rate is lower than the spill rate of LH2, a hydrogen pool will form. The risks of a hydrogen pool are the cold temperature and condensed air phase, where oxygen and nitrogen may co-exist with the pool in solid or liquid form. This condensed air phase is known for its extremely high ignition property. The MIE of the oxygen-rich hydrogen mixture is even four times lower than the hydrogen-air mixture to only $0.004mJ$ [7].

Established on the investigations of the literature review, BLEVE and RPT are not considered potential hazards nor implemented in the event tree diagram. Because there are no historical accidents for these two events to have happened before and researchers such as Ustolin et al. [110, 109] also concluded that these two hazards could be seen as incredible events. Furthermore, the inconceivable RPT event to have happened is also the primary consideration for LH2 water venting.

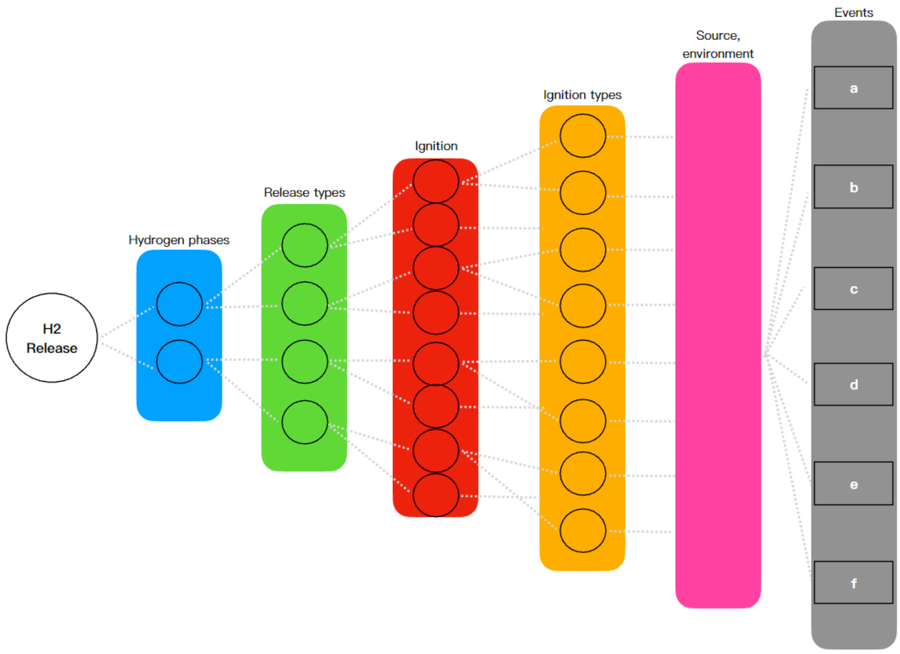

Figure 4.2: Proposed simplified event tree analysis by columns.

Table 4.5: Columns and states of the proposed ETA.

Column	**No.**	**States**
Hydrogen phases	2	Liquid; Gaseous
Release types	2	Instantaneous; Continuous
Ignition	2	Yes; No
Ignition types	2	Direct; Delayed
Source, environment	2	Confined space with strong source; others

Table 4.6: Consequences of proposed ETA.

No.	**Name**	GH2	LH2
a	Jet fire	✓	✓
b	Flash fire	✓	✓
c	Pool fire		✓
d	Explosion	✓	✓
e	Cold plume		✓
f	Hydrogen pool		✓
g	Gas fire ball	✓	

4.3. Scenario selection

Based on historical incident data, this section formulates potential causes contributing to hydrogen leakage within the system. Unlike most literature that assumed scenarios with fixed or constant release hole sizes, this research assessed leakage scenarios using representative component leakage frequencies as a function of the normalized leak size. For instance, a 10% leakage of 12mm pipes represents an 11.3 mm^2 leakage area. This method enhances the comprehensiveness of the system, as a single leakage event for components may not thoroughly cover all potential causes. Hydrogen leakage has been identified as the primary reason leading to hazards, and this approach provides a more comprehensive assessment of leakage scenarios.

The logical map depicting the selected scenarios is presented in a fault tree analysis, as illustrated in Figure 4.3. Based on incident data from [114], the mechanisms responsible for hydrogen leakage events are system design error, material/manufacture error, installation error, and human factors. However, some incidents occurred during the initial trials of hydrogen designs, where improper installations and human factors due to lack of experience were prevalent. However, these factors were not considered in this FTA. This analysis only accounts for the failure mode of each component. A detailed discussion of the frequency assessment for component failure/leakage is presented in Section 4.5. Figure 4.4 shows the FTA for random leaks of a single component, which is one of the logic gates inside the orange and blue blocks in Figure 4.3. Meanwhile, the whole FTA, which includes all components, is presented in Figure B.2 in Appendix B. Leakage scenarios were split into random leakage and catastrophic rupture. In this project, catastrophic ruptures were referred to as 100% LH2 tank and buffer tank leakages and external accidents. In contrast, random leakages were triggered by 0.01%-10% of tank-related failures and 0.01%- 100% of other components. These scenarios were selected according to the geometry of the components, i.e., a 100% of pipe leakage was still considered a continuous release since it is within the transportation line.

On the other hand, components such as tanks were considered terminals for storing devices. Therefore, 100% of leakage was assumed to cause an instantaneous large-scale release. The annual frequency of random leaks was calculated using Equation 4.2:

$$f_{RandomRelease,Component_i} = \Sigma N_{Component_i} * f_{Leakage,j,i} \tag{4.2}$$

Where i stands for the components' index, N for the number of components, and j for the leak area index with 0.01%, 0.1%, 1%, 10%, and 100% (For tanks, j only accounts from 0.01% to 10%). Table 4.7 summarises the components (i) that were considered in this system. Based on the upper part of FTA, the total frequency of random release can then be calculated as Equation 4.3:

$$f_{RandomRelease} = \Sigma f_{RandomRelease,Component_i} \tag{4.3}$$

Table 4.7: Components considered that lead to a hydrogen leakage.

$Components_i$	$GH2$	$LH2$
LH2 Tank		✓
Vaporiser		✓
Pipe	✓	✓
Flange	✓	✓
Valve	✓	✓
Buffer tank	✓	

As for the catastrophic rupture scenario, it can be presented as the summation of the frequency for the 100% full-bore rupture tanks plus the frequency of accidental events, as shown in Equation 4.4. The accidental events here referred to the external events such as collisions in storage tank or vaporiser, a frequency of $5 * 10^{-6}$ per year was added as recommended by Correa- Jullian et al. [19]. Finally, the total hydrogen leakage frequency can be expressed as equation 4.5.

$$f_{Catastrophicrupture} = \Sigma f_{Fullborerupture,k} + f_{accident} \tag{4.4}$$

$$f_{Hydrogenleakage} = f_{Randomleakage} + f_{Catastrophicleakage} \tag{4.5}$$

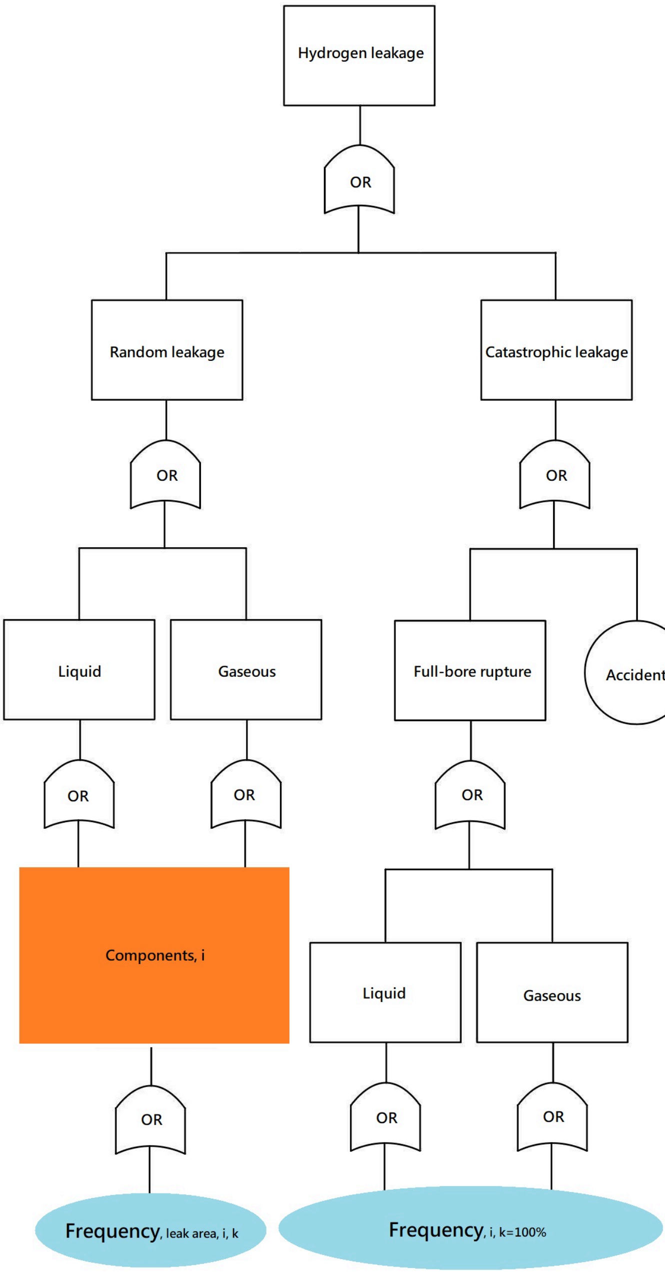

Figure 4.3: Simplified fault tree diagram of the system.

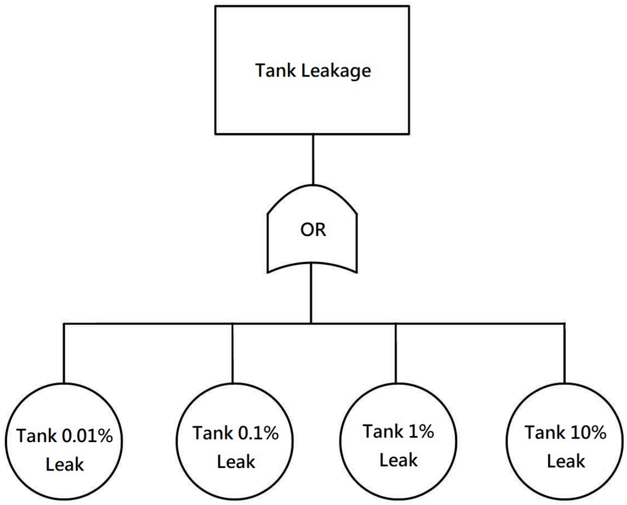

Figure 4.4: Fault tree for random leakages of tank.

4.4. Logical map of the system

The whole system's logic was established on the ETA and FTA from hazard identification and scenario selection. The FTA started with the predicted leakage frequency on every component with different hole sizes scenarios and ended up with the hydrogen leaking frequency of the system. At the same time, the initial event in this ETA was the hydrogen leakage, which propagated through several conditional states, contributing to the final hazards. The end of the FTA was the same as the start of the ETA. Therefore, these two analytical diagrams could be combined to form the logic of this system, as shown in Figure 4.5. This diagram is called a bow-tie diagram. The risk was then compiled by multiplying the frequency (FTA) with the probability (ETA).

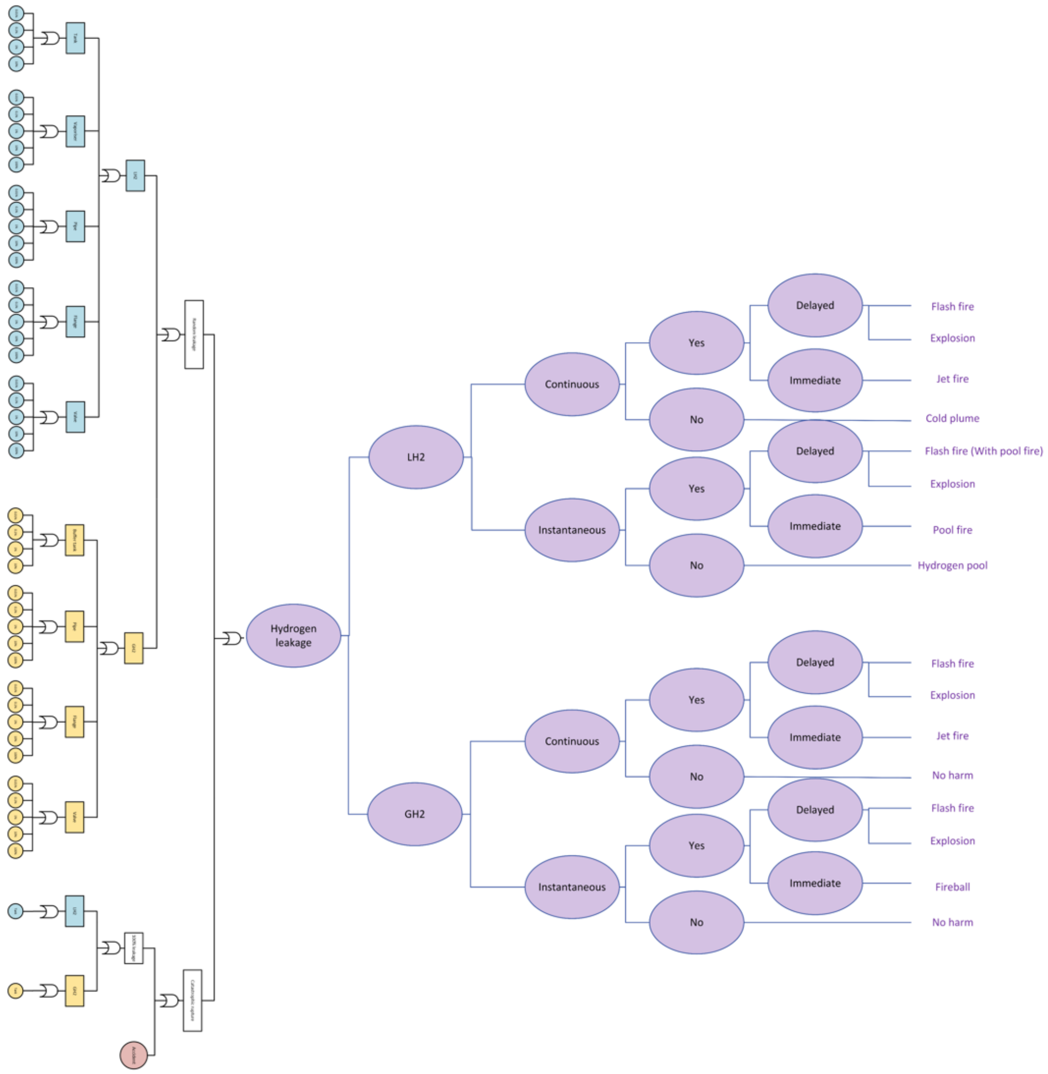

Figure 4.5: Bow-tie diagram of the maritime LH2-based propulsion system, by combining the fault tree and the event tree together.

4.5. Frequency assessment

The objective of this section is to quantify the Fault Tree Analysis (FTA) of the logical map as discussed earlier. As the mechanisms that contribute to the leakage of each component are intricate and include various factors such as vibration, structural deficiencies, failures to function, and other potential causes, it is more comprehensive to consider these factors collectively as a single leakage event. In other words, the frequency of component leakage with a given normalized leak size is the sum of the frequencies of all potential mechanisms, as obtained from relevant data sources.

The use of Bayesian statistics was proposed to predict the leakage frequencies of components operating with LH2. This is because operating hydrogen in components can result in different leakage frequencies compared to generic ones obtained from data sources. Additionally, the limited experience and operating data for liquid hydrogen pose a challenge. Bayesian updating was used to understand the probability of a specific parameter value given data by decomposing this probability into the probability of the data assuming that the specific parameter value multiplied by the probability of the parameter within that specific value. This can be formulated as follows:

$$p(A|B) = p(B|A) * p(A) \tag{4.6}$$

In Equation 4.6, the term $P(A|B)$ represents the posterior, while $P(B|A)$ represents the likelihood and $P(A)$ represents the prior. Typically, the posterior is the value that we want to determine, while the likelihood represents the information that we can observe, and the prior represents the initial belief about A. In this framework, the posterior becomes the prior for the next update and is propagated through the same rule. The mathematical model assumes that the log-leak frequency for each normalized leak size follows a normal distribution. Additionally, the mean of the normal distribution, $log(\mu_{LF,j})$, can be represented as a linear equation with α_1 as the intercept and α_2 as the slope, as shown in Equation 4.8 and Figure 4.6.

$$log(LF_j) \sim normal(\mu_{LF,j}, \tau_j) \tag{4.7}$$

$$log(\mu_{LF,j}) = \alpha_1 + \alpha_2 log(LA_j) \tag{4.8}$$

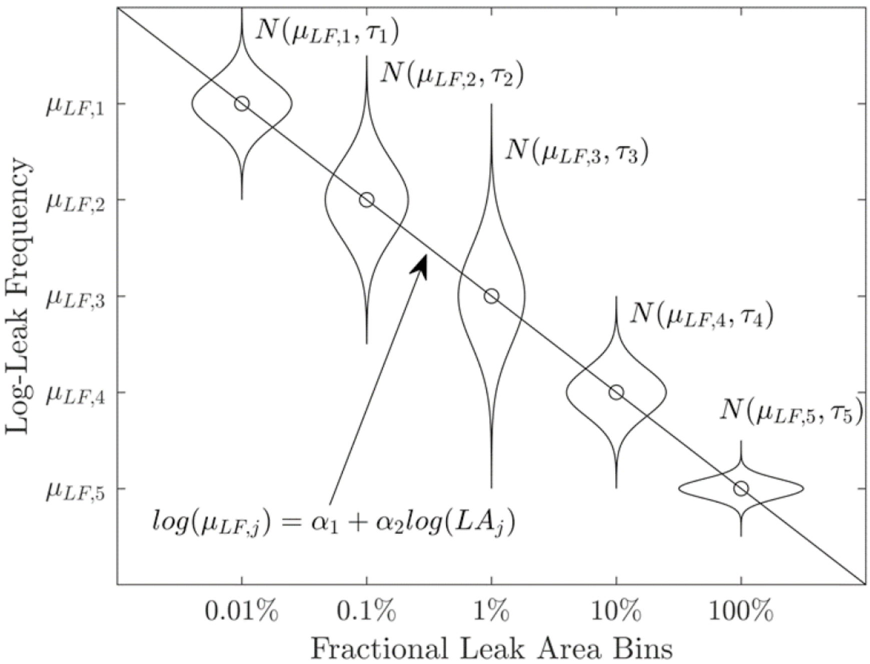

Figure 4.6: The mathematical log-normal distribution model for estimating frequencies as a function of fractional leak area, cited from Brooks et al. [20].

Furthermore, the intercept and slope, being the parameters of the log-normal distribution, can also be represented by a normal distribution. This is expressed in Equation 4.9. The prior distribution for these two parameters and the precision τ_j are the initial assumptions in the Bayesian-based model. Multiple data sets are then used as the likelihood to update the posterior distribution of the parameters.

$$\alpha_1 \sim normal(\alpha_{11}, \alpha_{12}) \;\; ; \;\; \alpha_2 \sim normal(\alpha_{21}, \alpha_{22}) \tag{4.9}$$

The Bayesian-based model was updated using two different categories of data. The first set of data comprised generic industry data and data from gaseous hydrogen systems, while the second set used LNG-related data to estimate the final LH2 frequency. LH2 leak frequencies were estimated from the model's results for α_1, α_2, and μ, taking into account the fact that LH2 properties lie between those of GH2 and LNG. The distribution of the 0.1% tank leakage frequencies in both logarithmic and normal spaces is shown in Figure 4.7, with a 95% confidence interval. The total component frequency diagrams can be found in Appendix A. The authors recommended using the **mode** as the leakage frequency, as it has the highest probability of occurring, while the **mean** provides a probability-weighted average of all possible values, as shown in the upper figure in Figure 4.7. Both values were selected as the frequencies to be applied in the system, and the formulation is as follows:

$$f_{mode} = e^{\mu - \sigma^2} = e^{log(f_{median}) - \tau} \tag{4.10}$$

$$f_{mean} = e^{\mu + \frac{1}{2}\sigma^2} = e^{log(f_{median}) + \frac{1}{2}\tau} \tag{4.11}$$

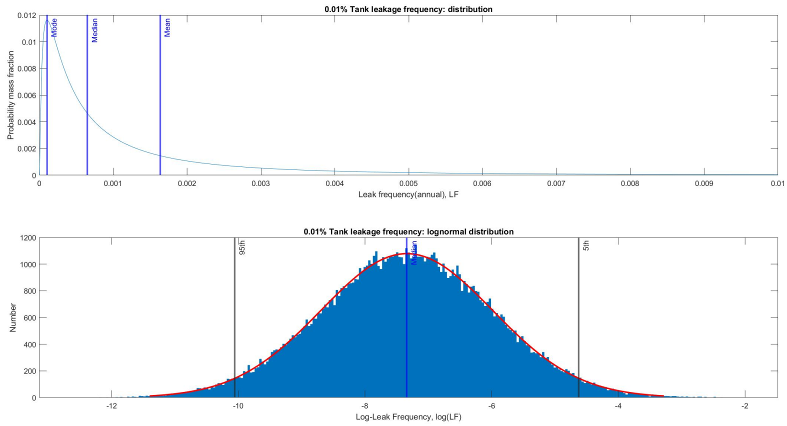

Figure 4.7: Frequency of 0.01% leakage tank, the median, mean, and mode are plotted in normal distribution space.

Nevertheless, this method has a limitation in that only components with available data can be evaluated. Thus, the vaporizer, which is unique to LNG systems, cannot be assessed using this Bayesian approach. To overcome this limitation, a new approach was applied in this study. The leakage frequency trends for LH2 and LNG components were compared and it was found that LH2 components tend to have higher frequencies at 0.01% and 0.1%, whereas they have lower leakage frequencies from 1% to 100%. Based on this comparison, an amplification factor was applied to update the LNG vaporizer leakage frequencies and better predict the frequencies for handling LH2.

The data sources utilized in this Bayes theorem only account for generic LNG and H2 leakage frequencies and do not account for the harsh marine operating environment. Three factors typically associated with failure rates in the marine environment are temperature, corrosion, and vibration. The temperature factor can be characterized by the k_t factor, which depends on the operating temperature and generic data temperature. However, in this study, the operating temperature was assumed to be $15°C \pm 20$, and the k_t factor was determined to have a negligible influence on the failure rate. In addition, Cadwallader [11] investigated the corrosion factor and found that it may take decades to weaken a component from the surface inward, indicating that it may not be a critical factor in affecting the failure rate. Lastly, the vibration of the mechanical components on the ship may accelerate the failure rate. Basquin's Law proposed by FIDES [30] can be used to model the modified failure rate as a function of root mean square vibration amplitude, g_{rms}, in the operating environment and the reference vibration amplitude, g_{rms0}, with a recommended value of 0.5g. This study considers the vibration of rotating machinery to influence the failure rate of each component, but irregular wave vibrations on the hull and components are negligible due to the low frequency of induced wave vibrations.

$$VF = (\frac{g_{rms}}{g_{rms0}})^{1.5} \tag{4.12}$$

To estimate the root mean square vibration amplitude of the ship, g_{rms}, the Power Density Function (PSD) is needed according to the definition of Basquin's Law [30]. However, the current vibration level for shipping as recommended by ISO 6954:2000 Mechanical Vibration and Shock – Guidelines for the overall evaluation of vibration in Merchant Ships (2000) [95] is presented in a Fast Fourier Transform (FFT) diagram, as shown in Figure 4.8. Therefore, a conversion from FFT to PSD was implemented to estimate the influence of vibrations on components' failure. In addition, the motions of the ship in terms of vertical acceleration were also evaluated, and the result showed that low-frequency wave-induced motions contribute little to the vibration factor. By taking the integral of the PSD spectrum in Figure 4.8 and taking the square root, g_{rms} can then be calculated.

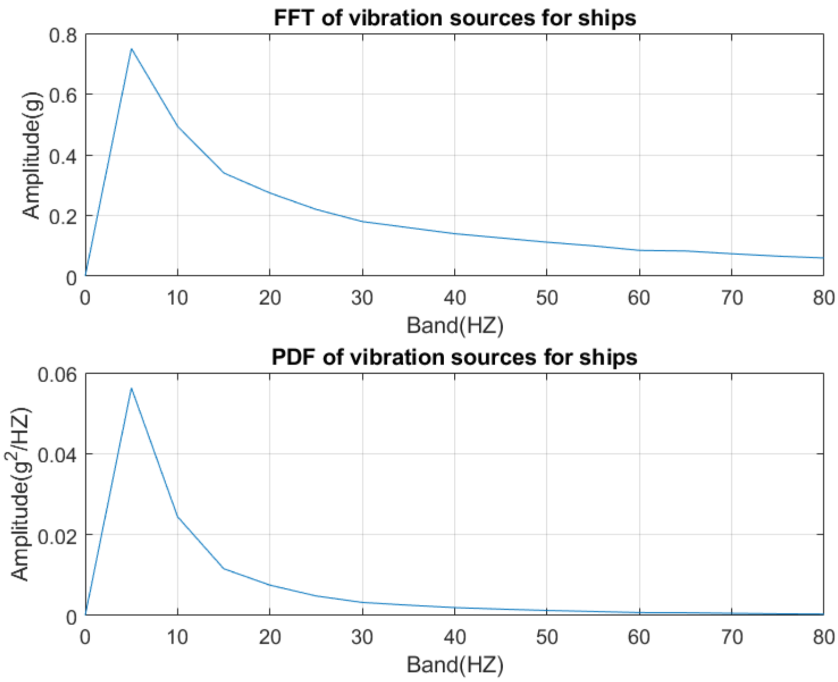

Figure 4.8: FFT and converted PDF of vibration sources for ships, FFT data was assessed from [95].

4.6. Consequence assessment

This section aims to quantify the ETA part of the system and provide answers to research question two. It comprises two parts: probability assessment and consequence modeling. First, the probability assessment part addresses the hydrogen ignition probability based on methane properties. A modified ignition model for LH2 was proposed. In contrast to previous literature, ignition probability for both continuous and instantaneous releases are individually distinguished and assessed. Besides, the likelihood of which consequences will occur was also evaluated here. Next, the consequence modeling part assesses SOTA modeling methods and compiles the hazard of each consequence as the fatal distance based on fatality criteria. Finally, the quantified risks can be evaluated by associating the likelihood of events with their consequences.

4.6.1. Probability assessment

Risk is defined as the product of frequency and probability. While the frequency component has been previously derived and quantified in section 4.5, this section will focus on assessing the probability component. As shown in ETA B.1, determining the ignition probability is necessary to compile the likelihood of the event in times per year. For continuous hydrogen releases, a GH2 ignition model was utilized that considered differences between the physical properties of hydrogen and methane. Methane is a commonly used hydrocarbon in industries that has been extensively studied over the years. Previous researchers, such as Tchouvelev et al. [107] and Aarskog et al. [3], have proposed ignition probability models that consider minimum ignition energy (MIE) and flammable cloud volume as primary factors contributing to ignitions. In comparing the properties of methane and hydrogen, Tchouvelev et al. [107] found that hydrogen and methane with identical molar release rates would result in a flammable cloud eight times larger for hydrogen, while a 7.3 higher flammable range would only account for approximately 16% of the total flammable cloud size. As a result, they proposed reducing leak flow ranges by a factor of eight and increasing gas ignition probability by 16%, as summarized in table 4.8. However, this model did not consider the MIE discrepancy between hydrogen ($0.02mJ$) and methane ($0.27mJ$) or gas accumulation conditions. Furthermore, recent studies have challenged the assumption of an eight times larger flammable cloud size, instead finding a 30-40 times larger volume for a similar mass flow rate.

Table 4.8: Ignition probabilities for different fuels, data collected from HyRAM [25].

(a) Hydrogen

Release Rate (kg/s)	Ignition Probability
<0.125	0.012
0.125-6.25	0.08
> 6.25	0.35

(b) Methane

Release Rate (kg/s)	Ignition Probability
<1	0.01
1-50	0.07
>50	0.3

As a result, a different ignition model was proposed in [3]. This model suggests a reduction of release rate by a factor of 40 to achieve comparable flammable cloud size, and updates the ignition probabilities based on the lower MIE. For instance, a release rate of $1.25kg/s$ gives a 30% ignition probability, while a release rate greater than $12.5kg/s$ has a 100% probability. Additionally, this model takes into account gas accumulation behavior in a confined space. Consequently, a final continuous relationship was proposed, which can be expressed as:

$$P_{ignition,gh2} = Minimum(1.0; 0.55 * rate^{0.87}; 0.267 * rate^{0.52}) \tag{4.13}$$

An LH2 ignition model was proposed to analyze and design a QRA system with lower uncertainty. LH2 has different physical properties compared to GH2, but no literature or data is available to determine the LH2 ignition probability. Thus, following the same thought as the GH2 model, a comparison of the flammable cloud volume shows that the ignition cloud volume of LH2 is in the same order as GH2. However, LH2 leakage events tend to form a cryogenic cloud or pool that may contain liquefied and solidified oxygen and nitrogen, resulting in an oxygen-dense mixture with an MIE reported to be as low as $0.0012mJ$, which is 15 times lower than GH2. However, 15 times difference does not mean 15 times more probability; it means more low-energy ignition sources would contribute to ignitions. Therefore, the amount of potential ignition sources is related to the ignition probability. To determine the ignition probability of LH2, the number of potential ignition sources was assumed to be distributed logarithmically. Using data from GH2 and methane, a logarithmic relation between ignition probability and MIE was interpolated at a release rate of $12.5g/s$, as shown in Figure 4.9. The proposed LH2 ignition model is presented in Figure 4.10.

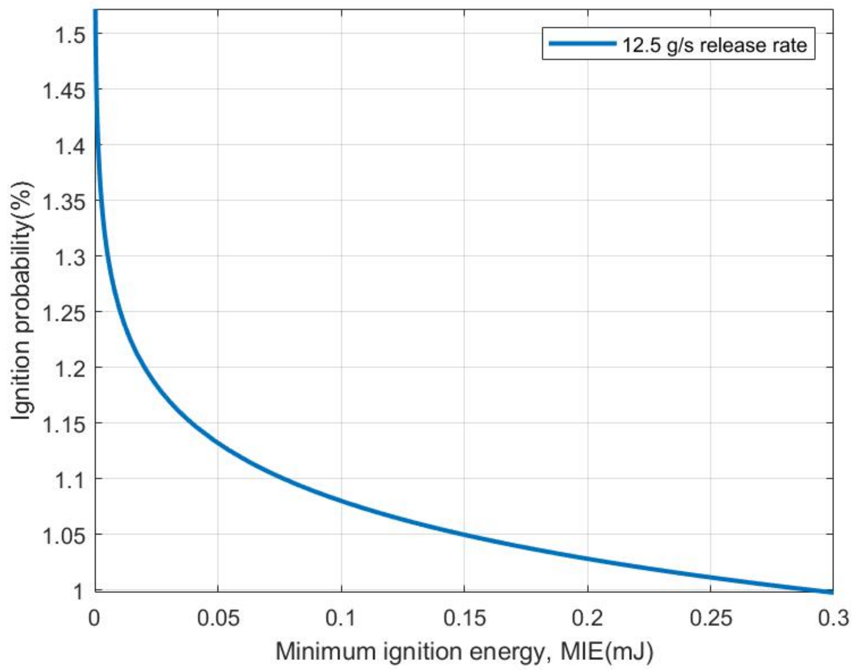

Figure 4.9: Ignition probability against minimum ignition energy at a release rate of 12.5 g/s, under the assumption of logarithm distribution.

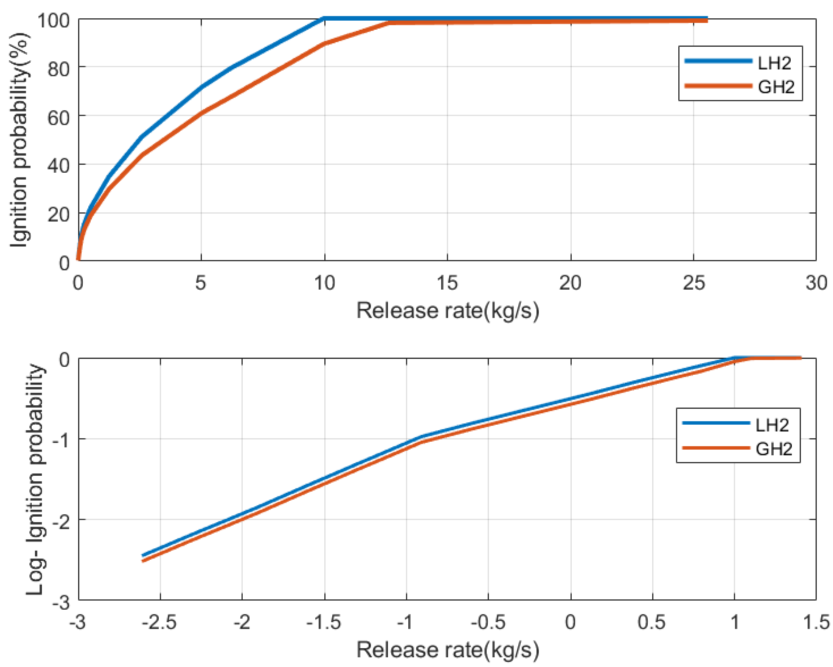

Figure 4.10: Proposed ignition probability of LH2, comparing to the existing GH2 ignition model.

The existing ignition models are only based on the release mass flow rate, which is only suitable for continuous releases. However, to fully assess risks, separate models for instantaneous releases are also necessary. In such cases, the amount of mass released is used to estimate ignition probability since the flow rate is unavailable. The RIVM Reference Manual Bevi Risk Assessment recommends a direct ignition probability of 20% for releases under 1000 kg, 50% for releases between 1000-10000 kg, and 70% for releases exceeding 10000 kg for extremely reactive substances. The same methods used for continuous releases were employed to assess the ignition probability of GH2 and LH2, with adjusted models for instantaneous releases based on a 40 times flammable volume and lower MIE. The resulting adjusted models for GH2 and LH2 are presented in Figure 4.11. It should be noted that for instantaneous releases, gas accumulation in a confined space was not applicable. Thus, no extra adjustments for high-release mass scenarios were developed.

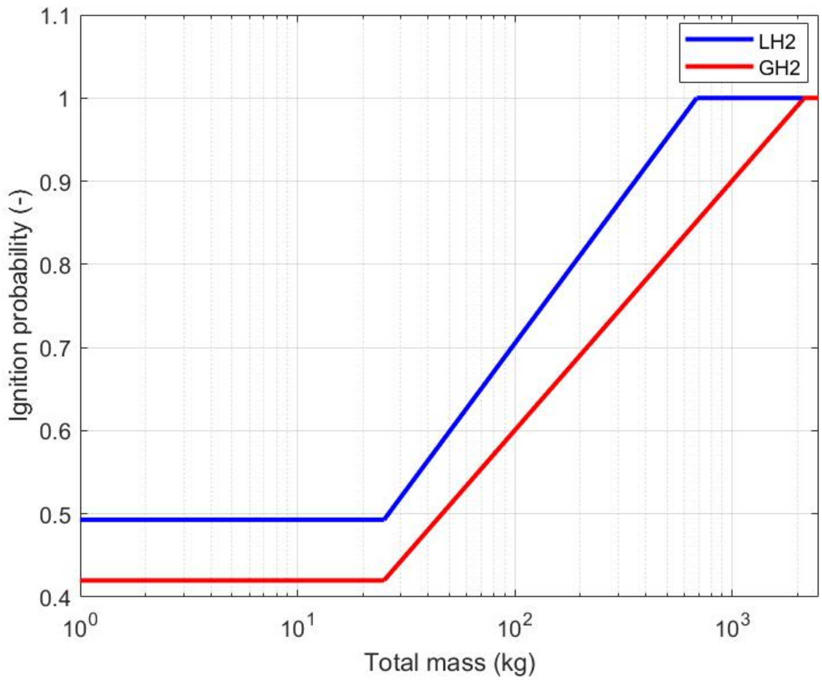

Figure 4.11: Proposed ignition probability for instantaneous releases.

In the last two states of the ETA map: Ignition types (Direct; Delayed) and hazards, as shown in Figure B.1. The portion of direct and delayed ignition was assigned to 2:1, according to a large number of hydrocarbon data collected by DNV. Furthermore, delayed ignitions may cause flash fires and explosions depending on the system's geometry. The default probability for flash fires was assigned to 0.6, while the probability of 0.4 for explosions for releases of flammable liquids. In addition, deflagration was assumed to be the only type of explosion that may occur in a confined space since detonations require strong ignition sources and confined space, which is unlikely to happen on board ships [90].

4.6.2. Consequence modelling

Release rate

The ignition probability of continuous releases is dependent on the released mass flow rate. Therefore, it is necessary to accurately estimate the flow rates of hydrogen leakages. Various methods for calculating leakage rates have been proposed in the literature, including the use of the Bernoulli equation combined with an orifice discharge coefficient or assuming an isentropic process. However, the accuracy of estimated mass flow rates using these methods has not been extensively validated. Thus, the aim of this subsection is to identify the most suitable method for calculating leakage rates.

Three different release rate models were discussed: a) the Bernoulli equation with discharge coefficient; b) the isentropic process equation according to Center for Chemical Process Safety guidelines; c) Nagase et al. model with under-expanded choke flow [78]. The first two models were most commonly used in hydrogen QRA studies. The formulations of these two methods are shown in equation 4.14 and 4.15.

$$\dot{m_A} = CA\sqrt{2\Delta P\rho} \tag{4.14}$$

$$\dot{m_B} = CA\sqrt{k\rho P(\frac{2}{k+1})^{\frac{k+1}{k-1}}} \tag{4.15}$$

The equation for calculating the leakage flow rate involves several variables, including the discharge coefficient (C), leakage area (A), pressure difference (ΔP), storing pressure (P), hydrogen density (ρ), and the ratio of specific heat capacity at constant pressure to constant volume (k). Despite the availability of this equation, it is important to validate the calculated leakage flow rates with experimental data to ensure accuracy. Figure 4.12 shows a significant deviation when comparing the evaluated mass flow rates with LH2 experimental data conducted by FFI [56]. The calculated leakage rates for model A, which used a discharge coefficient of 0.6, were found to be 4-5 times larger than the FFI experiments, while model B showed 2-3 times larger rates. Two potential reasons for this discrepancy are friction pressure losses and under-expanded momentum behavior.

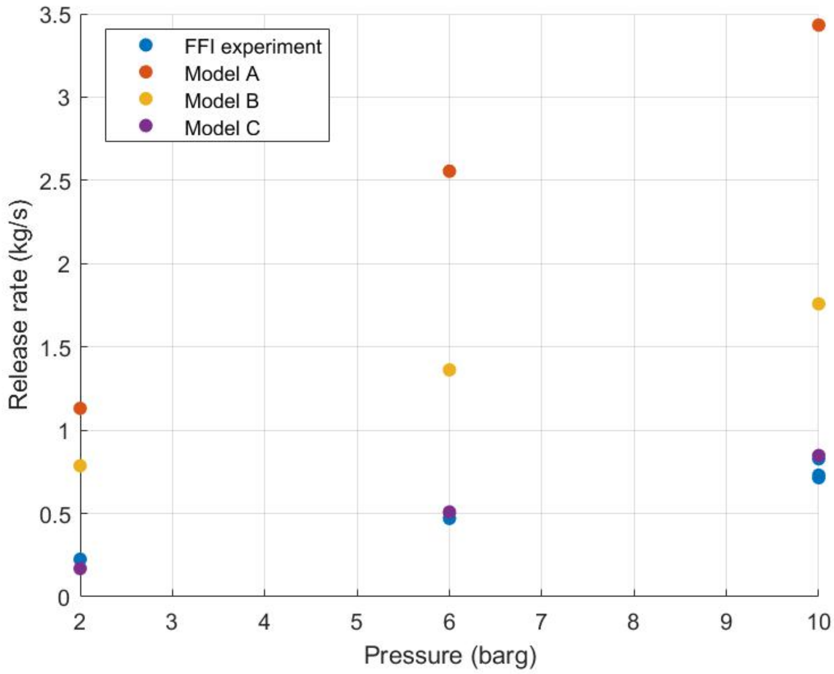

Figure 4.12: Comparison of three flow rate models with FFI experiment.

The most accurate model for estimating mass flow rates is Model C, which assumed that the hydrogen is in a saturated state at the exit of the leakage hole and predicts a choked flow behavior due to the differences between the initial and atmospheric pressure. A shrink coefficient of 0.8 was found to provide the best prediction of release rates, and the absence of hydrogen pools in all horizontal release tests from FFI supports the assumption of saturated gas. The choked, under-expanded theory is illustrated in Figure 4.13, where the exit velocity reaches one Mach number at the entrance, and a choked effect occurs. The main difference between this method and Model B is the density term in the formula, where the density of LH2 was used in Model B. In contrast, the density of saturated H2 was applied in Model C. The formulation is presented below:

$$\dot{m}_c = \sqrt{k(\frac{2}{k+1})^{\frac{k+1}{k-1}}}\frac{p_{01}cA}{\sqrt{RT_{01}}} \tag{4.16}$$

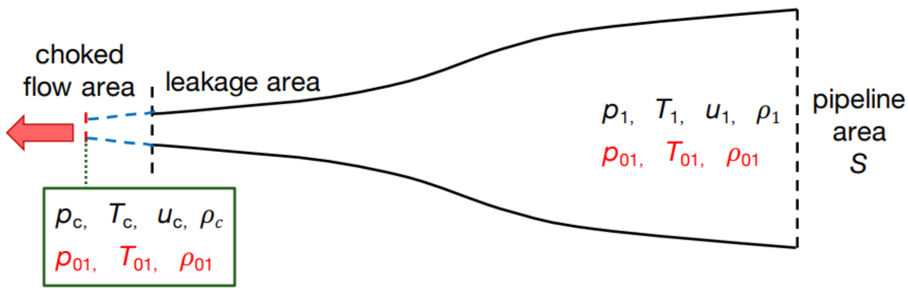

Figure 4.13: One-dimensional isentropic steady model of Model C [78].

4.6.3. Fires

As discussed in section 2.2.2, four potential fire-related consequences were assessed, which are jet fires, flash fires, pool fires, and gas fireballs. Among these hazards, criteria such as concentration, flame length and width, and heat flux will be modeled in this section, where the most suitable method will be implemented in the QRA system.

1. Jet fire

A number of small-scale cryogenic hydrogen jet fire tests have been conducted, all of which indicate that low-temperature releases result in larger jet fire areas and stronger heat radiation. For this study, three literature sources were selected that assume saturated gas releases under different conditions. However, it is important to note that these studies have only been validated through small-scale experiments and may not be applicable to large-scale scenarios, such as those that may occur with high-fractional area leakages. Friedrich et al. [1] analyzed experimental data at temperatures ranging from 35 to 65 K and pressures from 0.7 to 3.5 MPa, and proposed equations for ignition distance, $X_{IG} = 0.745d(\rho_0)^{1/2}$, and heat radiation, $q(r) = \frac{\dot{m}\Delta H X_{md}}{4\pi r^2}$. Where X_{IG} is the maximum ignition distance, m; d is the release diameter, m; ρ_0 is the release density, kg/m^3; $q(r)$ is the measured heat flux density at r, W/cm^2; $\dot{m}$ stands for release mass flow rate, g/s while ΔH is the hydrogen heat of combustion, kJ/g.

For conditions with higher temperatures, Panda and Hecht [87] conducted experiments ranging from 37 K to 295 K and 2-6 bar. They presented the flame length as a function of the more conventional Reynolds number, Re, and formulated the radiant fraction, x, as a function of the global flame residence time, $a_p \tau_G {T_f}^4$. Equations 4.17 and 4.18 show these relationships, where L represents the flame length, D is the hole diameter, a_P is the Planck-mean absorption coefficient for an optically thin flame (0.23 for hydrogen), T_f is the adiabatic flame temperature.

$$\frac{L}{D} = 0.86 * \sqrt{Re} \tag{4.17}$$

$$x = 9.45 * 10^{-9} [a_p \tau_G {T_f}^4]^{0.47} \tag{4.18}$$

Although Equation 4.17 showed a good agreement in cryogenic conditions, but the experimental data at room temperature are seriously scattered. Therefore, Yu et al. [122] governed the series of experiments and proposed the wider-range correlation for hydrogen jet fire with a temperature range of 133 - 273 K and a pressure range of 2 –400 bar. The flame characteristics can be shown as follow:

$$\frac{L_f}{d_j} = 530 * {p_0}^{0.43} * \frac{T_{atm}}{T_0}^{0.35} \tag{4.19}$$

$$\frac{W_f}{d_j} = 95 * {p_0}^{0.43} * \frac{T_{atm}}{T_0}^{0.35} \tag{4.20}$$

To compare the three jet fire models with our system, it was found that the method proposed by Yu et al. [122] is the most suitable. Method 1 shows a higher level of uncertainty with the experimental data, while the Reynolds number of our system does not fall within the applicable range for method 2.

To evaluate the risk of jet fires, an accurate assessment of heat radiation flux is crucial. The hazard level can be estimated using Equation **??**, which considers the lethal threshold of $35; KW/m^2$ heat radiation flux and radiation fraction, thereby enabling the determination of the fatal distance from the flame center. Additionally, Miller [73] investigated the geometry of the jet fire and found that the maximum radiation fraction occurs at a distance of 2/3 of the flame length, with a value of approximately 0.06. This knowledge can be leveraged to describe the shape of the jet fire and predict its potential consequences, including the fatal distance.

2. Flash fire

The flash fire is a phenomenon that occurs when the released hydrogen ignites and propagates horizontally to a concentration of at least 8% v/v and upward to a concentration above 4% v/v. For liquid hydrogen, a CFD-based mathematical model developed by Liu et al. [67] was selected to estimate the consequences of a flash fire as a function of wind speed and release rate, as depicted in Figure

4.14. The model results were found to be consistent with the HSL LH2 spill experiment. Equation 4.21 represents the mathematical formulation, which includes a safety coefficient γ ranging from 1.15 to 1.2 to ensure a conservative approach. The release rate Q and wind speed U are measured in kg/s and m/s, respectively.

$$L = \gamma \dot{m}^{0.1886}(-2.727U^2 + 21.37\dot{m}^{0.12}U + 12.38) \tag{4.21}$$

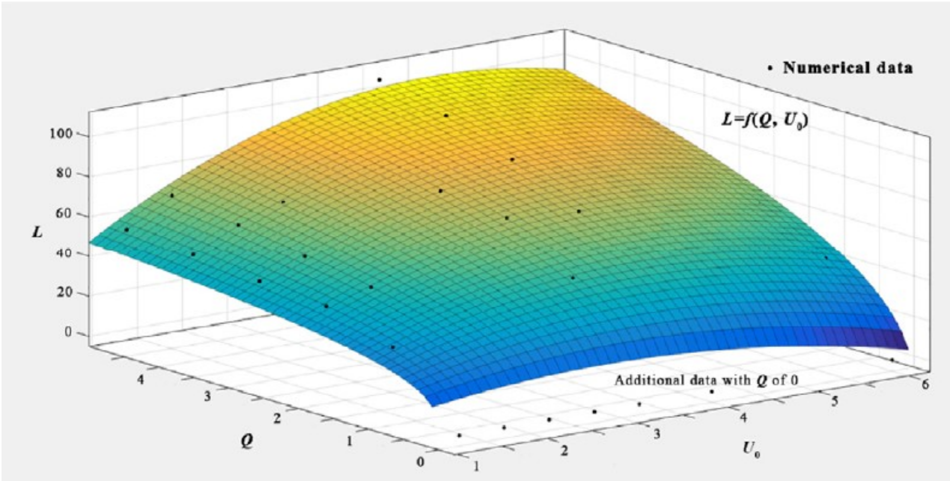

Figure 4.14: 8% hydrogen vol. concentration as a function of wind speed and released rate [67].

The dispersion of gaseous hydrogen has been the subject of numerous investigations, and the concentration can be expressed as a function of the diameter of the leakage hole, d, and the density, ρ_0. The concentration that is deemed fatal is usually set at 8% of CH_2. Furthermore, the concentration at a given distance, x, may be affected by the ambient density, ρ_a.

$$1/CH_2 = 0.011484 + 1.59 * 10^{-4}(\frac{x}{d})(\frac{\rho_a}{\rho_0})^{1/2} \tag{4.22}$$

3. Pool fire

The effective distance of a pool fire resulting from instantaneous liquid hydrogen releases is typically evaluated based on the pool diameter, which can be affected by several factors such as the evaporation rate, which, in turn, is influenced by weather conditions and the type of ground material. To estimate the LH2 pool diameter, an equilibrium LNG pool expression was adapted from Woodward and Pitblado [43], which was found to be applicable in the LH2 pool case. The expression includes the evaporation rate G_{eva} and was estimated to be $0.022kg/m^2/s$ for the concrete ground type under consideration. This formulation is in good agreement with the results obtained using commercial software FLACS, as shown in Figure 4.15.

$$R = (\frac{\dot{m}}{\pi G_{eva}})^{1/2} \tag{4.23}$$

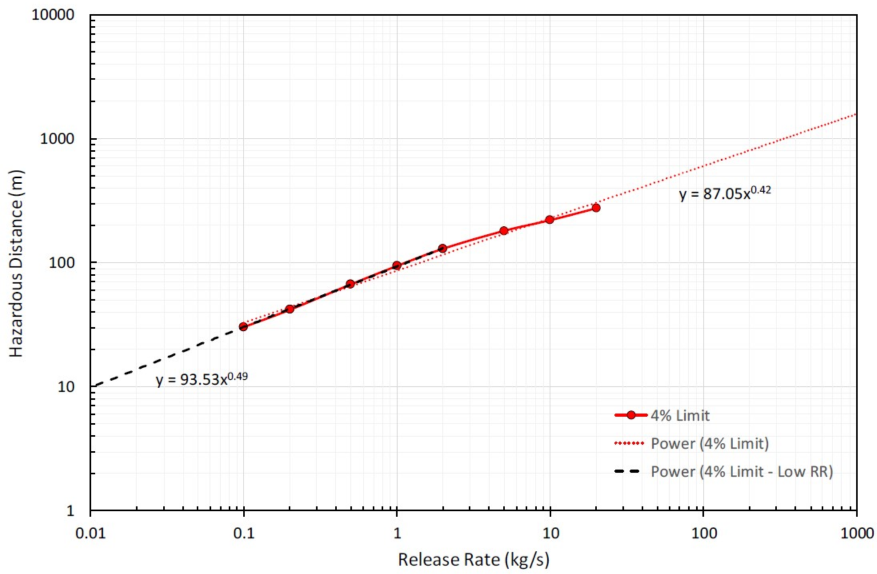

Figure 4.15: Pool fire radius expression shows good agreement with the FLACS simulation results [43].

4. Fireball

Fireball simulation methods have been extensively studied as a well-known hazard, and almost all models treat the fireball as a sphere based on observations and videos, with the fireball diameter and heat radiation determining the consequences (100% fatal area). The fireball diameter can be estimated using Equation 4.24, which was developed by Roberts [96]. In the equation, m_f represents the mass of fuel involved in kilograms, and D denotes the diameter of the sphere in meters.

$$D = 5.8 * {m_f}^{1/3} \tag{4.24}$$

To simulate heat radiation, a solid-flame approach has been used in previous studies [10, 70]. The heat flux at a specific distance from the fire can be calculated as a function of several parameters, including the surface emission power (SEP), atmospheric transmissivity (τ_a), and view factor (F_{view}). SEP can be calculated using an energy balance relation that takes into account the fraction of heat radiated (F_s), the heat of combustion (h_c), the burning rate (q_s), and the surface area of the fireball ($A_{fireball}$). Equation 4.26 shows the calculation of SEP, where the surface area of the fireball is estimated based on its spherical shape. The burning rate q_s depends on the mass of fuel m_f and its duration t_d, which are calculated using the equations listed below. Finally, the view factor F_{view} is based on the geometric relationship between the spherical fireball and a flat target located outside the fireball at a distance h in meters.

$$q = F_{view} * \tau_a * SEP \tag{4.25}$$

$$SEP = \frac{F_s * h_c * q_s}{A_{fireball}} \tag{4.26}$$

$$A_{fireball} = \pi * D^2 \tag{4.27}$$

$$q_s = \frac{m_f}{t_d} \tag{4.28}$$

$$t_d = 0.45 * m_f^{1/3} \quad For \;\; momentum - dominated \;\; fireballs \tag{4.29}$$

$$t_d = 2.6 * m_f^{1/6} \quad For \;\; buoyancy - dominated \;\; fireballs \tag{4.30}$$

$$F_{view} = \frac{R^2}{h^2} \tag{4.31}$$

4.6.4. Explosions

Explosions represent one of the most severe consequences that can occur in a hydrogen system. While extreme detonation is not a possibility due to the geometry of the LH2 tank, which will be installed in an open space, it is still essential to estimate positive overpressures resulting from potential explosions (deflagrations). Two popular methods used to estimate these overpressures are the TNO multi-energy and Baker-Strehlow-Tang (BST) methods. The TNO multi-energy method was selected for this study because of its better fit with existing experimental data on hydrogen explosions. In contrast, the BST method, which uses Mach numbers to estimate overpressures, always under-predicts the effects of hydrogen explosions due to the lack of ignition strength as a parameter in its model [72].

However, it should be noted that the overpressures estimated using the TNO multi-energy method are based on class numbers 1-10. The guideline to choose the appropriate class number was developed by Melani et al. [72] and can be found in Table 4.9. For this study, class number 7 was selected as the default number for the QRA tool, considering that no high ignition sources will be present on board the ship, and the system geometry is not expected to produce significant changes. Figure 4.16 shows the modeling details for each class number, while the scaled distance ($\bar{R}$) and dimensionless maximum static overpressure ($\Delta \bar{P}_s$) are presented in Equations 4.32 and 4.33, respectively. Here, R represents the distance in meters, P_a is the atmospheric pressure in Pascals, E is the combustion energy of the fuel-air mixture in stoichiometric quantity measured in joules per kilogram, and P is the positive over-pressure in Pascals.

Table 4.9: Guidelines for choosing the class number for the TNO multi-energy method for hydrogen explosion [72].

Ignition power	Obstruction	Volume (m^3)	Class number
Low ($0 - 150\ J$)	0 to 1%	5 to 2094	3
	1 to 15%	5 to 300	5 or 6
	4.40%	17	7 or 8
High ($150 - 5.2 * 10^4\ J$)	0%	300	9

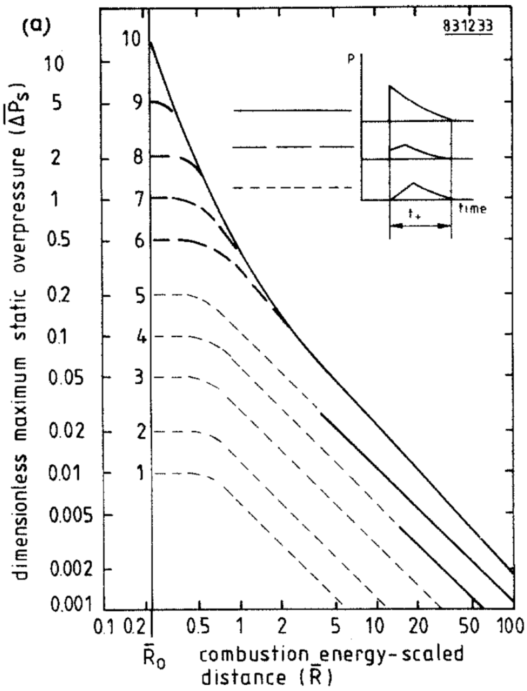

Figure 4.16: Multienergy method for overpressure distance [112].

$$\bar{R} = R * (\frac{P_a}{E})^{1/3} \tag{4.32}$$

$$\Delta \bar{P}_s = \frac{P}{P_a} \tag{4.33}$$

4.6.5. Non-ignited events

Non-ignited events are generally considered to be less severe than ignited events, but they can still have harmful effects. In the liquid hydrogen subsystem, the release of cryogenic temperatures can cause frostbite in humans. According to [43], the threshold for cryogenic injury is 200K. The author also investigated the hazardous distance for 200K cryogenic frostbites and found that it is significantly shorter than the 8% LFL criteria, as shown in Figure 4.17. Although the given frostbite effect will not cause fatality, it has a much shorter hazardous distance than other ignited events. Despite this, cryogenic effects have not been considered a significant risk in this study or in general risk criteria guidelines. Nevertheless, the consequence model for the 200K hazardous distance has been implemented in this QRA tool for further research.

Regarding other non-ignited events, no harmful effects were reported and investigated. In this design configuration, the operational pressures for the GH2 subsystem are in the range below $10bar$. Therefore, the release pressure wave will not cause hazards to humans.

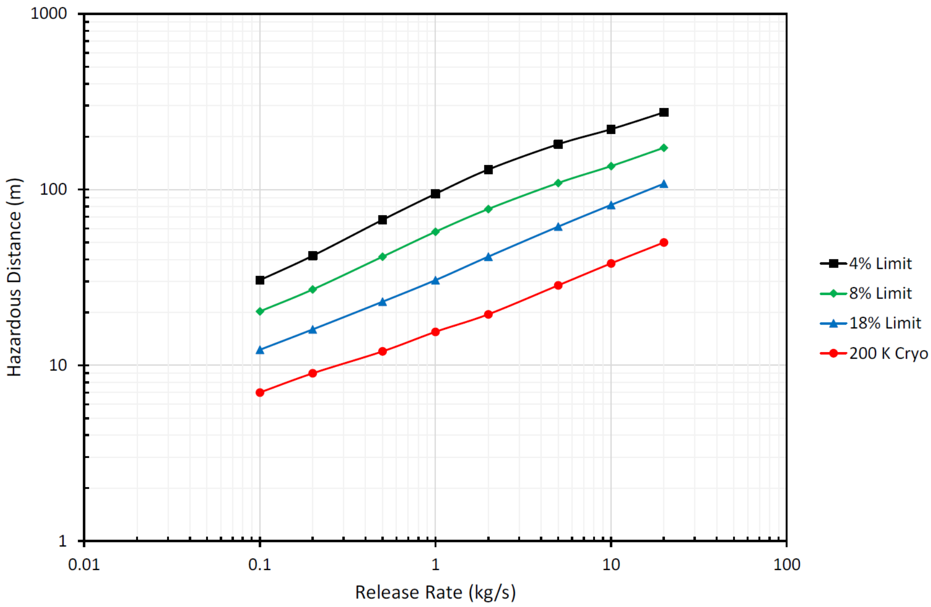

Figure 4.17: Modeling result of 200K cryogenic hazardous distance versus other LFL criteria [43].

4.7. System overview

To enable the automatic and efficient compilation of quantified risk, a Simulink model was developed using the aforementioned logic and methodologies. Figure 4.18 provides an overview of the system, and a more detailed diagram can be found in Appendix C. The model begins with the frequency assessment stage, where the leakage frequencies for both LH2 and GH2 components are implemented. Based on the logical map outlined above, each scenario is distributed to different states based on release types (Green block). Next, we perform the probability assessment by substituting estimated leakage rates into the module to calculate the ignition probability (Blue block). In the following light orange block, various consequence models are implemented to evaluate the fatal distance for each event. Finally, by associating the frequency and consequence of each event, the final risk can be compiled to check if the system meets the acceptance criteria.

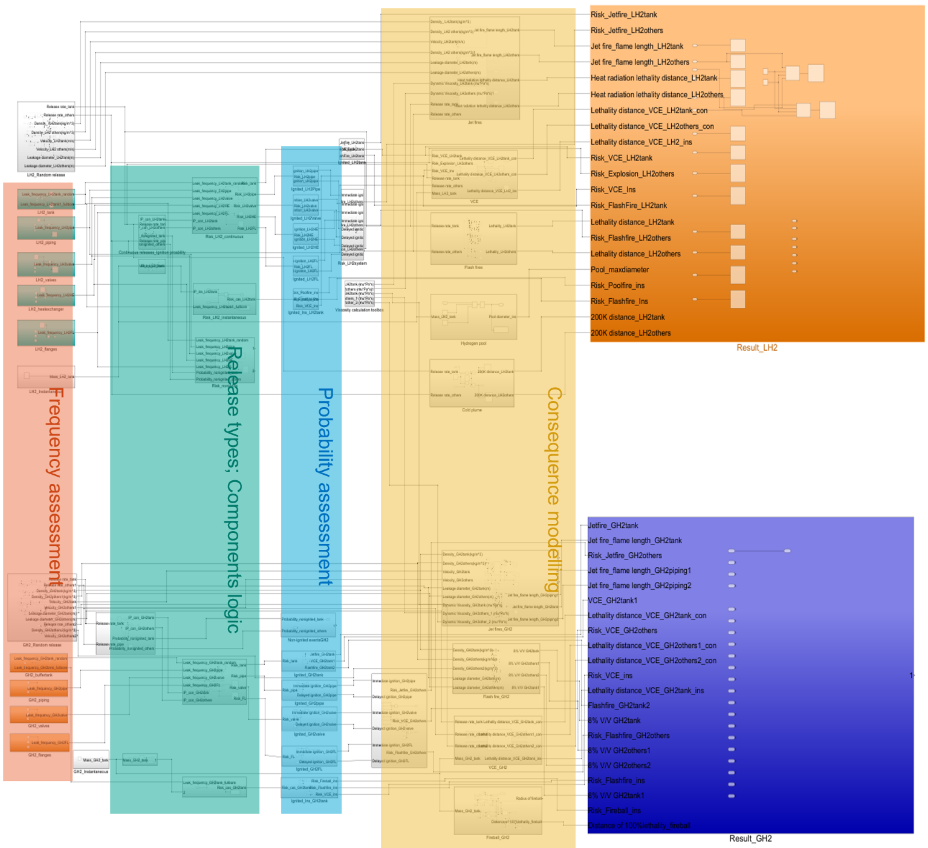

Figure 4.18: The developed Simulink model for the LH2 QRA tool, each block is denoted in a different color.

This page intentionally left blank

5 Modelling result

The definition of risk as the combination of frequency and consequence is widely accepted. Especially in the context of quantitative risk assessment, the results of this assessment are often expressed as Individual Risk (IR) and Societal Risk (SR). IR measures the risk to a single person in the proximity of a hazard and considers the potential severity of the injury, the likelihood of occurrence, and the time frame over which the injury might occur. On the other hand, SR measures the risk to a group of people.

In this chapter, the results of the risk assessment will be presented through individual risk contour plots and societal risk F-N curves. The design will be evaluated against acceptance criteria to determine if it is safe. Critical factors and scenarios will be analyzed, and mitigation measures will be suggested and implemented to reduce the overall risk.

5.1. Individual risk

Individual risk assessment is often represented through risk contours, where each contour represents the number of facilities that experience an event per year. Figure 5.1 displays the initial system's IR contours relative to the scale of the reference vessel. The individual risk on board a ship is considered a first-party risk as only crew members will be present, and the IR criteria should not exceed 10^{-4} per year. The line plot of IR against distance for the initial design is shown in Figure 5.2. Comparing this plot with the acceptance criteria showed that the risk distance of 10^{-4} was up to $51m$, covering almost half of the vessel. This result was unacceptable and indicated mitigation measures should be taken to improve the system's safety. However, it is important to note that this calculation assumed a 24/7 operational profile for the ship without considering its actual operational profile, which is not possible in real cases.

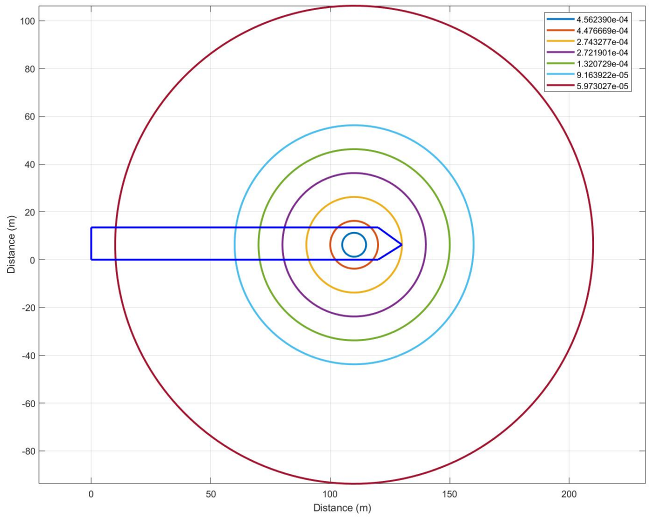

Figure 5.1: The IR contours for the original system design without mitigation measures, the vessel's outline is also plotted to better understand the effect of consequences.

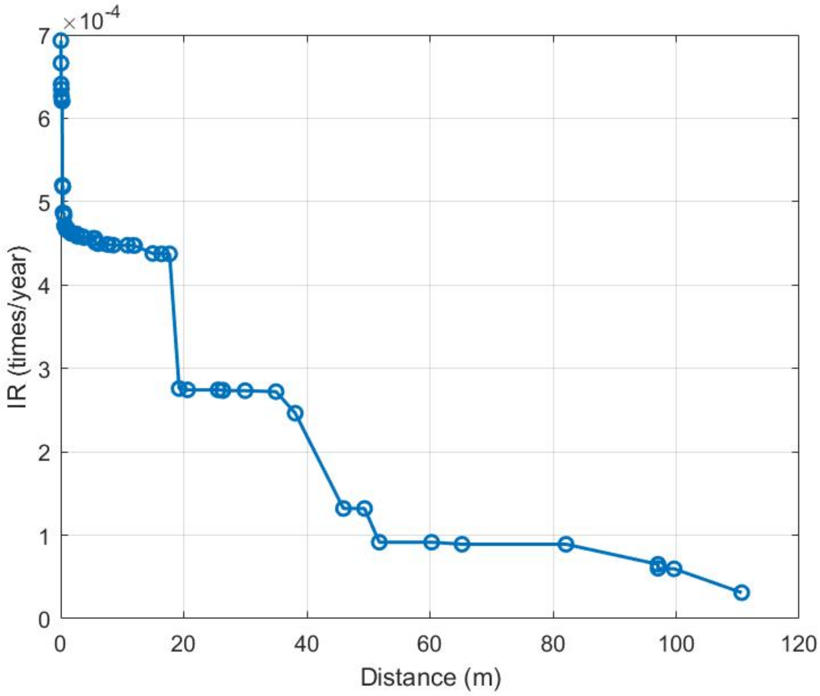

Figure 5.2: The IR line plot for the original system design without mitigation measures.

To determine the impact of each factor on risk, the severity ranking for each scenario is consolidated in Table 5.1. It can be observed that the highest impact on the total risk was caused by explosions resulting from small-scale leaks in the LH2 tank. Explosions of 0.01 and 0.1 LH2 tanks accounted for more than 55% of the total risk, followed by the 0.01% gaseous piping system explosions and flash fires from 0.01% LH2 tank leaks, which contributed approximately 15% and 6% respectively.

Similarly, the effect of each subsystem and the hazard is listed in Table 5.2 and 5.3. It was clear that the LH2 tank and VCE were the most critical subsystem and hazards. However, these contributions were only considered from the frequency perspective, whereas the fatal distance was evenly essential for risk assessment. For instance, in the case of 0.01% GH2 piping explosion, the lethal distance was only 0.26m though it accounted for 14.56% of total risk frequency. To solve this problem, a risk matrix was also applied to better understand each category's risk impact.

Table 5.1: Individual risk contributions for each scenario.

Scenarios	Frequency (Times/year)	Percentage (%)	Distance (m)
0.01 VCE LH2 tank	1.62E-04	23.31	17.69
0.1 VCE LH2 tank	1.14E-04	16.49	38.11
0.01 VCE GH2piping2	1.01E-04	14.56	0.26
0.01 Flash fire LH2 tank	4.04E-05	5.83	49.38
0.01 VCE GH2piping1	3.12E-05	4.50	0.36
0.1 Flash fire LH2 tank	2.86E-05	4.12	99.67
0.01 Jet fire GH2 piping2	2.70E-05	3.89	0.04
0.01 Jet fire LH2 tank	2.58E-05	3.73	34.99
0.01 Flash fire GH2 piping2	2.52E-05	3.64	0.05
1 VCE LH2 tank	2.40E-05	3.47	82.11
0.1 Jet fire LH2 tank	1.83E-05	2.64	110.65
0.1 VCE GH2piping2	1.21E-05	1.75	0.56
100 VCE LH2 piping	9.53E-06	1.38	12.00
0.01 Flash fire GH2 piping1	7.80E-06	1.13	0.11
Others	6.65E-05	<10	-

Table 5.2: Individual risk contributions for each subsystem.

Subsystem	Frequency (Times/year)	Percentage (%)
LH2 tank	4.34E-04	62.32
LH2 piping	2.75E-05	3.95
GH2 tank	1.52E-06	0.22
GH2 piping1	5.40E-05	7.77
GH2 piping2	1.79E-04	25.75
Total	6.96E-04	100

Table 5.3: Individual risk contributions for each hazard.

Hazards	Frequency (Times/year)	Percentage (%)
VCE	4.81E-04	69.20
Jetfires	9.06E-05	13.02
Flashfires	1.21E-04	17.40
Fireball	4.89E-08	0.01
Poolfire	2.57E-06	0.37

The risk matrix is composed of frequency (likelihood) and severity, whereas a 5*5 matrix is widely applied in the risk assessment field. Referring to the risk matrix from IDEALHY project [32], the risk matrix, and frequency and severity categories are shown as follows:

Likelihood

- 1: Extremely Unlikely (about 10^{-9} per year)
- 2: Unlikely (about 10^{-7} per year)
- 3: Possible (about 10^{-5} per year)
- 4: Very Possible (about 10^{-3} per year)
- 5: Probable (about 10^{-1} per year)

Consequence severity

- 1: Slight Effect (Cause almost no harm, fatality distance no more than 5m)
- 2: Minor Damage (Cause fatality more than 5m)
- 3: Moderate Damage (Cause fatality more than 10m)
- 4: Major damage (Cause fatality more than 30m)
- 5: Massive damage (Cause fatality more than 50m)

QRM			Consequence Severity				
			1	2	3	4	5
			Slight Effect	Minor Damage	Moderate Damage	Major Damage	Massive Damage
Likelihood	1	Probable	Low	Medium	High	High	High
	2	Very Possible	Low	Medium	Medium	High	High
	3	Possible	Low	Low	Medium	Medium	High
	4	Unlikely	Low	Low	Low	Medium	Medium
	5	Extremely Unlikely	Low	Low	Low	Low	Medium

Figure 5.3: Quantitative Risk Matrix.

Of the 75 scenarios evaluated, only three have been identified as high risks, 21 were considered medium risks, and the remainder was considered low risks. These three high-risk scenarios were the 0.1% LH2 tank jet fire, 0.1% LH2 tank flash fire, and 1% LH2 tank explosion, which yielded divergent results compared to the findings presented in the tables above. If the assessment were solely based on individual risk criteria, the focus would be to lower the frequency of the highest contributors to risk. However, after applying the Quantitative Risk Matrix (QRM) method, the scenarios that required the most mitigation measures have changed.

To mitigate the risk, the highest contributors from both the IR contours and risk matrix will be addressed. First, considering the IR contours, the top three scenarios were all associated with explosion events, as these have higher frequencies due to the high likelihood of ignition and occurrence. Regarding the risk matrix, the top three scenarios were also related to the LH2 tank, as it had the highest predicted frequency of leakage among all components. This result can be attributed to the LH2 tank's 2.4m cross-section diameter and high density within the system.

5.1.1. Operating time

The cases discussed above were all assumed to operate 24/7, but these would not be realistic for the vessels. The operational profile for inland vessels is around 20% a year, while other times are in the harbor. The result of implementing 20% operating time is shown in Figure 5.4 and 5.5. Compared to the risk criteria of 10^{-4}, only the distance within 1 meter was considered unsafe. Considering that in normal situations, no staff members would work and stay within a meter close to the tank connection space. Consequently, it can state that this liquid hydrogen-based propulsion design was approved from the perspective of individual risk. Further, if there is a need to prolong the operational time, the forbidden distances were also discussed and shown in Figure 5.6. It is evident that longer operational times result in larger forbidden areas. Thus, more reduction measures should be implemented for higher operational demand vessels.

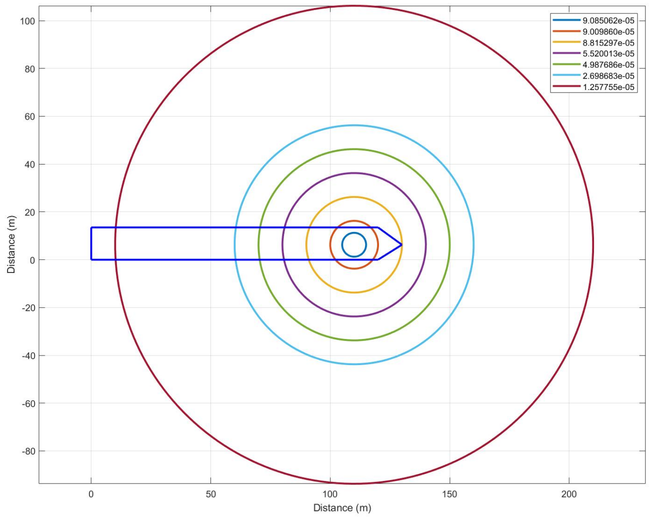

Figure 5.4: The IR contours for 20% operatiing time without mitigation measures, the vessel's outline is also plotted to better understand the effect of consequences.

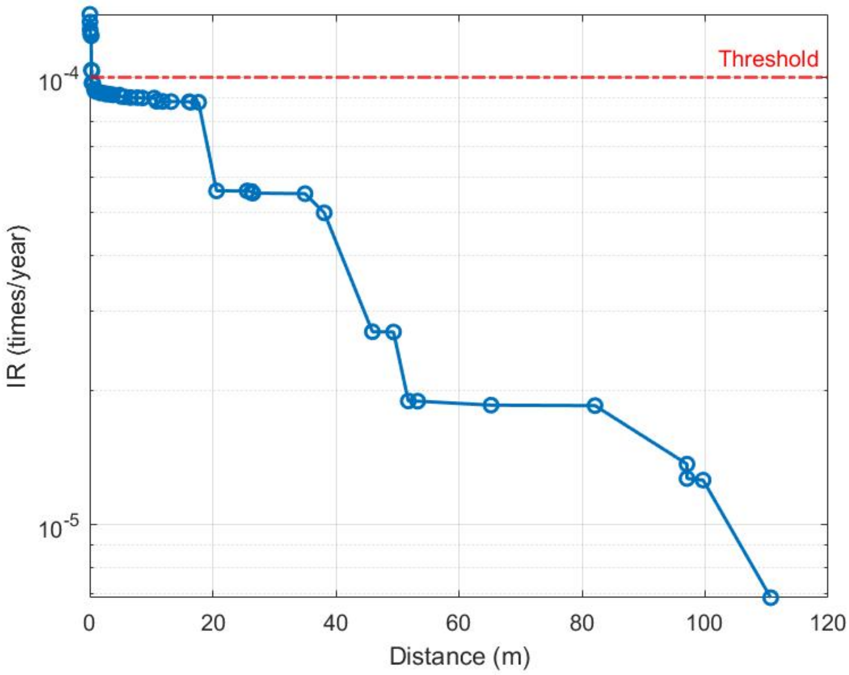

Figure 5.5: The IR line plot for 20% operating time.

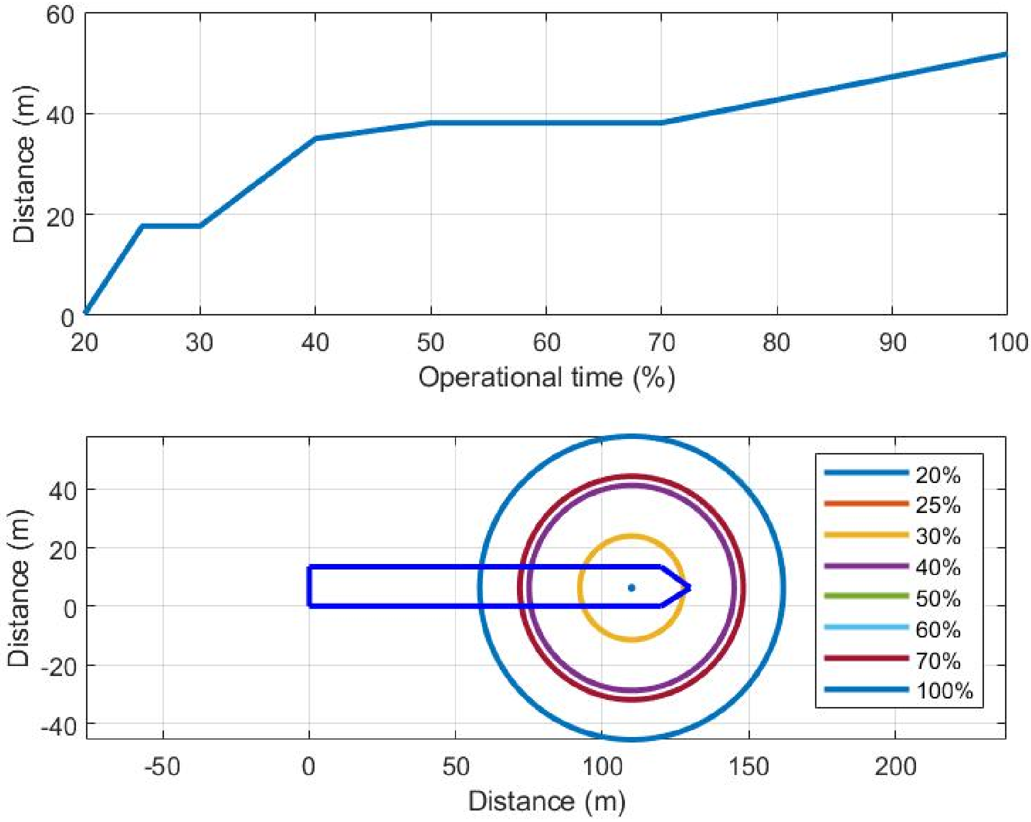

Figure 5.6: Forbidden distances against operational time, only the operational time below 20% is acceptable without mitigation measures.

To ensure the overall safety level, each scenario of 20% operating time was listed in the table below. Moreover, each result was substituted in the QRM to assess the risk. The result from QRM also proved that there are no scenarios identified as "high-risk", as can be shown in Figure 5.7, where the numbers of scenarios are compiled in matrix cells.

QRM			Consequence Severity				
			1	2	3	4	5
			Slight Effect	Minor Damage	Moderate Damage	Major Damage	Massive Damage
Likelihood	5	Probable	0	0	0	0	0
	4	Very Possible	0	0	0	0	0
	3	Possible	1	0	1	1	0
	2	Unlikely	22	3	6	2	12
	1	Extremely Unlikely	10	3	6	1	7

Figure 5.7: QRM for 20% operating time.

5.1.2. Mitigation measures

Based on the above discussions, the primary measures for reducing the risk were focused on mitigating the impact of explosion events and the LH2 tank. The over-pressure distance is mainly attributed to the mass of fuel, which is a function of the hydrogen's delayed time and leakage rate. In the initial design scenario, the delayed time was set to 20 seconds, while the leakage rate was estimated based on the system's pressure and temperature. To reduce the total mass of hydrogen, implementing an emergency shut-down (ESD) system could be a potential solution. The ESD system would rapidly shut down the hydrogen supply from the LH2 tank, thereby preventing continued releases from the LH2 piping, GH2 piping 1, and GH2 piping 2. Additionally, to reduce the leakage rate, a reduction in the cross-sectional area dimensions could be considered, as the current assessment considered leakage holes based on cross-sectional area fractions. A previous study has also suggested separating a large tank into smaller tanks to reduce the risk, and the effectiveness of this measure will be evaluated further.

Emergency shut-down system (ESD)

Implementing the Emergency Shut-Down (ESD) system was aimed at limiting the leak time in the event of a hydrogen leakage. The simulation assumed the ESD system could effectively shut down the hydrogen leakages within 10 seconds. This results in a fixed maximum hydrogen accumulated mass, regardless of the ignition delay time. The data presented in Figure 5.8 demonstrates that for certain IR levels, the fatal distances decrease as the delay time becomes shorter, particularly in the case of explosion, pool fire, and flash fire events which were related to delayed ignition. Figure 5.9 depicts the $2.8 * 10^{-4}$ risk contour among these simulations. It was evident that the implementation of the ESD system significantly lowered the lethal distance.

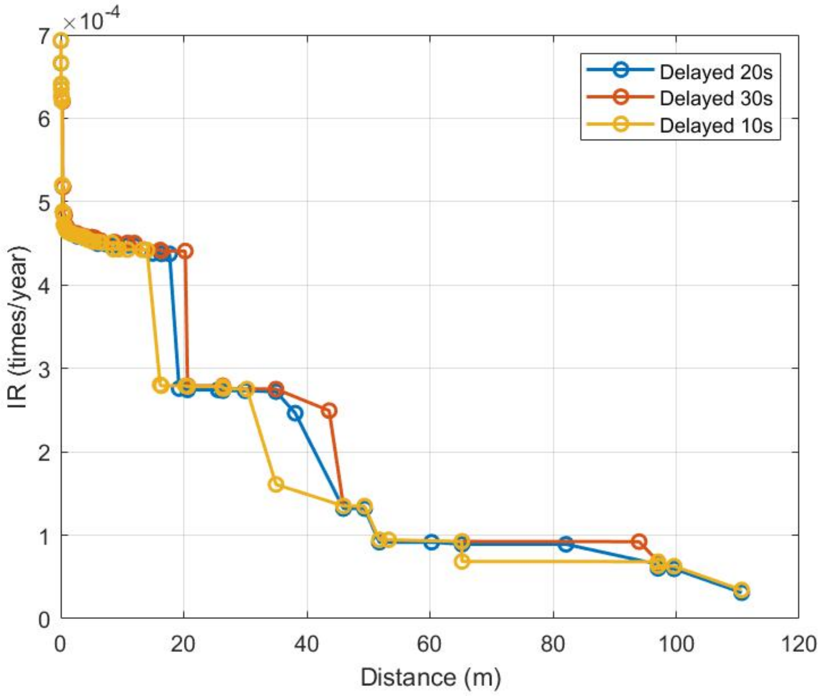

Figure 5.8: The risk line plot of $2.8 * 10^{-4}$ IR for different delayed ignition times

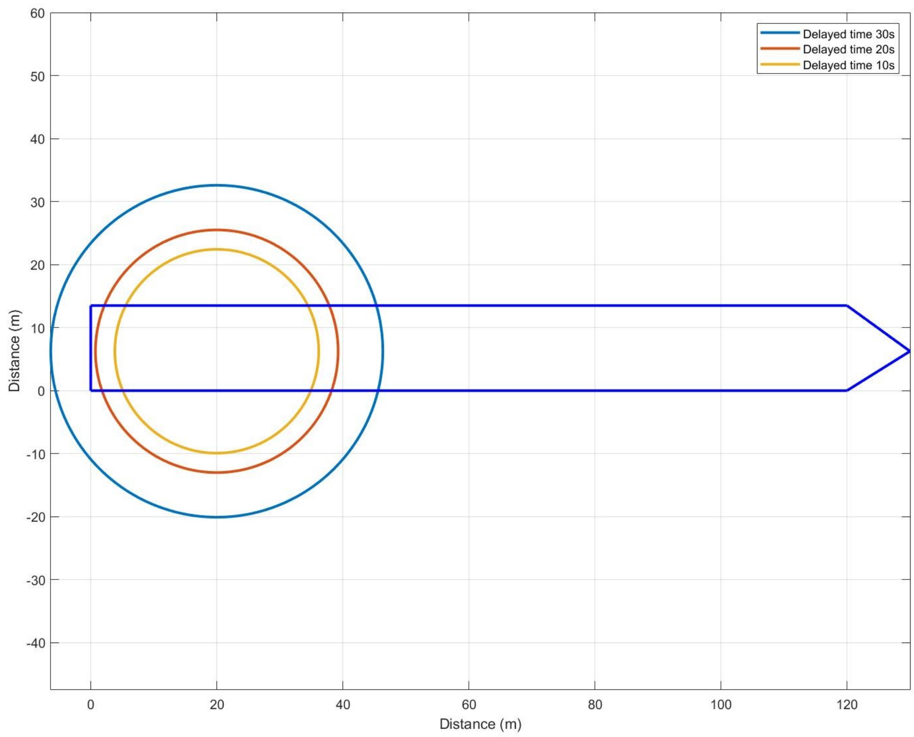

Figure 5.9: The contour plot of $2.8 * 10^{-4}$ IR for different delayed ignition times, which represents the effect of the emergency shutdown system.

Separating tanks

The mitigation measure of separating tanks has been suggested to reduce the impact of large-scale hydrogen releases at fatal distances in previous literature [3]. However, it was crucial to acknowledge that the overall risk is a composite of frequency and severity. While separating tanks may lead to a reduction in fatal distance, it may also augment the frequency of hydrogen leaks, as each tank constitutes an independent occurrence. This trade-off is demonstrated by the simulation results of different tank configurations, as illustrated in Figure 5.10. The figure shows that separating tanks indeed results in a decrease in the fatal distance in the case of large-scale releases. However, it is noteworthy that the fatal distances remain constant for low hydrogen release rates, such as those under 0.01% and 0.1%, as the released mass does not reach the maximum tank capacity within the given delayed time of 20 seconds. As depicted in Figure 5.11, the results of the individual risk (IR) assessment reveal that the effect of increased frequency overpowers the benefit of reduced fatal distance. In addition, incorporating these configurations into a risk assessment method, such as the Quantitative Risk Matrix (QRM), has resulted in an increase in incidents classified as ”high risk”.

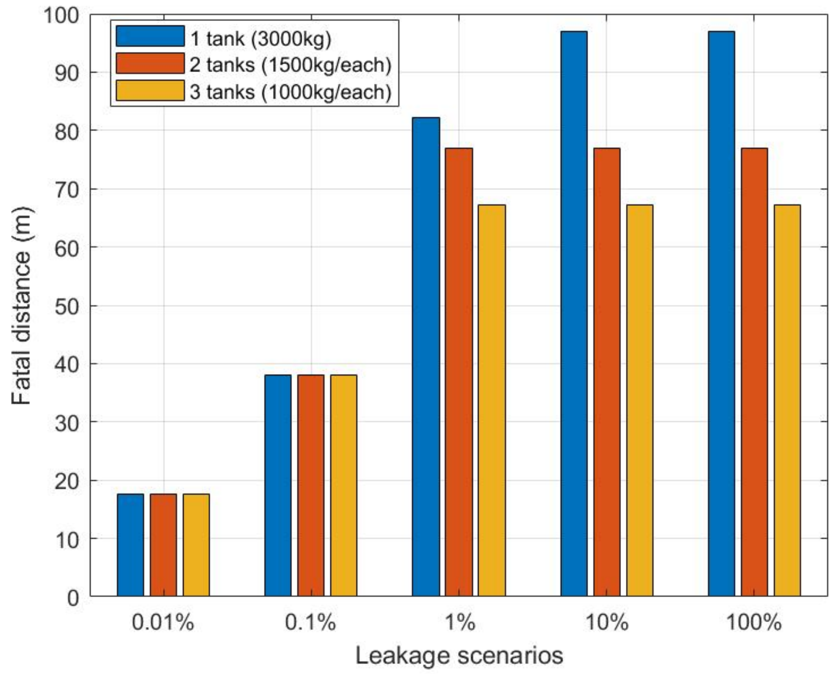

Figure 5.10: Fatal distances for different tank configurations, in the LH2 leakage scenario, explosion as a consequence.

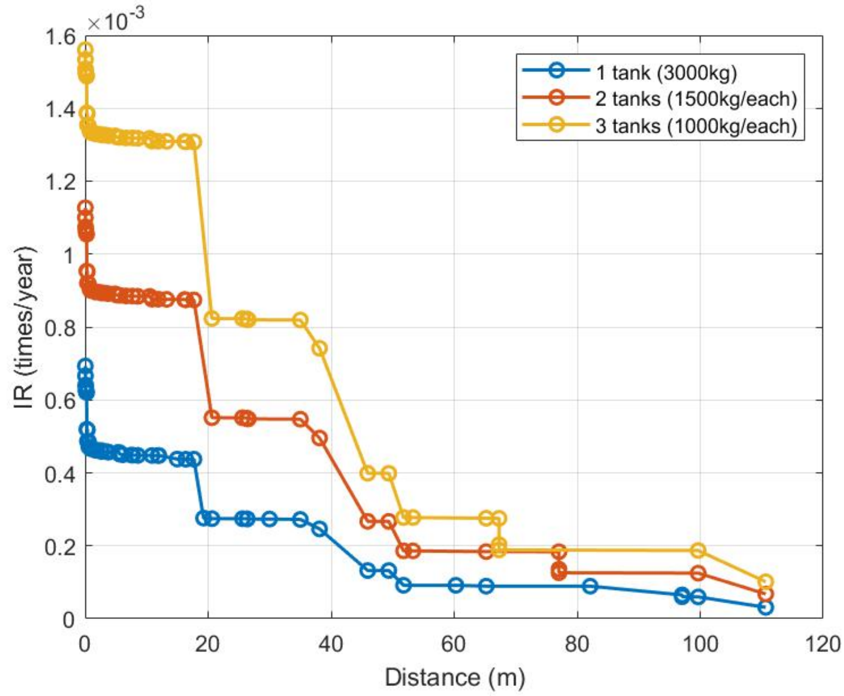

Figure 5.11: Individual risk of three different tank configurations.

Minimizing pipe dimensions

As previously discussed, the cross-sectional dimensions of the piping systems directly impact the release rates of hydrogen. Smaller piping dimensions result in lower release rates, which not only affect the fatal distances of incidents such as jet fires and flash fires, but also the probabilities of ignition. This presumption is demonstrated in Figure 5.12, where the lowest fatal distance is observed for the 8mm pipe diameter at a risk level near $1.3 * 10^{-4}$ and within a distance of 20 meters. It should be noted that the distances affected by the piping dimensions are typically within a 20-meter range. A zoomed-in version of the figure, depicted in Figure 5.12, further emphasizes that reducing the piping dimensions can decrease both the severity and likelihood of incidents.

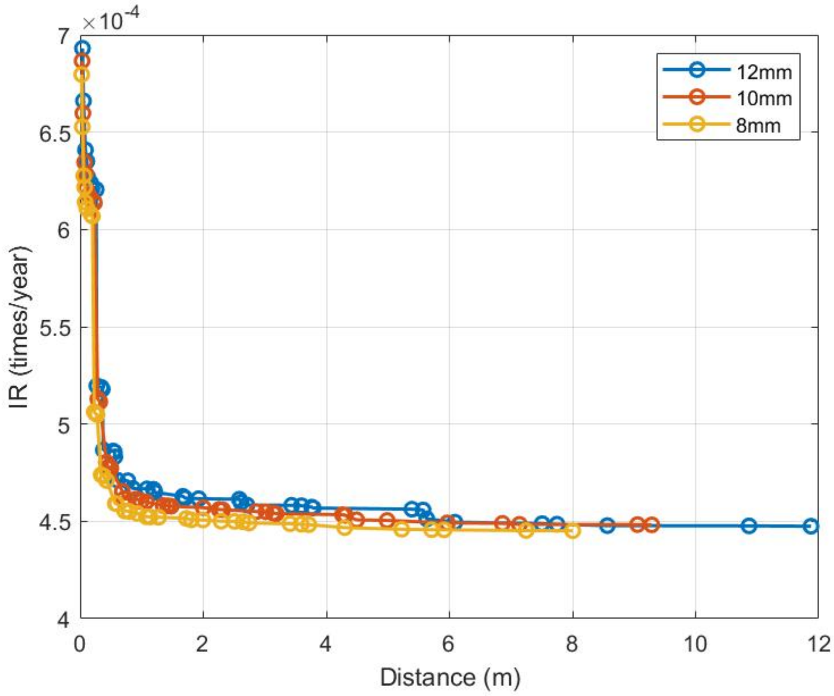

Figure 5.12: Individual risk of three different pipe diameters.

Vertical walls

Other risk reduction measures have not been simulated in this Quantitative Risk Assessment (QRA) system, primarily due to the high degree of uncertainty associated with the assumptions made. One direct method of mitigating the severity of releases is through the design of vertical walls surrounding the hydrogen tank and tank connection space. This design can help prevent the spread of fire consequences and over-pressures horizontally, directing them upwards instead. However, one of the main challenges in simulating such designs is the variability in the properties and strength of the material used for the walls. The temperature and pressure encountered at different distances are highly diverse, contributing to a large number of uncertainties that can impact the results of the mitigation measures.

Double wall design

In addition to design measures, reducing the likelihood of releases is another way to mitigate risk. For example, methods such as a double-wall design for tanks and pipes can help reduce the frequency of leaks while reducing the number of components and decreasing the pipe length can directly lower the likelihood of releases. Especially for the LH2 tank design, though the existing LH2 tanks are all equipped with a double-wall design, the expected leakage frequencies in this study are still comparably high to other components, and even an order higher than the CH2 tank. The reason behind this was speculated to be the lack of the LH2 handling database and the nature of the Bayesian theorem. Without exiting LH2 operating data, Bayesian update enables the prediction of the frequencies from CH2 and LNG existing data. However, these predicted results are generic leakage data without considering the special design measures. As a result, the uncertainty of the LH2 leakage frequencies can only be improved until more and more real LH2 data is published.

5.2. Societal risk

Assessing the SR is crucial when evaluating the potential impact of large-scale hydrogen releases. The Frequency-Number (F-N) Curve is a widely used tool for determining the risk of harm to a group of people. The x-axis of the curve represents the number of fatalities, while the y-axis denotes the frequency of N or more fatalities per year. The geometry and distribution of individuals within the area being evaluated can significantly affect the outcome of the SR calculation. The Dutch VROM has established the acceptable criteria for SR [37], with the unacceptable limit represented by Equation 5.1. The range between the negligible criteria, Equation 5.2, and the unacceptable limit is known as the As Low As Reasonably Practicable area.

$$F = 10^{-3}N^{-2} \ \ per \ \ year \tag{5.1}$$

$$F = 10^{-5}N^{-2} \ \ per \ \ year \tag{5.2}$$

Two scenarios were considered in the calculation of SR: 1) during operation and 2) in port. During operation, the ship is assumed to be executing missions 20% of the time and is considered to be isolated, meaning the SR is only related to the first-party risks to the staff members on board. In the harboring scenario, the ship is in port 80% of the time in a year, and the risks to third parties are the main concern, which will be addressed in the following section.

5.2.1. Risk when operating

The influence of system geometry and population distribution on societal risk is significant. In the case of the FPS Rijn vessel, the crew consists of only five individuals, with their accommodations located near the stern below the superstructure. The location of the LH2 propulsion system is examined through the use of an SR diagram. Due to the uniform frequencies of one to five fatalities, the SR calculation is simplified, resulting in a straight-line diagram. The placement of the LH2 system at the bow and 10 meters ahead of the superstructure is illustrated in Figure 5.13.

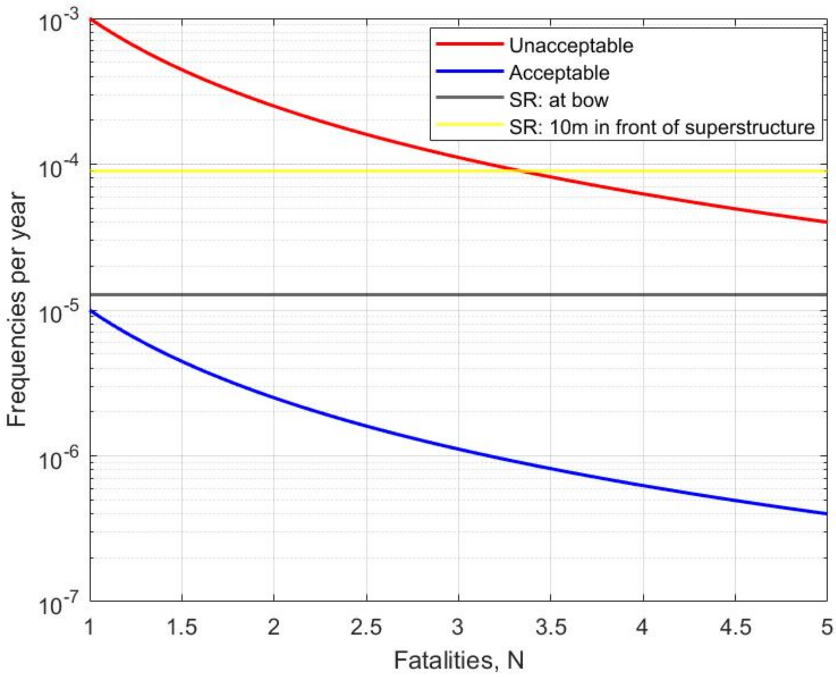

Figure 5.13: SR for FPS Rijn when in operation, with two different LH2 system locations.

The analysis indicates that the optimal location for the LH2 system is at the bow of the ship, as this placement results in the greatest distance between the LH2 system and crew quarters, and the entire SR curve falls within the ALARP region. However, when the LH2 tank is positioned 10m from the crew quarters, the risk becomes unacceptable when the number of fatalities exceeds 3.3. According to the SR criteria and assuming a crew of 5, the distance between the LH2 system and crew quarters should not be lower than 45m.

5.2.2. Risk in the port

For this scenario, it is postulated that the vessel has five crew members in the surrounding port area. Consequently, a larger population is potentially impacted compared to the operational scenario. When the vessel is in the port, it is assumed that all systems, except for the LH2 tank, are not functional, with the tank still containing hydrogen. Based on the average population density in Rotterdam, an estimated 24 individuals may be impacted within a given 100m contour outside the ship. It is important to note that this assessment is regarded as conservative, given that the port of Rotterdam would have a lower population density than the average value.

The societal risk of the port scenario is depicted in Figure 5.14, where the yellow line indicates the SR of the tank storing 3000kg of hydrogen at all times, and the risk is deemed acceptable when the fatalities exceed 8. However, this scenario is not considered realistic as the tank will eventually be drained after missions. Conversely, given that the tank is designed to be swappable, the duration of time that the tank is handling a full capacity of hydrogen (3000kg) can be controlled. The purple line represents the scenario where the tank is filled with hydrogen for only 10% of the time in port. As a result, the SR falls within the ALARP region, indicating that the risk to individuals in the harbor is acceptable.

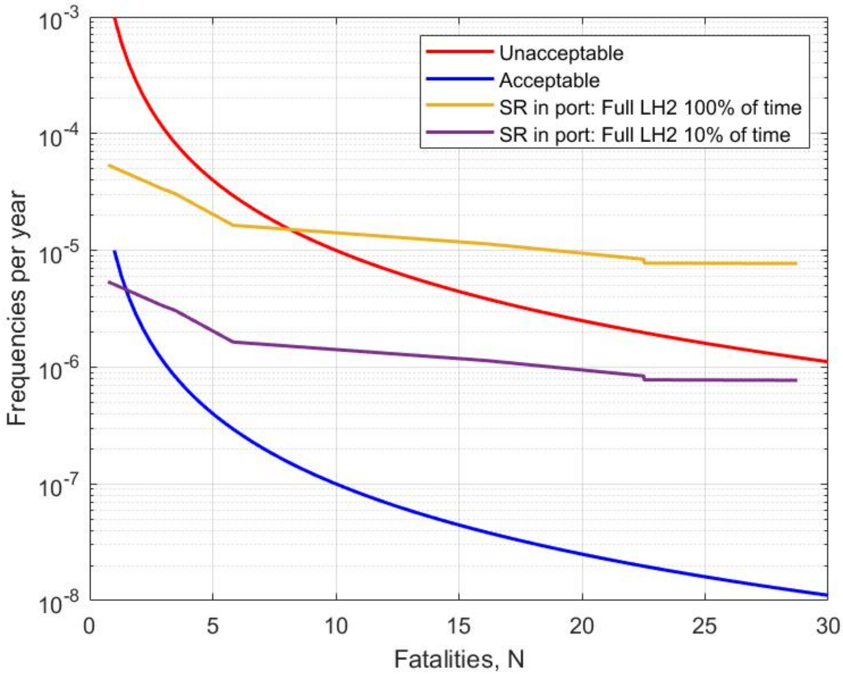

Figure 5.14: SR for FPS Rijn when in harbor, with LH2 full capacity time percentage.

5.3. Potential of operating 24/7 with mitigation measures

Although the risk assessment for the FPS Rijn without any mitigation measures showed promise, its operational time is currently limited to only 20% annually. It is, however, worthwhile to explore the possibility of 100% up-time, as it would increase flexibility and potentially encourage future development, provided that the safety requirements are met.

To reduce the risks associated with 24/7 operation, two measures were implemented: an ESD device and vertical walls. The ESD device effectively limits the duration of any hydrogen leak, thereby reducing the total mass of hydrogen released into the environment and minimizing the severity of the consequences. Additionally, vertical walls were installed 5m away from the LH2 tank to block heat radiation, flame envelopes from jet fires and fireballs, and overpressures from explosions. However, the effect of flash fire was not considered to be mitigated due to the delayed ignition characteristic. The hydrogen can still disperse across the vertical walls to the nearby area, though hydrogen is expected to concentrate in a comparably high position. It is important to note that distances closer than 5m were considered inaccessible. Finally, as in the initial design consideration, the LH2 tank is always installed in an open space on the deck to avoid detonations.

Figure 5.15 shows the IR line plot for operating 24/7 with the two mitigation measures mentioned earlier. The risk is acceptable for all areas outside the 5m contour (vertical walls' location). From the figure, there is a significant drop at a distance of 49m, owning to the 0.01% LH2 tank leaks flash fire event. As discussed before, this delayed consequence cannot be mitigated by vertical walls. Therefore, it can only recommend decreasing the potential ignition sources within that area. Similarly, Figure 5.16 depicts the societal risk for operating 100% annually, which also shows an acceptable safety level. The LH2 system is installed at the bow and located 100m away from the crew rooms.

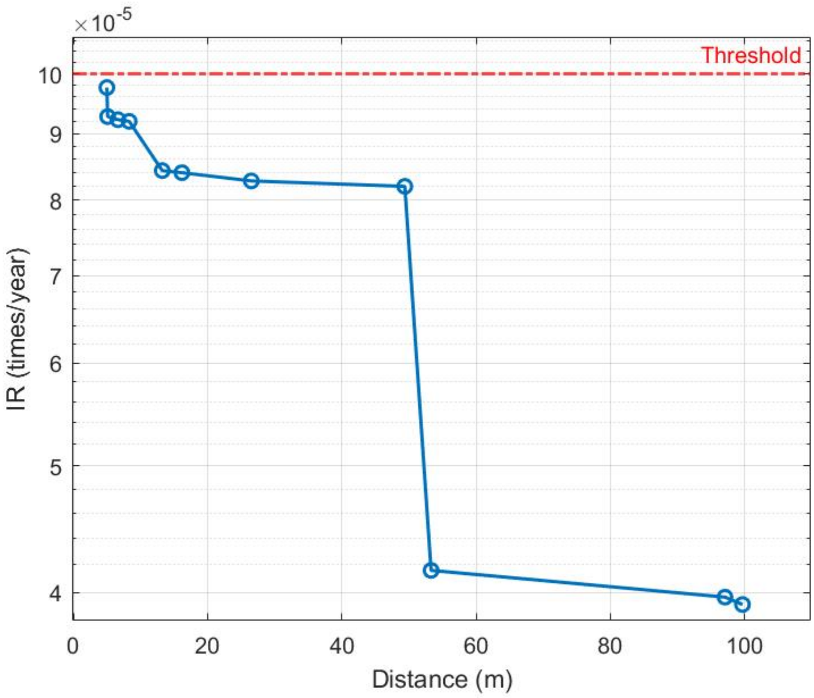

Figure 5.15: FPS Rijn operates 24/7 with mitigation measures (with vertical walls and ESD device).

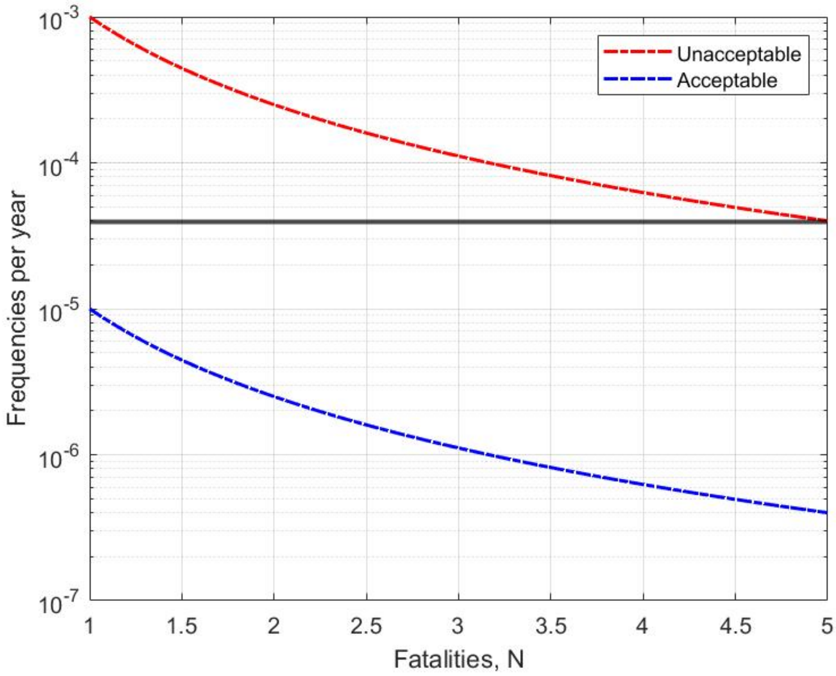

Figure 5.16: Societal risk of FPS Rijn operates 24/7 with mitigation measures (with vertical walls and ESD device).

5.4. Comparison to compressed hydrogen design

To address research sub-question 3, whether the higher energy density of LH2 solutions leads to higher risks compared to existing CH2 solutions, a comparison between the risk results of LH2 and CH2 was intended. However, due to differences in the selection of scenarios and configurations of the systems, a direct comparison was not possible. To address this, a new QRA model for CH2 was developed based on information from the literature and an extension of the GH2 subsystem used in the LH2 QRA tool. The scenarios considered in the CH2 model were similar to those of the LH2 system, and the system's capacity was also set to 3000 kg of hydrogen. This approach would provide a more comprehensive understanding of the risks associated with CH2 and LH2 systems and enable a meaningful comparison.

5.4.1. Design logic

For the purpose of comparing the LH2 and CH2 solutions, it is necessary to ensure that the selected scenarios are consistent. Thus, we consider leakages with cross-sectional area fractions of 0.01%, 0.1%, 1%, 10%, and 100% for this system. However, unlike the LH2 system, the CH2 system includes additional filters but excludes the heat exchanger. Furthermore, based on the operational conditions and locations of the components, we can group them into three subsystems: the CH2 Tank, the High-Pressure Piping Subsystem (HPPS), and the Low-Pressure Piping Subsystem (LPPS). For each subsystem, it also contains different leakage scenarios, where only the 100% tank leakage was considered instantaneous release.

Following the scenarios, hazards associated with gaseous hydrogen, including jet fires, flash fires, fireballs, and explosions, have been previously discussed in the LH2 system. The total logical map of the conceptual CH2 QRA system is illustrated in Figure 5.17. While it appears to be less complicated and similar to the LH2 system, the differences in the number of components, types, and physical characteristics could lead to significant changes. Assumed component parameters and amounts are presented in Table 5.4, and these numbers are based on existing literature and published product manuals.

Table 5.4: System parameters of the conceptual 300 bar CH2 system.

<table>
<tr><th colspan="4">CH2 tank</th></tr>
<tr><td></td><td>Pressure (Bar)</td><td>Temperature (k)</td><td>Size (kg*number)</td></tr>
<tr><td>Tank</td><td>300</td><td>300</td><td>40ft (500*6)</td></tr>
<tr><th colspan="4">HPPS</th></tr>
<tr><td></td><td>Pressure (Bar)</td><td>Temperature (k)</td><td>Number</td></tr>
<tr><td>Pipe</td><td rowspan="4">300</td><td rowspan="4">300</td><td>25 (m)</td></tr>
<tr><td>Valve</td><td>8</td></tr>
<tr><td>Joint</td><td>20</td></tr>
<tr><td>Filter</td><td>1</td></tr>
<tr><th colspan="4">LPPS</th></tr>
<tr><td></td><td>Pressure (Bar)</td><td>Temperature (k)</td><td>Number</td></tr>
<tr><td>Pipe</td><td rowspan="4">10</td><td rowspan="4">300</td><td>10 (m)</td></tr>
<tr><td>Valve</td><td>2</td></tr>
<tr><td>Joint</td><td>10</td></tr>
<tr><td>Filter</td><td>1</td></tr>
</table>

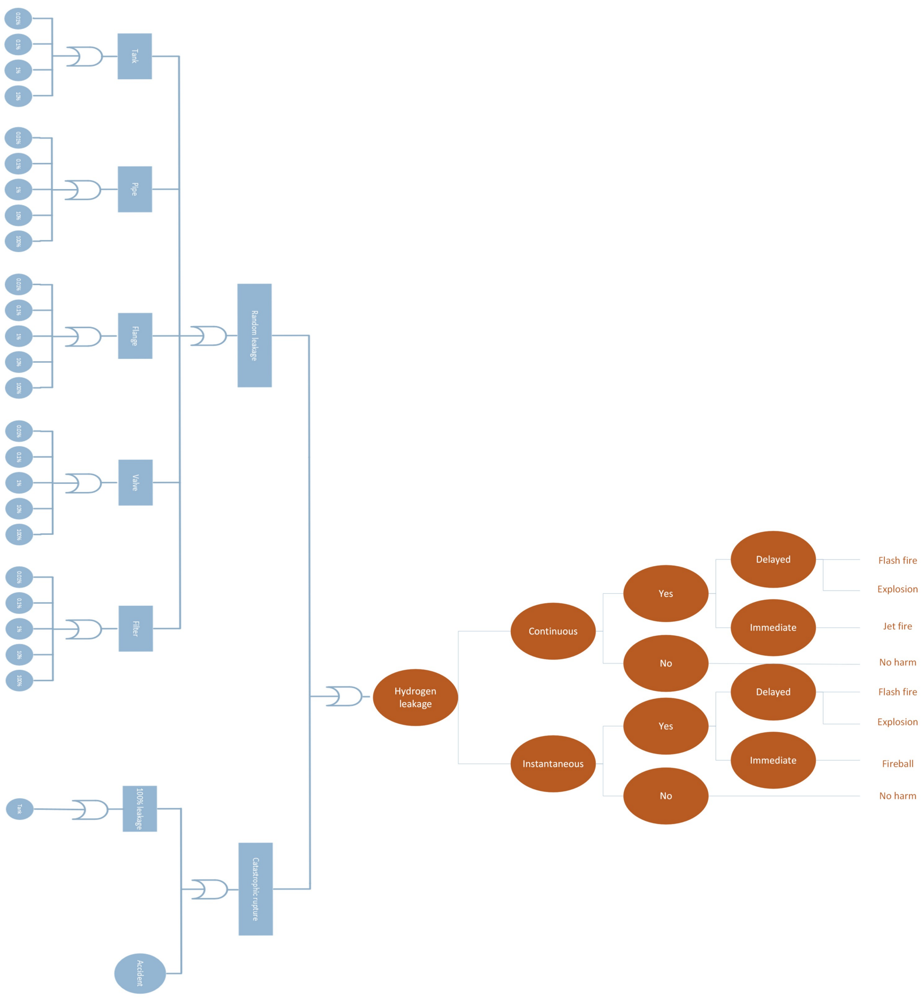

Figure 5.17: Logical map of the CH2 system, the light blue part shows the selected scenarios that could lead to hydrogen leakages while the orange part indicates all the potential hazards for hydrogen leaking events.

5.4.2. Model implementation

The compressed hydrogen leakage frequencies were based on results from Sandia National Laboratory's research [40], using generic system leak frequencies and data from compressed hydrogen systems. Regarding the ETA part, the gaseous hydrogen ignition probability was determined using the continuous release model proposed by Aarskog et al. [3] (Figure 4.10), and the instantaneous releases model from RIVM [90] (Figure 4.11). These probabilities were calculated based on the release rate and total mass of each scenario.

In terms of consequence modeling, the same models used in the GH2 system were employed for the CH2 system. This is because the relevant parameters in the CH2 system were also applicable and could be implemented in the modeling process.

5.4.3. Result & Comparison

To validate the results of the proposed CH2 QRA system, a comparison was made with the only existing QRA literature on maritime applications. This study analyzed the total individual risk of a compressed hydrogen high-speed light craft in Norway with 450 kg of hydrogen stored, using the same design parameters as Aarskog's study. Figure 5.18 shows the IR line plot for these two methods. Notably, the two methods have similar values for distances around 5m, but the proposed system yields higher individual risk values for larger distances. This can be attributed to differences in design logic, such as frequency adjustment, release rate model, and risk reduction measures.

In the proposed model, a vibration factor was implemented to account for the severe maritime environment, and assumed values for leakage rates were updated using the under-expanded choke flow. The vibration factor increases the frequency of leaking, while the calculated leakage rates are lower than those assumed in Aarskog's study, thus reducing the ignition probability. Furthermore, Aarskog's study implemented vertical walls near the high-pressure piping subsystem, assuming that heat radiation and fire flames would be limited to 5m. This may be the primary reason why the proposed system dominated the risk outside the 5m contour. Lastly, since the area within vertical walls is forbidden, the IR plot was plotted to start from 5m.

All in all, quantitatively, the proposed model innovated the risk assessment methods and models and provided the risk value in a similar range as the previous literature.

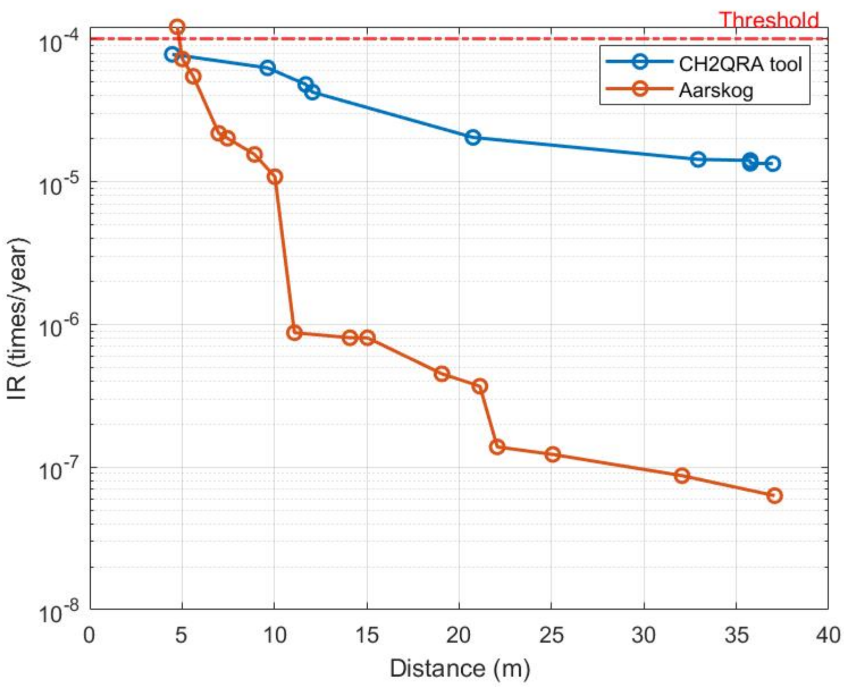

Figure 5.18: Comparison of two methods for GKP7H2 hydrogen driven fast passenger ferry with 20% operational time, data collected from [3].

The aim of the above comparison was to verify the accuracy of the quantified result. Apart from this, the comparison between the LH2 and CH2 solutions was discussed here to answer the research question. Overall, the individual risk of the proposed conceptual 3000kg CH2 design is deemed acceptable. The risk analysis shows that the HPPS contributed the most to the risk result. On the other hand, although the tank storage system has lower frequencies, it has more significant impacts on the severe consequences. Figure 5.19 demonstrates the individual risk for both conceptual designs (LH2 and CH2) with the 20% operational time.

From the IR perspective, both systems are deemed acceptable beyond the 1 meter contour with 20% operational time. The CH2 system exhibits higher IR than the LH2 system for distances within 1 meter, owing to the frequent occurrence of HPPS leakages at a rate of 0.01%. Conversely, beyond the 1-meter distance, the IR of the LH2 system dominates that of the CH2 system. This is attributed to the fact that LH2 tank leakages contribute significantly to the risk result, owing to the large amount of hydrogen in a single tank (3000kg), which leads to high fatal distances. Consequently, the crucial contributions in the IR of tank leakage events can be shown as the IR line of the LH2 system remains nearly horizontal before the 17-meter distance (for LH2 tank 0.01% leak), as well as at 38 meters, 82 meters, and 97 meters (for LH2 tank leaks of 0.1%, 1%, and 10%, respectively).

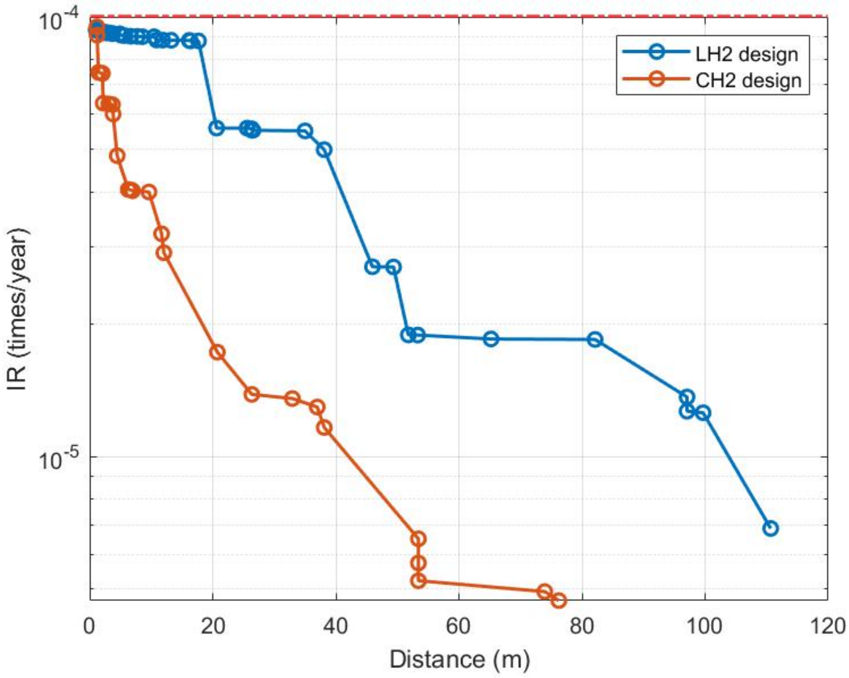

Figure 5.19: Comparison of LH2 (1 tank of 3000kg) and CH2 (6 tanks of 500kg) designs without mitigation measures when operating 20% of time in a year.

The SR result of the CH2 conceptual design was also compiled and compared to the LH2 design, as can be seen in Figure 5.20 for the vessel in operation. The figure shows the SR when the hydrogen system is installed at the bow, which indicates that the SR is acceptable in this scenario for both designs. Moreover, following the assumption of 5 crew members, the minimum acceptable distances between the hydrogen system and the crew rooms are 45m and 4.5m for liquefied and compressed storage.

Two scenarios were analyzed for the SR in the port: one in which the hydrogen tanks were at 100% capacity all the time and another in which they were at 10% capacity. This assumption was based on the tank's design, which allows for easy swapping and control over the amount of hydrogen. As shown in Figure 5.21, both designs were found to be unacceptable for the numbers of people over 5 and 14. However, it was unlikely that the tanks would remain at full capacity after the entire mission, as the amount of hydrogen was typically determined based on the sailing route. As such, the amount of hydrogen would be relatively low at the end of the mission. Figure 5.22 represented a more realistic scenario in which the tanks were only swapped to new ones before starting a new mission. Accordingly, the risk associated with the 10% full capacity time fraction was acceptable in this scenario.

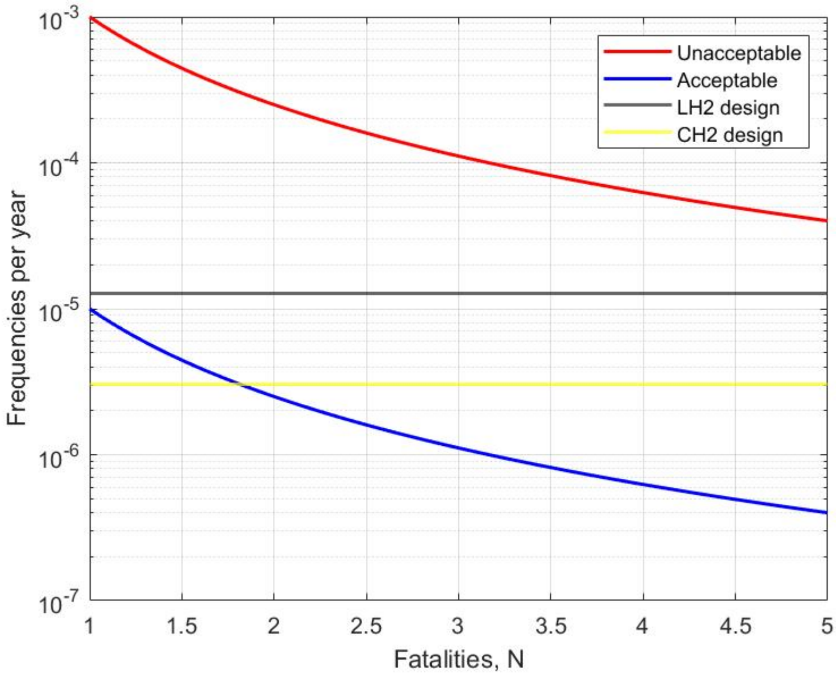

Figure 5.20: Comparison of SR for LH2 and CH2 designs without mitigation measures when operating 20% of time in a year.

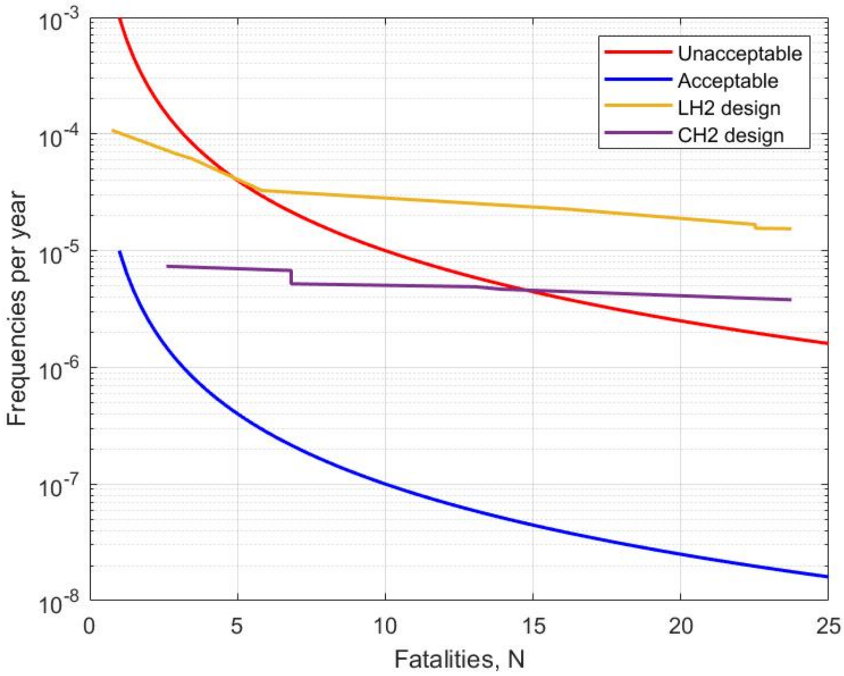

Figure 5.21: SR in the port scenario, with 100% of time having full hydrogen capacity (3000kg).

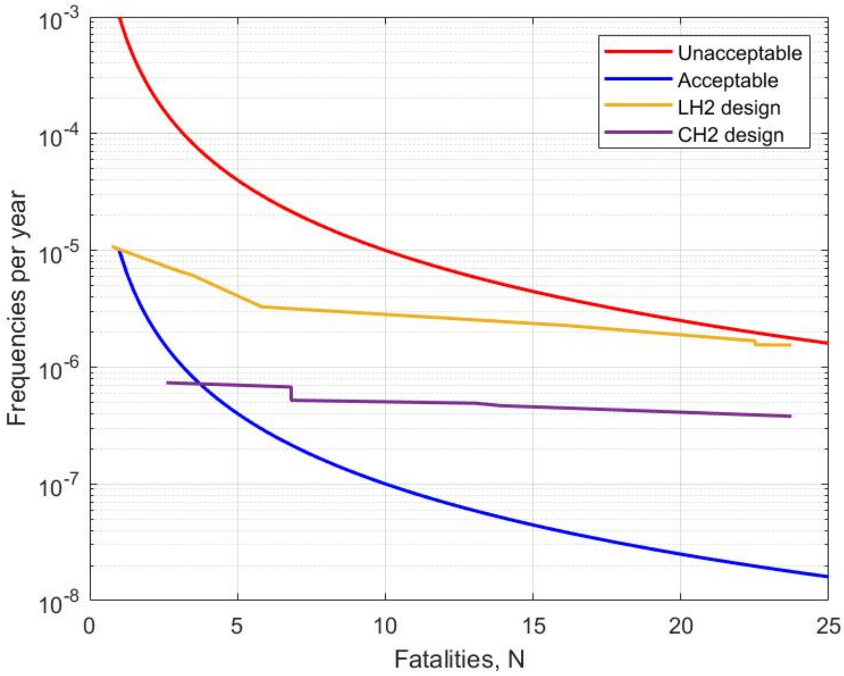

Figure 5.22: SR in the port scenario, with 10% of time having full hydrogen capacity (3000kg).

5.4.4. Feasibility analysis

In this section, we will assess the feasibility of liquid hydrogen-based maritime solutions in terms of their capabilities and risks. LH2 storage solutions offer approximately six times the energy density of existing 350-bar compressed hydrogen storage solutions, enabling much longer distance missions with the same storage space. Since current CH2 vessels are only suitable for inland transportation, more energy-dense LH2 solutions could be a viable option for seagoing transportation. However, LH2 solutions present higher risks both in terms of individual and societal risks due to higher leakage frequencies and larger storage capacities of LH2 tanks. Despite this, our case study on the FPS Rijn indicates that the overall individual and societal risks are acceptable when sailing for 20% of the time without mitigation measures. Regarding the acceptable level of societal risk in the harbor, it is necessary to swap the full hydrogen tank before each mission. Moreover, for such an LH2 design, it is also tested to be possible to operate 100% of the time when mitigation measures are implemented, providing the future design's potentiality.

Although this study does not consider the economic impact, it is worth noting that the LH2 designs are more complex, requiring a subsystem for GH2 and LH2. Particularly in the LH2 subsystem, the double-walled design with specific materials prevents heat transfer and leakage, which can increase costs. All in all, the design of a 3000kg LH2 container vessel is a feasible solution for long-distance maritime transportation with zero emissions. However, it is important to note that each design carries its own unique set of risks. Therefore, it is crucial to thoroughly analyze the initial individual and societal risks associated with a design and develop effective mitigation measures to ensure that the acceptance criteria are met. By doing so, we can pave the way for the safe and sustainable future development of LH2-based solutions in the maritime industry.

This page intentionally left blank

6 Discussion

The role of QRA is to ensure that the risk of the new design is sufficiently safe with conventional designs. However, one critical question can be addressed here, how do you know the final result is accurate enough? To answer this question, the uncertainty analysis of this system will be discussed here. In addition, the assumptions were made with conservative approaches to avoid underestimating the risk effect.

To assess the uncertainties of the QRA system, every progress within the logical map was analyzed qualitatively.

6.1. Uncertainties in leakage frequencies

Starting with the frequency of hydrogen leakage, there were significant uncertainties associated with the available data. As previously mentioned, the lack of data on handling LH2 means that the only way to estimate these leakage frequencies is through the use of the Bayesian updating method. However, the predicted LH2 leakage data used in this analysis was based on generic data that did not take into account the double-wall design of current LH2 components, which is intended to increase safety and prevent heat dissipation. Therefore, it is reasonable to speculate that the actual frequency of LH2 leakage from these components may be lower than predicted.

Regarding the frequency of CH2 leakage, the availability of published operating data has enabled a more mature and accurate estimation of the associated frequencies. However, it is worth noting that the reviewed literature all used the same CH2 data set to assess these risks, which did not account for operating pressure as a variable. This omission introduces additional uncertainties into the system analysis, as higher-pressure systems are generally more prone to leakage.

In order to provide a more conservative assessment of the system's performance, we also took into account the harsh maritime environment in which the system will operate. Specifically, we considered the effect of vibrations from the machinery and ship motions on the frequency of leakage events.

6.2. Uncertainties in probability assessment

In this study, the ignition probability of gaseous hydrogen was evaluated using an up-to-date model proposed by Aarskog et al. [3], which was developed based on a comparison of the physical properties of gaseous hydrogen and methane. However, as liquid hydrogen exhibits unique characteristics compared to its gaseous form, it was necessary to propose a new ignition probability model to reduce uncertainty in the evaluation of hydrogen-related risks.

To address this need, a novel liquid hydrogen ignition probability model was proposed in this study, which accounts for the distinct characteristics of liquid hydrogen. It is important to note that the ignition probability is closely related to the release rate, as ignition models are dependent on this parameter. Therefore, a best-fit release rate theory was also presented and validated with experimental data, which surprisingly has a 2-3 times lower release rate than the models used in other QRA literature.

In order to assess the risks associated with hydrogen storage and transport systems, it is necessary to consider the probabilities of various hazards occurring. In this study, the probabilities of delayed and immediate ignition were assigned based on a 1:2 ratio, as recommended by DNV's data.

However, it should be noted that the likelihood of hazards occurring depends on numerous factors, such as the environment, geometry, and weather. As these details cannot be fully simulated in the model, a simpler method of assigning probabilities was applied. While this approach has been recommended in some risk assessment guidelines, it can also contribute to the uncertainties in the system.

6.3. Uncertainties in consequence modeling

As the last step of the QRA procedure, each hazard was assessed in terms of its potential consequences, which were expressed as fatal distances calculated based on specific fatality criteria. For instance, heat radiation over $35KW/m^2$ and pressure wave over $0.82barg$ was considered 100% fatal. Although the modeling tools were carefully selected and compared to identify the most appropriate methods, some of the consequences resulting from large-scale releases could not be validated due to the lack of experimental data. Consequently, these contributed the most uncertainties to the consequence modeling process. It is worth noting, however, that the likelihood of such large-scale releases occurring is extremely low. Therefore, the impact of the higher uncertainties associated with them can be minimized and may even be regarded as inedible scenarios.

6.4. Uncertainties in human errors

In this research, accidental risks caused by human error were not taken into account, as they are largely dependent on the training and experience of personnel operating hydrogen systems. However, as noted in the study by Wen et al. [115], human errors account for 29% of hydrogen accidents based on the HIAD2.0 database. To mitigate this risk and its uncertainty, it is recommended that crew members receive comprehensive training and education to reduce the likelihood of human error.

6.5. Individual risk

This research presents individual risk as contour plots and line plots that combine fatal distances and chances of occurrence. To establish acceptance criteria for individual risk assessment, DNV's recommendation of a most conservative value of $1 * 10^{-4}$ per annum was referenced. The resulting consequences were only considered the distance within 100m due to the scale of the case vessel and the insignificant happening frequencies. However, this posed a disadvantage for individual risk assessment since the acceptance criteria only consider the frequency perspective and do not factor in consequences. Therefore, this research also assessed system risks using the risk matrix and societal risk to ensure overall safety.

The main source of uncertainty in individual risk assessment is the assumption that all subsystems are located at the same point (LH2 tank location). This assumption was made because the risks (both frequencies and consequences) of the LH2 and CH2 subsystems were mild compared to the LH2 tank, and it simplified and accelerated the analytical process. However, in reality, it is advisable to evaluate each event based on its specific location to obtain risk contours that reflect irregular shapes.

Regarding the effect of implementing mitigation measures, the result demonstrates a significant drop in the final risk plot. It is acceptable to even operate 24/7 if the risk reduction measures are well-considered and designed properly.

6.6. Societal risk

Societal risk is typically represented by an F-N curve, and in this research, the acceptance criteria were derived from VROM, the Dutch authorities. The F-N curves for both operating and porting scenarios fall within the ALARP area, indicating that risk reduction measures are not mandatory but should be implemented if feasible. The study found that installing a 3000kg LH2 tank at the bow is an acceptable design for a 5-crew member inland container vessel, and it is even practical for operating 100% of the time. However, for more severe cases, such as an LH2 ferry carrying a much larger number of people, mitigation measures would be necessary to bring the societal risk to an acceptable level.

In the porting scenario, a conservative assumption was made by taking the population density of Rotterdam in the harbor. Without any special safety design, it is acceptable to contain full LH2 capacity for 10% of the time in the harbor. This is considered practical since the LH2 tank is swappable, and it replaces with a new one before the missions.

6.7. Comparison with existing hydrogen QRA studies

The innovative approaches of this study provide quick and accurate risk results for maritime hydrogen applications, which surpass other studies in several ways. Firstly, the logic map developed in this study is unique as it covers both LH2 and GH2 subsystems, their specific leak frequencies and scenarios, and additional hazards such as flash fires and hydrogen pools. In comparison with HyRam's LH2 QRA tool and the studies by Yoo et al. and Li et al., the former only considered jet fires and explosions as hazards, while the last two works did not include specific leakage frequency data for hydrogen or consider a wide range of leakage hole scenarios for each component [25, 121, 65].

Secondly, this study takes into account the maritime environment by introducing a unique way of considering the vibration factor, which reduces system uncertainty. Additionally, a newly proposed liquid hydrogen ignition model and the different ways of assessing continuous and instantaneous releases provide a more comprehensive approach. In contrast, Yoo et al. [121] and Li et al. [65, 123, 124] assume a constant, discontinuous hydrocarbon ignition probability for hydrogen, which underestimates the likelihood and increases uncertainty. While HyRam [25] and Aarskog et al. [3] propose ignition models for gaseous hydrogen, formulated as a function of mass flow rates, which are not applicable for instantaneous releases.

Finally, the release rate model was validated with experimental data, and SOTA consequence modeling tools were selected to provide reliable consequence results.

This page intentionally left blank

7 Conclusion

This research has successfully developed a quantitative risk assessment system for maritime liquid hydrogen-based solutions, providing a valuable design tool to evaluate the risks quantitatively associated with this innovative technology. As an alternative design, it is requested that LH2-based solutions meet the same safety standards as conventionally fuelled vessels. The study has focused on assessing the fatality risk related to the liquid hydrogen systems on a container vessel, both in terms of individual and societal risk. The quantitative analysis has shown that the individual risk for the 3000kg LH2-based inland vessel is acceptable for the 20% operational time, as is the societal risk with a minimum distance of 45m between the LH2 system and the crew room. It should be noted that these are still without mitigation measures. Additionally, the research has assessed the societal risk for the port scenario conservatively with the population density data in Rotterdam. Overall, this study has contributed to understanding the risks associated with LH2-based solutions in the maritime industry and provided insights into ensuring the safety of future maritime LH2-based propulsion solutions.

Furthermore, this research proposes an innovative methodology that effectively reduces the uncertainties of the results by using a comprehensive hazard identification process, a newly proposed liquid hydrogen ignition model, leakage frequencies adapted to a severe maritime environment, and validated consequence models. In addition, the feasibility of maritime LH2-based solutions was compared to CH2-based designs in terms of risk. As a result of the low volumetric energy density, maritime CH2 solutions are limited to inland missions. However, the findings of this study illustrate that maritime LH2-based solutions not only offer the potential for longer seagoing missions but also demonstrate an acceptable level of safety.

Several mitigation measures have been proposed to reduce the risk associated with maritime LH2-based solutions, focusing primarily on the LH2 tank and explosions. These measures include implementing a double-wall design for the LH2 tank, introducing emergency shut-down devices to reduce release time, minimizing the cross-sectional diameter of tanks and pipes, and incorporating vertical walls to decrease the over-pressure effect. These methods can effectively reduce the frequency of leakage and fatal distances, as demonstrated that the risk is even acceptable when operating 100% of the time. Additionally, the QRA system has been extended to allow users to define their design parameters, increasing its applicability to different vessel types, operational profiles, and design geometries. Overall, this maritime liquid hydrogen-based quantitative risk assessment system consolidates and updates existing information and theories, providing a convenient and efficient environment for compiling quantified risk in the design early-stage phase across a wide variety of vessels.

7.1. Research sub-questions

1. What is the system configuration of the maritime liquid hydrogen propulsion system and how can potential hazards and scenarios be identified and assessed to evaluate the risks?

   The system configuration of the maritime liquid hydrogen comprises both liquid hydrogen and gaseous hydrogen subsystem. The liquid storage method provides a higher volumetric energy density than compressed hydrogen solutions, while the gaseous part is designed for supplying fuel cells. Therefore, a heat exchanger is required to evaporate the hydrogen from the liquid phase to the gaseous phase. In addition, since hydrogen is a highly reactive substance, the safety system, including the venting system and mitigation measures such as emergency shut-off devices and vertical walls, will also be implemented.

   The potential hazards have been carried out in the literature study, which included fires (jet fire, flash fire, fireball, and pool fire), explosions (deflagration and detonation), and non-ignited events (cold plume and hydrogen pool). These hazards are triggered by different conditions, such as ignition and leakage types. The scenarios were only considered hydrogen leakage, where all components have their own failure frequencies that lead the hydrogen to leak.

2. What are the most suitable methods for quantitatively and accurately assessing the risks (likelihoods and consequences) of maritime liquid hydrogen propulsion systems?

   In contrast to existing literature, this research examines the differing frequencies of LH2 and CH2 leakage. It investigates the additional hazards associated with LH2. Our validated models provide improved predictions of the consequences of such events. Given the cryogenic nature of LH2, it has the potential to freeze surrounding air, creating an oxygen-dense mixture that is highly combustible. To account for this risk, we developed an innovative ignition model for LH2.

   Finally, the harsh maritime environment in which the system operates with its mechanical vibrations, motions, and loading can increase hydrogen leakage frequencies. To address this issue, we developed an adaptive factor that uses Fast Fourier Transform diagrams of vibration sources for ships to provide a more accurate risk estimate.

3. What is the comparative feasibility, in terms of risks and capabilities, of maritime liquid hydrogen propulsion systems and existing compressed hydrogen propulsion systems?

   Liquid hydrogen outweighs compressed hydrogen for its higher volumetric energy density, enabling it to execute longer-distance missions. However, the development of LH2 systems and associated technologies is complex and still not fully matured. This study compared the risks associated with maritime LH2 and CH2 propulsion solutions. The results showed that LH2 solutions have higher risks than CH2 designs without appropriate mitigation measures. However, LH2 solutions can achieve the same or even higher levels of safety than CH2 designs with the implementation of appropriate mitigation measures or safety designs.

4. What are the potential risks associated with maritime liquid hydrogen propulsion systems, and what mitigation measures can be implemented to reduce these risks to acceptable levels?

   In the case of the FPS Rijn, we assessed four risk methods to determine the level of risk associated with the LH2 system. Based on both individual risk and risk matrix analyses, we found that the system had a sufficient level of safety without the need for mitigation measures.

   In terms of societal risk, our analysis showed that there must be at least 45 meters of distance between the LH2 system and crew rooms during operation. Additionally, in port scenarios, the fraction of time when the system is at full hydrogen capacity must be limited to 10% to mitigate the risk of potential incidents.

However, for the design in which the risk is unacceptable, risk reduction measures are required. Resulting of each contributor to the risk, measures to mitigate the LH2 tank leakage and explosion hazards can effectively lower the risk of the design. Consequently, the implementation of vertical walls surrounding the LH2 system, and emergency shut-off devices are the solutions for the larger-scale and longer operational time development. It was even shown that the risk is acceptable when operating 100% with these risk reduction measures.

5. To what extent can this quantified risk assessment system be applied?

   Each design carries its own risks, and to account for this, the original system was expanded to allow users to input their own design parameters. Figure 7.1 illustrates how the LH2 and CH2 subsystems and the operational profile are used to compile the frequencies and fatal distances of LH2 designs. However, it should be noted that this QRA system is restricted to assessing risks for specific LH2 designs that utilize buffer tanks and heat exchangers. This system does not include designs that use pumps for transporting liquid hydrogen or lack buffer tanks.

   Apart from LH2 solutions, this study also developed an innovative CH2 QRA system that improved existing information and adjusted for the harsh maritime environment. The final quantified risk as compared to previous work in the literature that used the same input parameters. As a result, the quantified values fell within a similar range, further establishing the credibility of this system.

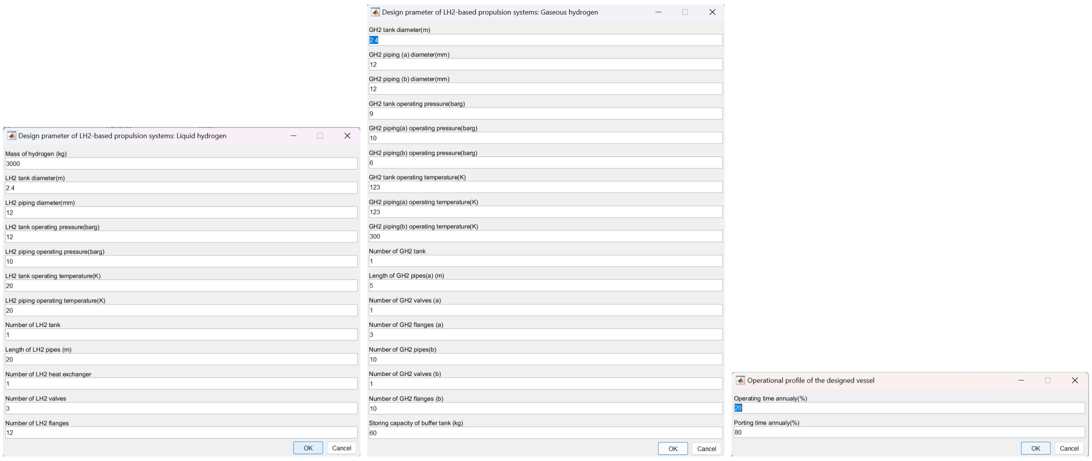

Figure 7.1: User inputs of the system.

This page intentionally left blank

8 Recommendations

The developed quantitative risk assessment system is the first tool for maritime liquid hydrogen-based propulsion solutions. It enables future engineers to analyze risks in the early design stage. However, due to the innovation of such a technology, this is still in the early stage of development of this topic. The recommendations and ideas for improving the system's accuracy and applicability are consolidated below for future development.

8.1. LH2 leak frequencies update

Due to the lack of real data, the main uncertainty of this system is presumed to be the LH2 leak frequencies. The existing quantitative leak frequencies were predicted using the Bayesian updating process. While this approach is one of the most promising methods for predicting leak frequencies, it is essential to note that more updating processes with real LH2 data are required to obtain a better prediction. It is expected that all LH2 components have a double-wall design, which should result in a lower leakage frequency compared to GH2 components. However, existing data shows a much higher value than that of GH2 components. This discrepancy may be attributed to the fact that the predicted data is for a generic design rather than a special double-wall design.

8.2. Large-scale consequences validation

In the consequence modeling section, it is possible to validate the results of large-scale releases, including catastrophic scenarios such as jet fires or flash fires. While the likelihood of these events may be low, it is still essential to conduct research in case a real accident occurs. Validating these consequences can lead to the implementation of measures and regulations to adjust to potential risks.

8.3. Consideration of harmful effects

While this study and other risk-related documents have assessed risks in terms of fatality, it is important to note that harmful effects can also cause severe injuries to humans and damage to other properties. As such, it is recommended to consider the harmful perspective and how it can impact other aspects, such as cargo and structures. By considering these additional factors, a more comprehensive risk assessment can be performed.

8.4. Assessing risks based on the specific location of each event

To simplify the risk-analysis process, the risks were assessed assuming all subsystems were located in the same place. This was done because the LH2 tank has the greatest impact on the total risk, and assuming all subsystems were located together would not significantly affect the consequences of the overall risk. However, in cases where all subsystems have similar risk contributions, a more detailed assessment is necessary, which can also assist in developing risk plans and structural designs.

8.5. The design of CCH2 propulsion solutions

Currently, developed QRA tools have been developed for both CH2 and LH2 configurations. Furthermore, a higher energy-dense solution, CCH2, could be explored in future research. The characteristics of CCH2 lie between those of CH2 and LH2, allowing for similar consequence modeling but without the liquefied effects. However, assessing leak frequencies for CCH2 components will pose a challenge due to its high-pressure, low-temperature properties, making storage and handling even more difficult. Therefore, further investigation is needed to identify special designs and measures for risk prevention.

8.6. More comprehensive feasibility analysis of maritime LH2-based propulsion solutions

In this study, the feasibility of maritime LH2 solutions was compared to CH2 solutions from a technical perspective. However, economic factors are equally important and critical for market development. For instance, price differences between LH2 and CH2, as well as capital and operating expenditures, may vary and should be considered in future research.

This page intentionally left blank

Bibliography

[1] Friedrich A et al. “IGNITION AND HEAT RADIATION OFCRYOGENIC HYDROGEN JETS”. In: *International Journal of Hydrogen Energy* 37.22 (2012), pp. 17589–17598.

[2] Ballard Power Systems Europe A/S. *Fuel Cell Power Module for Marine Applications*. Ballard Power Systems Europe A/S. 2022.

[3] Fredrik G. Aarskog et al. “Concept risk assessment of a hydrogen driven high speed passenger ferry”. In: *International Journal of Hydrogen Energy* 45.2 (Jan. 2020), pp. 1359–1372. DOI: 10.1016/j.ijhydene.2019.05.128.

[4] G.P. Ackroyd and S.G. Newton. “An investigation of the electrostatic ignition risks associated with a plastic coated metal”. In: *Journal of Electrostatics* (2003).

[5] Mojtaba Afzali. “Modeling of evaporation of hydrogenduring accidental releases”. MA thesis. The University of South-Eastern Norway, May 2021.

[6] Norsk Hydro ASA and DNV. *acceptance criteria for H2 refuelling stations*. Norsk Hydro ASA and DNV. 2003.

[7] Ryo Ono1 Ayumi Kumamoto1 Hiroto Iseki1 and Tetsuji Oda2. “Measurement of minimum ignition energy in hydrogenoxygen-nitrogen premixed gas by spark discharge”. In: *Journal of Physics: Conference Series 301 (2011) 012039* (2011). URL: https://iopscience.iop.org/article/10.1088/1742-6596/301/1/012039/pdf.

[8] W. E. Baker et al. *Explosion hazards and evaluation. In Fundamental studies in engineering, Vol. 5.* Amsterdam: Elsevier Scientific Publishing Company, 1983.

[9] Somtochukwu Godfrey Nnabuife Bernard Chukwudi Tashie-Lewis. “Hydrogen Production, Distribution, Storage and Power Conversion in a Hydrogen Economy - A Technology Review”. In: *Chemical Engineering Journal Advances* 8 (2021), p. 100172. DOI: 10.1016/j.ceja.2021.100172. URL: https://doi.org/10.1016/j.ceja.2021.100172.

[10] Hans Boot and Sonia Ruiz Perez. “Why a Hydrogen fireball should not be modelled as a BLEVE event”. In: *Chemical Engineering Transactions* 90 (May 2022), pp. 49–54. DOI: 10.3303/CET2290009. URL: https://www.cetjournal.it/index.php/cet/article/view/CET2290009.

[11] L. C. Cadwallader. *Failure Rate Estimates for Passive Mechanical Components*. Tech. rep. Idaho National Laboratory, 2018.

[12] Ciro Caliendo and Gianluca Genovese. “Quantitative Risk Assessment on the Transport of Dangerous Goods Vehicles Through Unidirectional Road Tunnels: An Evaluation of the Risk of Transporting Hydrogen”. In: *Risk Analysis* 41.9 (Dec. 2020), pp. 1522–1539. DOI: 10.1111/risa.13653.

[13] Arnab Chakrabarty, Sam Mannan, and Tahir Cagin. “Chapter 2 - Process Safety”. In: *Multiscale Modeling for Process Safety Applications*. Ed. by Arnab Chakrabarty, Sam Mannan, and Tahir Cagin. Boston: Butterworth-Heinemann, 2016, pp. 5–110. ISBN: 978-0-12-396975-0. DOI: https://doi.org/10.1016/B978-0-12-396975-0.00002-4. URL: https://www.sciencedirect.com/science/article/pii/B9780123969750000024.

[14] Yuanjiang Chang et al. “Dynamic Bayesian network based approach for risk analysis of hydrogen generation unit leakage”. In: *International Journal of Hydrogen Energy* (2019). DOI: .org/10.1016/j.oceaneng.2021.109259.

[15] NewYork: American Institute of Chemical Engineers. *Guidelines for Chemical Process Quantitative Risk Analysis*. Center for Chemical Process Safety (CCPS), 1989.

[16] Ariel Chiche et al. “Feasibility and impact of a Swedish fuel cell-powered rescue boat”. In: *Ocean Engineering* 234 (2021), p. 109259. ISSN: 0029-8018. DOI: https://doi.org/10.1016/j.oceaneng.2021.109259. URL: https://www.sciencedirect.com/science/article/pii/S002980182100679X.

[17] Choeng Hoon Choi et al. “Development and demonstration of PEM fuel-cell-battery hybrid system for propulsion of tourist boat”. In: *International Journal of Hydrogen Energy* 41.5 (2016), pp. 3591–3599. ISSN: 0360-3199. DOI: https://doi.org/10.1016/j.ijhydene.2015.12.186. URL: https://www.sciencedirect.com/science/article/pii/S0360319915028438.

[18] Bikram Roy Chowdhury and Ethan S. Hecht. “Dispersion of cryogenic hydrogen through high-aspect ratio nozzles”. In: *International Journal of Hydrogen Energy* 46.23 (2021). ICHS 2019 Conference, pp. 12311–12319. ISSN: 0360-3199. DOI: https://doi.org/10.1016/j.ijhydene.2020.09.072. URL: https://www.sciencedirect.com/science/article/pii/S0360319920334923.

[19] Camila Correa-Jullian and Katrina M. Groth. “Data requirements for improving the Quantitative Risk Assessment of liquid hydrogen storage systems”. In: *International Journal of Hydrogen Energy* 47.6 (Jan. 2022), pp. 4222–4235. DOI: 10.1016/j.ijhydene.2021.10.266.

[20] Brooks D.M, Ehrhart B.D, and C LaFleur. “DEVELOPMENT OF LIQUID HYDROGEN LEAK FREQUENCIES USING A BAYESIAN UPDATE PROCESS”. In: Sandia National Laboratories. 2021.

[21] Mohammad Dadashzadeh et al. “Risk assessment methodology for onboard hydrogen storage”. In: *International Journal of Hydrogen Energy* 43.12 (2018), pp. 6462–6475. ISSN: 0360-3199. DOI: https://doi.org/10.1016/j.ijhydene.2018.01.195. URL: https://www.sciencedirect.com/science/article/pii/S0360319918303422.

[22] Lutz Decker. *Liquid Hydrogen Distribution Technology- HYPER Closing Seminar*. Linde. 2019.

[23] Jorgen Depken et al. “Safety Considerations of Hydrogen Application in Shipping in Comparison to LNG”. In: *Energies* 15.9 (Apr. 2022), p. 3250. DOI: 10.3390/en15093250.

[24] DMI. “Types of major chemical/industrial hazards - fire.” In: 2021.

[25] Brian D. Ehrhart and Ethan S. Hecht. “Hydrogen Plus Other Alternative Fuels RiskAssessment Models (HyRAM+) Version 4.1Technical Reference Manual”. In: Sandia Natinal Laboratories. 2022.

[26] Breeding RJ. Eisenberg NA Lynch CJ. *Vulnerability model. A simulation system for assessing damage resulting from marine spills.* Tech. rep. 1975.

[27] Børre J. Paaske Erling Håland. *Main Report - Survey of Hydrogen Risk Assessment Methods rev 2*. Tech. rep. DNV Research & Innovation, Jan. 2008.

[28] Samuel Glasstone and Philip J. Dolan. *The Effects of Nuclear Weapons. Third Edition*. UNITED STATES DEPARTMENT OF DEFENSE, the ENERGY RESEARCH, and DEVELOPMENT ADMINISTRATION, 1977.

[29] Frederick D. Gregory. *Safety Standard for Hydrogen and Hydrogen Systems*. English. 1997. URL: https://ntrs.nasa.gov/citations/19970033338.

[30] FIDES Group. *FIDES guide 2009, Edition A, Reliability Methodology for Electronic Systems*. Tech. rep. FIDES Group, 2009.

[31] Jonathan Hall. *Ignited Releases of Liquid Hydrogen - Final reformat.docx*. Tech. rep. Health and Safety Laboratory, 2014.

[32] G. Hankinson and B. J. Lowesmith. *Qualitative Risk Assessment of Hydrogen Liquefaction, Storage and Transportation*. Tech. rep. 3.11. Oct. 31, 2013.

[33] Olav R. Hansen and D. Michael Johnson. “Improved far-field blast predictions from fast deflagrations, DDTs and detonations of vapour clouds using FLACS CFD”. In: *Journal of Loss Prevention in the Process Industries* 35 (2015), pp. 293–306. ISSN: 0950-4230. DOI: https://doi.org/10.1016/j.jlp.2014.11.005. URL: https://www.sciencedirect.com/science/article/pii/S0950423014001831.

[34] Olav R. Hansen et al. “Using computational fluid dynamics (CFD) for blast wave predictions”. In: *Journal of Loss Prevention in the Process Industries* 23.6 (2010). Papers Presented at the 2009 International Symposium of the Mary Kay O’Connor Process Safety Center, pp. 885–906. ISSN: 0950-4230. DOI: https://doi.org/10.1016/j.jlp.2010.07.005. URL: https://www.sciencedirect.com/science/article/pii/S0950423010000914.

[35] Olav Roald Hansen. “Hydrogen infrastructure—Efficient risk assessment and design optimization approach to ensure safe and practical solutions”. In: *Process Safety and Environmental Protection* 143 (Nov. 2020), pp. 164–176. DOI: 10.1016/j.psep.2020.06.028.

[36] Olav Roald Hansen. “Liquid hydrogen releases show dense gas behavior”. In: *International Journal of Hydrogen Energy* 45.2 (2020). International Hydrogen and Fuel Cell Conference 2018, Trondheim, Norway, pp. 1343–1358. ISSN: 0360-3199. DOI: https://doi.org/10.1016/j.ijhydene.2019.09.060. URL: https://www.sciencedirect.com/science/article/pii/S0360319919333749.

[37] Nilsen S Haugom G Rikheim H. *Hydrogen applications. Risk acceptance criteria and risk assessment methodology*. Tech. rep. DNV , The Research Council of Norway, Norsk Hydro ASA, 2003.

[38] Health and Safety Executive(HSE). “Failure Rate and Event Data for use within Risk Assessments”. In: 2017.

[39] Health and Safety Executive(HSE). *REDUCING RISKS, PROTECTING PEOPLE. HSE’s decision-making process*. Health and Safety Executive(HSE), 2021.

[40] Ethan S. Hecht and Bikram Roy Chowdhury. “Characteristic of cryogenic hydrogen flames from high-aspect ratio nozzles”. In: *International Journal of Hydrogen Energy* 46.23 (2021). ICHS 2019 Conference, pp. 12320–12328. ISSN: 0360-3199. DOI: https://doi.org/10.1016/j.ijhydene.2020.08.265. URL: https://www.sciencedirect.com/science/article/pii/S0360319920333243.

[41] Ethan S. Hecht and Pratikash P. Panda. “Mixing and warming of cryogenic hydrogen releases”. In: *International Journal of Hydrogen Energy* 44.17 (Apr. 2019), pp. 8960–8970. DOI: 10.1016/j.ijhydene.2018.07.058.

[42] Laurens Van Hoecke et al. “Challenges in the use of hydrogen for maritime applications”. In: *Energy &amp Environmental Science* 14.2 (Jan. 7, 2021), pp. 815–843. DOI: 10.1039/d0ee01545h.

[43] P.G. Holborn, C.M. Benson, and J.M. Ingram. “Modelling hazardous distances for large-scale liquid hydrogen pool releases”. In: *International Journal of Hydrogen Energy* 45.43 (2020), pp. 23851–23871. ISSN: 0360-3199. DOI: https://doi.org/10.1016/j.ijhydene.2020.06.131. URL: https://www.sciencedirect.com/science/article/pii/S0360319920322692.

[44] J Hord. *IS HYDROGEN A SAFE FUEL?**. Tech. rep. con-. Feb. 9, 1978.

[45] Seyed Ehsan Hosseini and Brayden Butler. “An overview of development and challenges in hydrogen powered vehicles”. In: *International Journal of Green Energy* 17.1 (2020), pp. 13–37. DOI: 10.1080/15435075.2019.1685999. URL: https://doi.org/10.1080/15435075.2019.1685999.

[46] W. Houf and R. Schefer. “Analytical and experimental investigation of small-scale unintended releases of hydrogen”. In: *International Journal of Hydrogen Energy* 33.4 (2008), pp. 1435–1444. ISSN: 0360-3199. URL: https://www.sciencedirect.com/science/article/pii/S0360319907007203.

[47] William Houf and Robert Schefer. “Predicting radiative heat fluxes and flammability envelopes from unintended releases of hydrogen”. In: *International Journal of Hydrogen Energy* 32.1 (2007), pp. 136–151. ISSN: 0360-3199. DOI: https://doi.org/10.1016/j.ijhydene.2006.04.009. URL: https://www.sciencedirect.com/science/article/pii/S0360319906001704.

[48] Yimiao Huang and Guowei Ma. “A grid-based risk screening method for fire and explosion events of hydrogen refuelling stations”. In: *International Journal of Hydrogen Energy* 43.1 (Jan. 2018), pp. 442–454. DOI: 10.1016/j.ijhydene.2017.10.153.

[49] *IGC Doc 75/07/E/rev. DETERMINATION OF SAFETY DISTANCES*. Tech. rep. European Industrial Gases Association, 2007.

[50] IMO. *GUIDELINES FOR THE APPROVAL OF ALTERNATIVES AND EQUIVALENTS AS PROVIDED FOR IN VARIOUS IMO INSTRUMENTS, MSC.1/Circ.1455*. Tech. rep. European Industrial Gases Association, 2013.

[51] *IMO Resolution MSC.391(95). INTERNATIONAL CODE OF SAFETY FOR SHIPS USING GASES OR OTHER LOW-FLASHPOINT FUELS (IGF CODE)*.

[52] ISO/IEC. *Safety aspects — Guidelines for their inclusion in standards*. English. 2014. URL: `https://cdn.standards.iteh.ai/samples/53940/eed8e9480a434fd2810d25c5cd95458e/ISO-IEC-Guide-51-2014.pdf`.

[53] S. Hawksworth J. Gummer. "Spontaneous ignition of hydrogen: Literature Review". In: Health and Safety Laboratory. 2008.

[54] Simon Jallais et al. *Pre-normative REsearch for Safe use of Liquid HYdrogen (PRESLHY)*. Tech. rep. May 2018.

[55] Lachance Jeffrey et al. "Analyses to Support Development of Risk-Informed Separation Distances for Hydrogen Codes and Standards". In: Mar. 2009.

[56] Øyvind Voie Jorunn Aaneby Thor Gjesdal. *Large scale leakage of liquid hydrogen (LH2) - tests related to bunkering and maritime use of liquid hydrogen*. Tech. rep. Norwegian Defence Research Establishment (FFI), Jan. 2021.

[57] Kenneth L. Kaiser. *Electrostatic Discharge*. CRC Press, 2005.

[58] S KIKUKAWA, H MITSUHASHI, and A MIYAKE. "Risk assessment for liquid hydrogen fueling stations". In: *International Journal of Hydrogen Energy* 34.2 (Jan. 2009), pp. 1135–1141. DOI: `10.1016/j.ijhydene.2008.10.093`.

[59] S KIKUKAWA, F YAMAGA, and H MITSUHASHI. "Risk assessment of Hydrogen fueling stations for 70MPa FCVs". In: *International Journal of Hydrogen Energy* 33.23 (Dec. 2008), pp. 7129–7136. DOI: `10.1016/j.ijhydene.2008.08.063`.

[60] L.E. Klebanoff, J.W. Pratt, and C.B. LaFleur. "Comparison of the safety-related physical and combustion properties of liquid hydrogen and liquid natural gas in the context of the SF-BREEZE high-speed fuel-cell ferry". In: *International Journal of Hydrogen Energy* 42.1 (Jan. 2017), pp. 757–774. DOI: `10.1016/j.ijhydene.2016.11.024`.

[61] Hiroaki Kobayashi et al. "Experimental study on cryo-compressed hydrogen ignition and flame". In: *International Journal of Hydrogen Energy* 45.7 (2020), pp. 5098–5109. ISSN: 0360-3199. DOI: `https://doi.org/10.1016/j.ijhydene.2019.12.091`. URL: `https://www.sciencedirect.com/science/article/pii/S0360319919346270`.

[62] M Komori and K Kikukawa. "SAFETY STUDY OF HYDROGEN SUPPLY STATIONS FOR THE REVIEW OF HIGH PRESSURE GAS SAFETY LAW IN JAPAN". In: 2002.

[63] Ayumi Kumamoto et al. "Measurement of minimum ignition energy in hydrogen-oxygen-nitrogen premixed gas by spark discharge". In: *Journal of Physics: Conference Series* 301 (Jan. 2011), p. 012039. DOI: `10.1088/1742-6596/301/1/012039`. URL: `https://doi.org/10.1088/1742-6596/301/1/012039`.

[64] Kolbjørn Berge Lars Alvestad. *HANDBOOK FOR HYDROGEN-FUELLED VESSELS*. Tech. rep. June 2021.

[65] Zhiyong Li et al. "Study on the harm effects of releases from liquid hydrogen tank by consequence modeling". In: *International Journal of Hydrogen Energy* 37.22 (2012). HySafe 1, pp. 17624–17629. ISSN: 0360-3199. DOI: `https://doi.org/10.1016/j.ijhydene.2012.05.141`. URL: `https://www.sciencedirect.com/science/article/pii/S0360319912012840`.

[66] Arthur Litile, Spacey Adnltntstration, and Nasa Lewis. *AN ASSESSMENT OF THE CRASH FIRE HAZARD OF LIQUID HYDROGEN FUELED AIRCRAFT*. Tech. rep. NASA, Feb. 1982.

[67] Yuanliang Liu et al. "Evaluation and prediction of the safe distance in liquid hydrogen spill accident". In: *Process Safety and Environmental Protection* 146 (2021), pp. 1–8. ISSN: 0957-5820. DOI: `https://doi.org/10.1016/j.psep.2020.08.037`. URL: `https://www.sciencedirect.com/science/article/pii/S0957582020317067`.

[68] B.J. Lowesmith, G. Hankinson, and S. Chynoweth. "Safety issues of the liquefaction, storage and transportation of liquid hydrogen: An analysis of incidents and HAZIDS". In: *International Journal of Hydrogen Energy* 39.35 (2014), pp. 20516–20521. ISSN: 0360-3199. DOI: `https://doi.org/10.1016/j.ijhydene.2014.08.002`. URL: `https://www.sciencedirect.com/science/article/pii/S0360319914022435`.

[69] Kieran Lyons et al. “Theory and analysis of ignition with specificconditions related to cryogenic hydrogen”. In: 2020.

[70] William E. Martinsen and Jeffrey D. Marx. “AN IMPROVED MODEL FOR THE PREDICTION OF RADIANT HEAT FROM FIREBALLS”. In: *1999 International Conference and Workshop on Modeling Consequences of Accidental Releases of Hazardous Materials* (1999). URL: `http://www.questconsult.com/`.

[71] Hidenori Matsui and John H. Lee. “On the measure of the relative detonation hazards of gaseous fuel-oxygen and air mixtures”. In: *Symposium (International) on Combustion* 17.1 (1979). Seventeenth Symposium (International) on Combustion, pp. 1269–1280. ISSN: 0082-0784. DOI: `https://doi.org/10.1016/S0082-0784(79)80120-4`. URL: `https://www.sciencedirect.com/science/article/pii/S0082078479801204`.

[72] L Mélani, I Sochet, and X Rocourt. “REVIEW OF METHODS FOR ESTIMATING THE OVERPRESSURE AND IMPULSE RESULTING FROM A HYDROGEN EXPLOSION IN A CONFINED/OBSTRUCTED VOLUME”. In: 2009.

[73] Derek Miller. “New model for predicting thermal radiation from flares and high pressure jet fires for hydrogen and syngas”. In: *Process Safety Progress* 36.3 (2017), pp. 237–251. DOI: `https://doi.org/10.1002/prs.11867`. URL: `https://aiche.onlinelibrary.wiley.com/doi/abs/10.1002/prs.11867`.

[74] Toshio Mogi et al. “Self-ignition and flame propagation of high-pressure hydrogen jet during sudden discharge from a pipe”. In: *International Journal of Hydrogen Energy* 34.14 (2009). 2nd International Conference on Hydrogen Safety, pp. 5810–5816. ISSN: 0360-3199. URL: `https://www.sciencedirect.com/science/article/pii/S0360319909006491`.

[75] Iraj Mohammadfam and Esmaeil Zarei. “Safety risk modeling and major accidents analysis of hydrogen and natural gas releases: A comprehensive risk analysis framework”. In: *International Journal of Hydrogen Energy* 40.39 (2015), pp. 13653–13663. ISSN: 0360-3199. DOI: `https://doi.org/10.1016/j.ijhydene.2015.07.117`. URL: `https://www.sciencedirect.com/science/article/pii/S0360319915019205`.

[76] V. Molkov and S. Kashkarov. “Blast wave from a high-pressure gas tank rupture in a fire: Stand-alone and under-vehicle hydrogen tanks”. In: *International Journal of Hydrogen Energy* 40.36 (2015), pp. 12581–12603. ISSN: 0360-3199. DOI: `https://doi.org/10.1016/j.ijhydene.2015.07.001`. URL: `https://www.sciencedirect.com/science/article/pii/S0360319915017280`.

[77] Foivos Mylonopoulos et al. “Hydrogen vs. Batteries: Comparative Safety Assessments for a High-Speed Passenger Ferry”. In: *Applied Sciences* 12.6 (2022). ISSN: 2076-3417. DOI: `10.3390/app12062919`. URL: `https://www.mdpi.com/2076-3417/12/6/2919`.

[78] Y. Nagase et al. “NUMERICAL INVESTIGATION OF HYDROGEN LEAKAGE FROM A HIGH-PRESSURE TANK AND PIPELINE”. In: *7th International Conference on Hydrogen Safety* (2017).

[79] Weyandt NC. “Vehicle bonfire to induce catastrophic failure of a 5000-psig hydrogen cylinder installed on a typical SUV.” In: Motor Vehicle Fire Research Institute. 2006.

[80] NFPA. *NFPA 2: “Hydrogen Technologies Code”.2020 edition*. Tech. rep. 2020.

[81] Hoi Dick Ng and John H.S. Lee. “Comments on explosion problems for hydrogen safety”. In: *Journal of Loss Prevention in the Process Industries* 21.2 (2008). Hydrogen Safety, pp. 136–146. ISSN: 0950-4230. DOI: `https://doi.org/10.1016/j.jlp.2007.06.001`. URL: `https://www.sciencedirect.com/science/article/pii/S0950423007000873`.

[82] International Association of Oil and Gas Producers. “OGP risk assessment data directory report No. 434.” In: Mar. 2010.

[83] Ryo Ono et al. “Minimum ignition energy of hydrogen–air mixture: Effects of humidity and spark duration”. In: *Journal of Electrostatics* 65.2 (2007), pp. 87–93. ISSN: 0304-3886. DOI: `https://doi.org/10.1016/j.elstat.2006.07.004`. URL: `https://www.sciencedirect.com/science/article/pii/S0304388606000726`.

[84] IMO-International Maritime Organization. *Fourth Greenhouse Gas Study 2020*. URL: https://www.imo.org/en/OurWork/Environment/Pages/Fourth-IMO-Greenhouse-Gas-Study-2020.aspx. (accessed: 15.08.2022).

[85] IMO-International Maritime Organization. *Initial IMO GHG Strategy*. URL: https://www.imo.org/en/MediaCentre/HotTopics/Pages/Reducing-greenhouse-gas-emissions-from-ships.aspx. (accessed: 15.08.2022).

[86] B.J.M. Ale P.A.M. Uijt de Haag. "Guidelines for quantitative risk assessment, 'Purple book'". In: 2005.

[87] Pratikash P. Panda and Ethan S. Hecht. "Ignition and flame characteristics of cryogenic hydrogen releases". In: *International Journal of Hydrogen Energy* 42.1 (Jan. 2017), pp. 775–785. DOI: 10.1016/j.ijhydene.2016.08.051.

[88] OREDA Participants. "OREDA Offshore Reliability Data Handbook 4th edition". In: DNV. 2002.

[89] HyFacts project. "Chapter IM. Hydrogen ignition mechanisms. Prevention and mitigation of ignition." In: 2012.

[90] National Institute of Public Health and the Environment (RIVM) Centre for External Safety. *Reference Manual Bevi Risk Assessments*. Tech. rep. July 2009.

[91] Ravichandra Pula et al. "Revised fire consequence models for offshore quantitative risk assessment". In: *Journal of Loss Prevention in the Process Industries* 18.4-6 (July 2005), pp. 443–454. DOI: 10.1016/j.jlp.2005.07.014.

[92] Knystautas R. "Measurement of cell size in hydrocarbon-air mixtures and predictions of critical tube diameter, critical initiation energy and detonability limits". In: *Progress in Astronautics and Aeronautics* 94 (1984), pp. 23–37.

[93] D K Pritchard & W M Rattigan. *Hazards of liquid hydrogen*. English. 2010. URL: https://www.hse.gov.uk/research/rrpdf/rr769.pdf.

[94] Lloyd's Register. *ShipRight Design and Construction, Additional Design Procedures -Risk Based Designs (RBD)*. Tech. rep. Lloyd's Register, 2018.

[95] Lloyd's Register. *Ship Vibration and Noise- Guidance Notes*. English. 2006.

[96] A.F. Roberts. "Thermal radiation hazards from releases of LPG from pressurised storage". In: *Fire Safety Journal* 4.3 (1981), pp. 197–212. ISSN: 0379-7112. DOI: https://doi.org/10.1016/0379-7112(81)90018-7. URL: https://www.sciencedirect.com/science/article/pii/0379711281900187.

[97] Chiara Dall'Armi Rodolfo Taccani Stefano Malabotti and Diego Micheli. "High energy density storage of gaseous marine fuels: An innovative concept and its application to a hydrogen powered ferry". In: *International Shipbuilding Progress* 67 (2020), pp. 33–56. DOI: 10.3233/ISP-190274. URL: http://dx.doi.org/10.1002/andp.19063240204.

[98] M Royle and D Willoughby. *Releases of unignited liquid hydrogen*. Tech. rep. Health and Safety Laboratory, 2014.

[99] Kashkarov S., Li Z., and Molkov V. "Nomograms for Assessment of Hazard Distances From a Blast Wave After High-Pressure Hydrogen Cylinder Rupture in a Fire". In: 2016.

[100] M Sherman, S Tieszen, and W Benedick. "The Effect of Obstacles and Transverse Venting on Flame Acceleration and Transition to Detonation for Hydrogen-Air Mixtures at Large Scale". In: Apr. 1989.

[101] MAN Energy Solutions. "MAN CRYO". In: Mar. 2019.

[102] John Spouge. "LEAK FREQUENCIES FROM THE HYDROCARBON RELEASE DATABASE". In: DNV Consulting. 2006.

[103] J Statharas et al. "Analysis of data from spilling experiments performed with liquid hydrogen". In: Dec. 6, 2015. DOI: 10.1016/S0304-3894(00)00252-1.

[104] Meryem Gizem Sürer and Hüseyin Turan Arat. “Advancements and current technologies on hydrogen fuel cell applications for marine vehicles”. In: *International Journal of Hydrogen Energy* 47.45 (2022). The Fifth International Hydrogen Technologies Congress, pp. 19865–19875. ISSN: 0360-3199. DOI: `https://doi.org/10.1016/j.ijhydene.2021.12.251`. URL: `https://www.sciencedirect.com/science/article/pii/S0360319921050552`.

[105] K Takeno et al. “PHENOMENA OF DISPERSION AND EXPLOSION OF HIGH PRESSURIZED HYDROGEN”. In: 2004.

[106] Keiji Takeno et al. “Experimental Study on Open Jet Diffusion Flame and Unconfined Explosion for Leaked High — pressurized Hydrogen”. In: *Journal of Japan Society for Safety Engineering* (2005).

[107] A Tchouvelev, R Hay, and P Benard. “COMPARATIVE RISK ESTIMATION OF COMPRESSED HYDROGEN AND CNG REFUELLING OPTIONS”. In: 2008.

[108] S. Tretsiakova-McNallTretsiakova-McNallyy. “LECTURE. Sources of hydrogen ignition and prevention measures”. In: 2016.

[109] Federico Ustolin. “Modelling of Accident Scenariosfrom Liquid HydrogenTransport and Use”. PhD thesis. Norwegian University of Science and Technology, July 2021.

[110] Federico Ustolin, Nicola Paltrinieri, and Gabriele Landucci. “An innovative and comprehensive approach for the consequence analysis of liquid hydrogen vessel explosions”. In: *Journal of Loss Prevention in the Process Industries* 68 (2020), p. 104323. ISSN: 0950-4230. DOI: `https://doi.org/10.1016/j.jlp.2020.104323`. URL: `https://www.sciencedirect.com/science/article/pii/S0950423020306100`.

[111] L. van Biert et al. “A review of fuel cell systems for maritime applications”. In: *Journal of Power Sources* 327 (2016), pp. 345–364. ISSN: 0378-7753. URL: `https://www.sciencedirect.com/science/article/pii/S0378775316308631`.

[112] A Van Den Berg. “THE MULTI-ENERGY METHOD A FRAMEWORK FOR VAPOUR CLOUD EXPLOSION BLAST PREDICTION”. In: 1985.

[113] K. VERFONDERN and B. DIENHART. “EXPERIMENTAL AND THEORETICAL INVESTIGATION OF LIQUIDHYDROGEN POOL SPREADING AND VAPORIZATION”. In: *International Journal of Hydrogen Energy* 22.7 (1997), pp. 649–660.

[114] Jennifer X. Wen et al. “Statistics, lessons learned and recommendations from analysis of HIAD 2.0 database”. In: *International Journal of Hydrogen Energy* 47.38 (2022), pp. 17082–17096. ISSN: 0360-3199. DOI: `https://doi.org/10.1016/j.ijhydene.2022.03.170`. URL: `https://www.sciencedirect.com/science/article/pii/S0360319922012976`.

[115] Jennifer X. Wen et al. “Statistics, lessons learned and recommendations from analysis of HIAD 2.0 database”. In: *International Journal of Hydrogen Energy* 47.38 (2022), pp. 17082–17096. ISSN: 0360-3199. DOI: `https://doi.org/10.1016/j.ijhydene.2022.03.170`. URL: `https://www.sciencedirect.com/science/article/pii/S0360319922012976`.

[116] R. D. WITCOFSKI and J. E. CHIRIVELLA. “EXPERIMENTAL AND ANALYTICAL ANALYSES OF THE MECHANISMSGOVERNING THE DISPERSION OF FLAMMABLE CLOUDS FORMED BYLIQUID HYDROGEN SPILLS”. In: *International Journal of Hydrogen Energy* 9.5 (1984), pp. 425–435.

[117] wurster. “acceptance criteria for H2 refuelling stations.PDF”. In: 2000.

[118] Eisuke Yamada et al. “Mechanism of high-pressure hydrogen auto-ignition when spouting into air”. In: *International Journal of Hydrogen Energy* 36.3 (2011). The Third Annual International Conference on Hydrogen Safety, pp. 2560–2566. ISSN: 0360-3199. DOI: `https://doi.org/10.1016/j.ijhydene.2010.05.011`. URL: `https://www.sciencedirect.com/science/article/pii/S0360319910009468`.

[119] Fuyuan Yang et al. “Review on hydrogen safety issues: Incident statistics, hydrogen diffusion, and detonation process”. In: *International Journal of Hydrogen Energy* 46.61 (2021), pp. 31467–31488. ISSN: 0360-3199. DOI: `https://doi.org/10.1016/j.ijhydene.2021.07.005`. URL: `https://www.sciencedirect.com/science/article/pii/S0360319921025520`.

[120] Arda Yapicioglu and Ibrahim Dincer. “Performance assesment of hydrogen and ammonia combustion with various fuels for power generators”. In: *International Journal of Hydrogen Energy* 43.45 (2018), pp. 21037–21048. ISSN: 0360-3199. DOI: https://doi.org/10.1016/j.ijhydene.2018.08.198. URL: https://www.sciencedirect.com/science/article/pii/S0360319918327915.

[121] Byung-Hoon Yoo et al. “Comparative risk assessment of liquefied and gaseous hydrogen refueling stations”. In: *International Journal of Hydrogen Energy* 46.71 (Oct. 2021), pp. 35511–35524. DOI: 10.1016/j.ijhydene.2021.08.073.

[122] Xing Yu et al. “Flame characteristics of under-expanded, cryogenic hydrogen jet fire”. In: *Combustion and Flame* 244 (2022), p. 112294. ISSN: 0010-2180. DOI: https://doi.org/10.1016/j.combustflame.2022.112294. URL: https://www.sciencedirect.com/science/article/pii/S0010218022003091.

[123] Li Zhiyong, Pan Xiangmin, and Ma Jianxin. “Quantitative risk assessment on a gaseous hydrogen refueling station in Shanghai”. In: *International Journal of Hydrogen Energy* 35.13 (2010). ISMF-09, pp. 6822–6829. ISSN: 0360-3199. DOI: https://doi.org/10.1016/j.ijhydene.2010.04.031. URL: https://www.sciencedirect.com/science/article/pii/S0360319910006956.

[124] LI. Zhiyong, PAN. Xiangmin, and MA. Jianxin. “Quantitative risk assessment on 2010 Expo hydrogen station”. In: *International Journal of Hydrogen Energy* 36.6 (2011). 3rd International Workshop in Hydrogen Energy, pp. 4079–4086. ISSN: 0360-3199. DOI: https://doi.org/10.1016/j.ijhydene.2010.12.068. URL: https://www.sciencedirect.com/science/article/pii/S0360319910024109.

[125] W Zhu. “Study on flow characteristics of high pressure and low temperature hydrogen”. In: *China Academy of Launch Vehicle Technol* (2019).

A

LIQUID HYDROGEN LEAKAGE FREQUENCY DATA

A.1. Tank/Vessel leakage

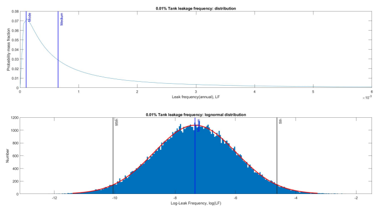

Figure A.1: Frequency of 0.01% leakage tank.

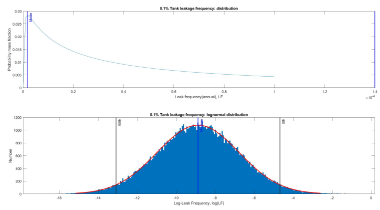

Figure A.2: Frequency of 0.1% leakage tank.

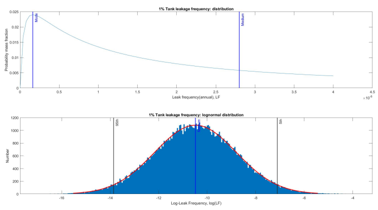

Figure A.3: Frequency of 1% leakage tank.

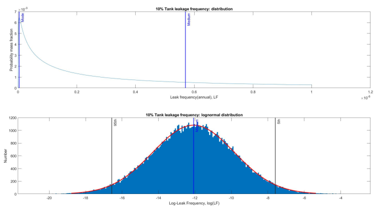

Figure A.4: Frequency of 10% leakage tank.

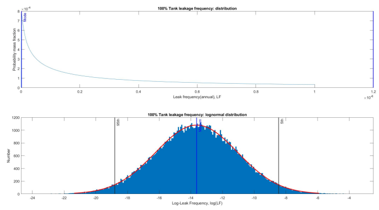

Figure A.5: Frequency of 100% leakage tank.

A.2. Pipe leakage

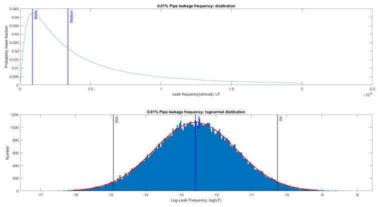

Figure A.6: Frequency of 0.01% leakage pipe.

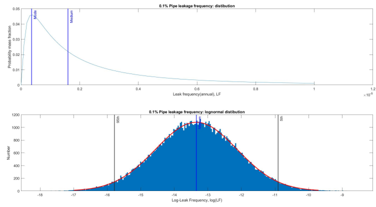

Figure A.7: Frequency of 0.1% leakage pipe.

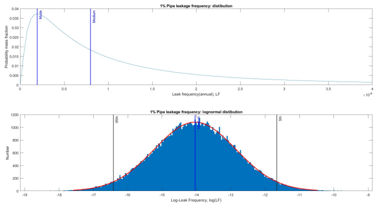

Figure A.8: Frequency of 1% leakage pipe.

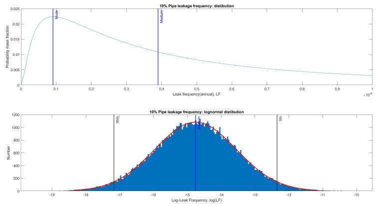

Figure A.9: Frequency of 10% leakage pipe.

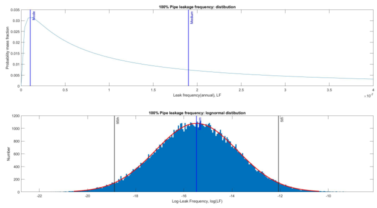

Figure A.10: Frequency of 100% leakage pipe.

A.3. Valve leakage

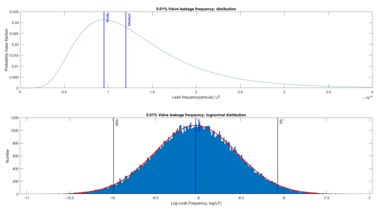

Figure A.11: Frequency of 0.01% leakage valve.

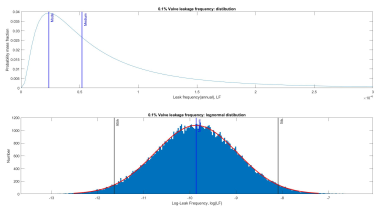

Figure A.12: Frequency of 0.1% leakage valve.

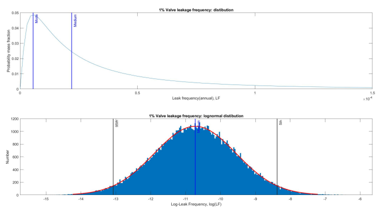

Figure A.13: Frequency of 1% leakage valve.

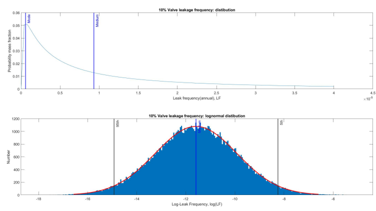

Figure A.14: Frequency of 10% leakage valve.

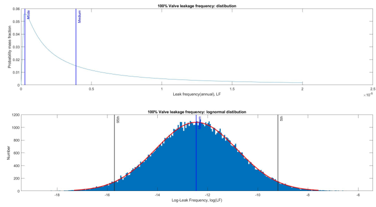

Figure A.15: Frequency of 100% leakage valve.

A.4. Flange leakage

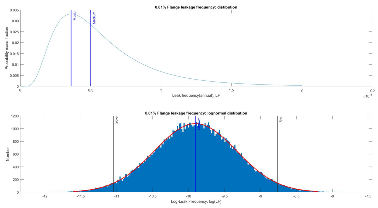

Figure A.16: Frequency of 0.01% leakage flange.

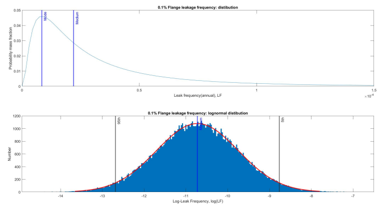

Figure A.17: Frequency of 0.1% leakage flange.

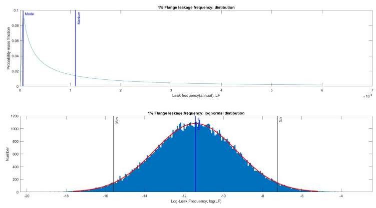

Figure A.18: Frequency of 1% leakage flange.

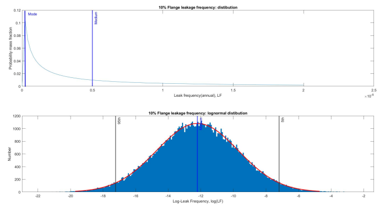

Figure A.19: Frequency of 10% leakage flange.

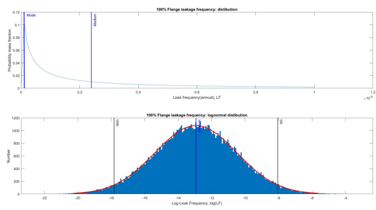

Figure A.20: Frequency of 100% leakage flange.

A.5. Heat exchanger leakage

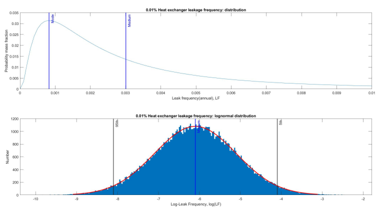

Figure A.21: Frequency of 0.01% leakage heat exchanger.

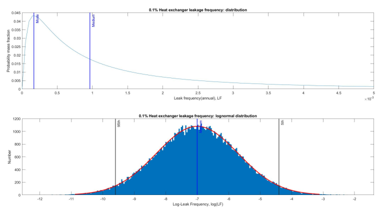

Figure A.22: Frequency of 0.1% heat exchanger.

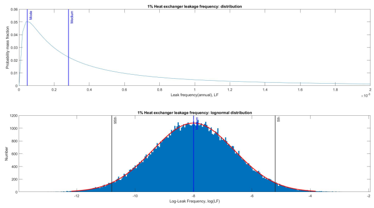

Figure A.23: Frequency of 1% leakage heat exchanger.

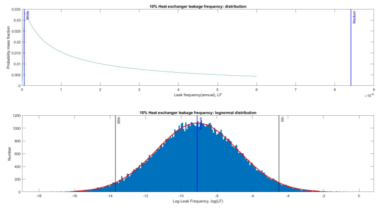

Figure A.24: Frequency of 10% heat exchanger.

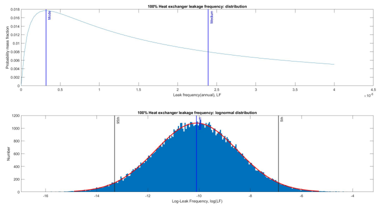

Figure A.25: Frequency of 100% leakage heat exchanger.

B

LOGICAL DIAGRAM

B.1. Event tree analysis

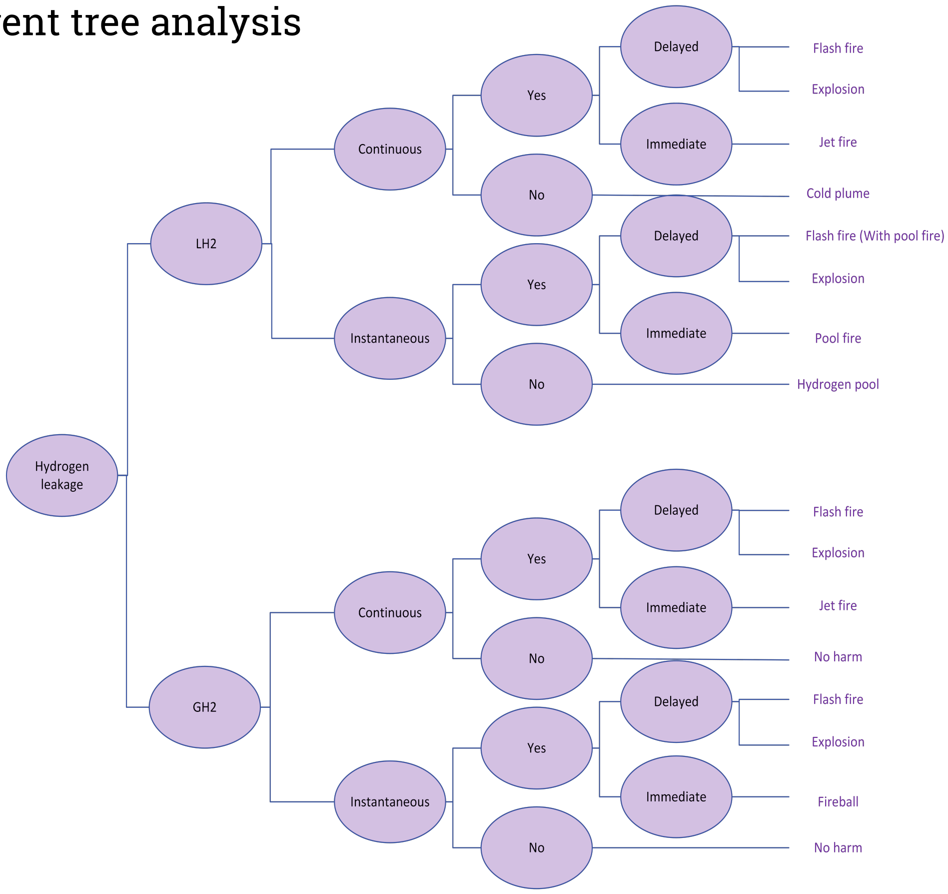

Figure B.1: Event tree analysis for the hazards of maritime LH2 propulsion system.

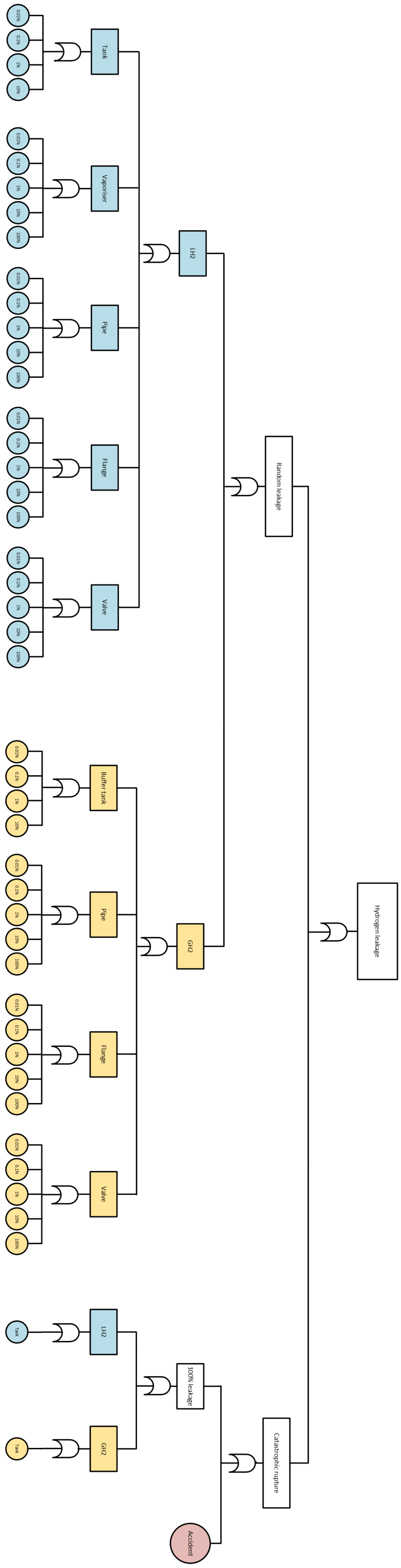

Figure B.2: Fault tree analysis for the hazards of maritime LH2 propulsion system.

C
SIMULINK MODEL

C.1. MARITIME LH2 PROPULSION SOLUTIONS' QUANTITATIVE RISK ASSESSMENT SYSTEM

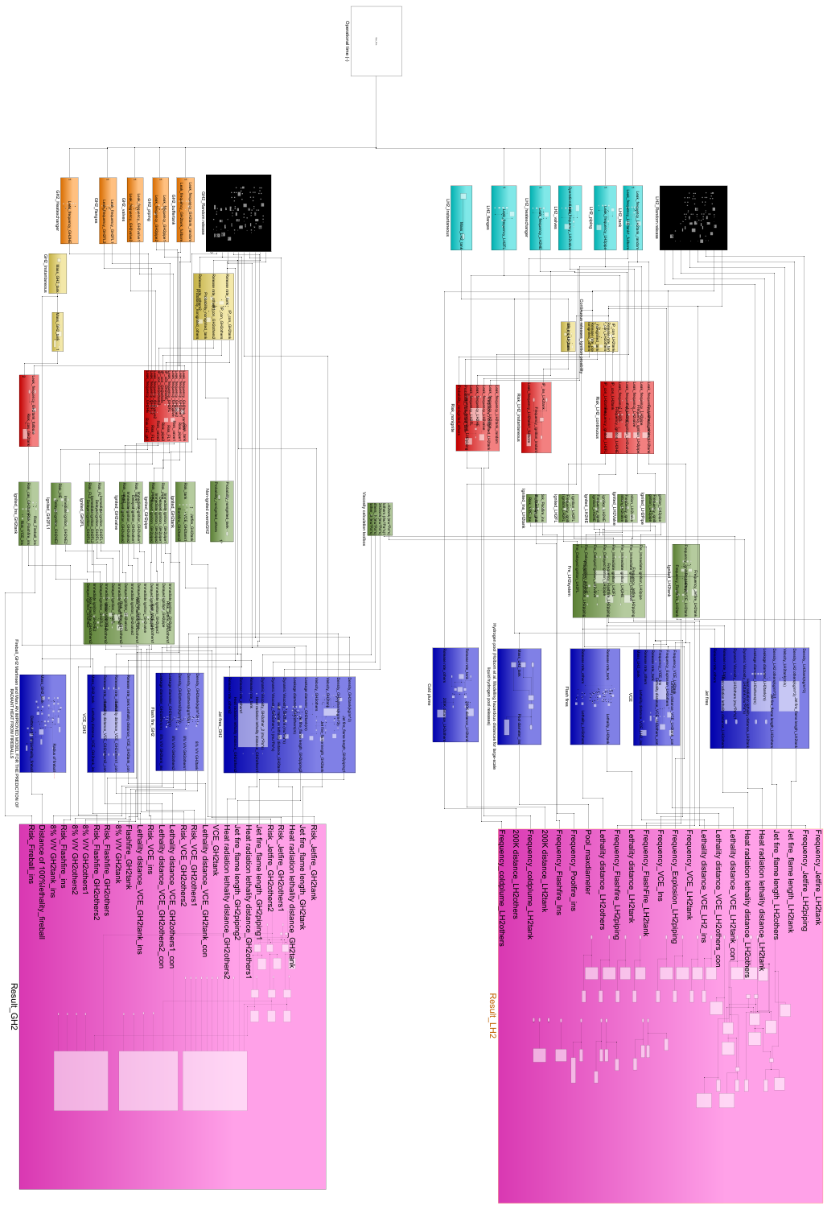

Figure C.1: Simulink model for the LH2 QRA system.

C.2. MARITIME CH2 PROPULSION SOLUTIONS' QUANTITATIVE RISK ASSESSMENT SYSTEM

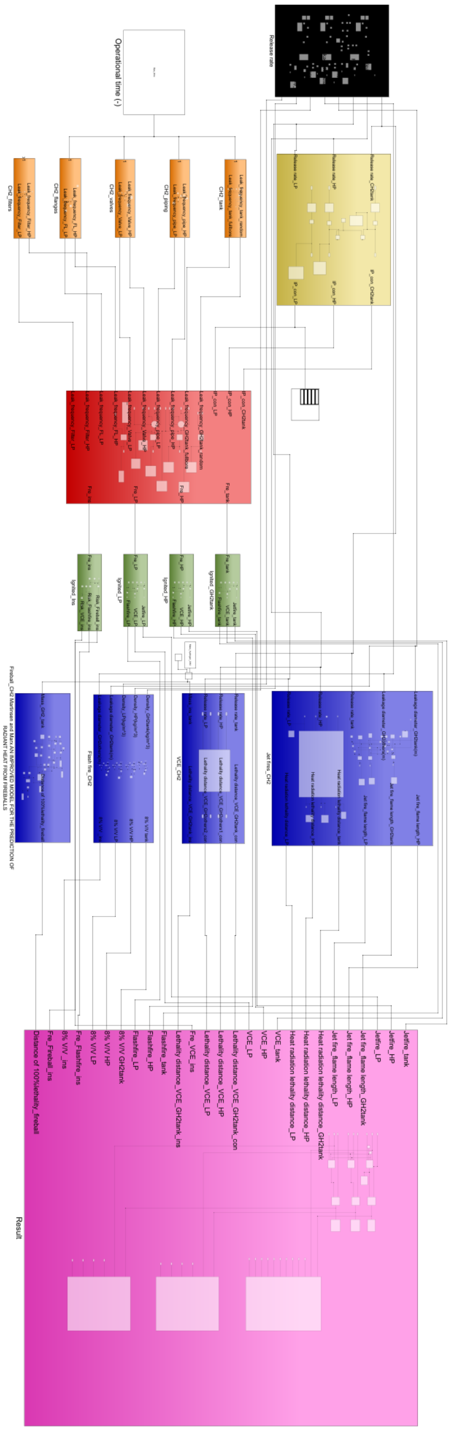

Figure C.2: Simulink model for the CH2 QRA system.